

PLEIOTROPHIN ENHANCE NERVE REGENERATION ACROSS
LONG GAP PERIPHERAL NERVE DEFECTS

by

SWARUP NARAYAN DASH

Presented to the Faculty of the Graduate School of
The University of Texas at Arlington in Partial Fulfillment
of the Requirements
for the Degree of

DOCTOR OF PHILOSOPHY

THE UNIVERSITY OF TEXAS AT ARLINGTON

August 2012

Copyright © by Swarup Narayan Dash

All Rights Reserved

ACKNOWLEDGEMENTS

Completing graduate school and getting a doctoral degree would not have been possible without the love and support of several people. First, I would like to acknowledge the enormous guidance and support from my advisor and mentor Dr. Mario Romero-Ortega throughout my graduate school. He has been instrumental in making me believe in my potentials and approach scientific research in a methodical manner. On a personal note, he has been very friendly and willing to help anytime I had tough days with my research.

Also, I would like to thank my committee members: Dr. Liping Tang, Dr. Jian Yang, Dr. Yuan Bo Peng at UT Arlington and Dr. Jonathan Cheng at UT Southwestern for their valuable time and support towards my academic research.

Abdul and Andrew, I would not have become successful in completing the long gap experiments without your immense help along with late nights and weekends in the lab. Also, I have to thank Parisa for always being supportive in the lab. Tarik and Dianna, thanks for being such awesome mentees all the time. I would also like to thank Nesreen and Ben for doing some amazing collaborative research in the lab. Finally many thanks to Jon and Mike for being the nicest mentors during my internship at Life Technologies and teaching me gene therapy based stem cell line productions and molecular genetics.

Last but absolutely not the least; I would thank my family including mom, dad and Anup for being very supportive of my graduate school endeavors. Most significantly, I extend my acknowledgement to my lovely wife Tabassum, without whom this achievement would have been impossible. Thank you for the continuous support and understanding all through my graduate school.

July 16, 2012

ABSTRACT

PLEIOTROPHIN ENHANCE NERVE REGENERATION ACROSS LONG GAP PERIPHERAL NERVE DEFECTS

Swarup Narayan Dash, PhD

The University of Texas at Arlington, 2012

Supervising Professor: Mario Romero-Ortega

Peripheral nerve injuries resulting in extensive loss in nerve continuity pose a challenge in reconstructive surgery. Autografts still remain the treatment of choice for nerve defects despite the need of donor nerve harvest and the associated morbidity of this procedure. In contrast to short gap injuries, isografts achieve sub normal functional recovery for gaps longer than a critical 30 mm length, and simple tubularization methods fail completely. The regenerative failure of peripheral nerves through long gaps can be postulated to the lack of appropriate growth substrate and trophic support. We hypothesize that for successful nerve regeneration across long-gap nerve defects, growth factor support and early vascularization of the regenerated nerve are critical factors. Vascular endothelial growth factor (VEGF) and Pleiotrophin (PTN) have growth promoting effects on neurons as well as the supporting cells, hence suitable for axonal regeneration. Here we described the development of a next generation multi-luminal biodegradable nerve implant repair strategy supplemented with growth factor delivery system, as a construct to bridge the transected neurons across critical peripheral nerve gaps and achieve functional recovery.

TABLE OF CONTENTS

ACKNOWLEDGEMENTS	iii
ABSTRACT	iv
LIST OF ILLUSTRATIONS	ix
LIST OF TABLES	xiii
Chapter	Page
1. INTRODUCTION.....	1
1.1 Peripheral Nerve Injury	1
1.1.1 Injury Classification	2
1.1.2 Cellular response after injury	4
1.1.3 Wallerian Degeneration.....	5
1.2 Nerve Regeneration Strategies.....	5
1.2.1 Autografts: the current gold standard.....	6
1.2.2 Synthetic Nerve Guides	7
1.2.3 Luminal fillers	9
1.2.3.1 ECM proteins	10
1.2.3.2 Cellular support	11
1.2.3.3 Growth Factors.....	11
1.2.4 Modified Scaffolds.....	13
1.2.4.1 Microfibers.....	13
1.2.4.2 Microchannels	14
1.3 Multiluminal Biosynthetic Nerve Implant (BNI) Approach.....	16
1.4 Hypothesis	18

1.5 Specific Aims.....	19
2. PLEIOTROPHINSUPPORT IN LONG GAP PERIPHERAL NERVE REPAIR	21
2.1 Introduction	22
2.2 Materials and Methods.....	25
2.2.1 Animals	25
2.2.2 BNI Nerve guides with multiluminal pleiotrophin support	25
2.2.3 BNI nerve repair.....	26
2.2.4 Nanoparticle Fabrication	26
2.2.5 Bioactivity evaluation of nanoparticle encapsulation of PTN and VEGF	28
2.2.6 Immunocytochemistry	29
2.2.7 Myelinated axon quantification.....	29
2.2.8 Electrophysiology	30
2.2.9 Behavioral function recovery.....	30
2.2.10 Statistical analysis.....	31
2.3 Results	31
2.3.1 Sustained release of biologically active VEGF or PTN within agarose microchannels	31
2.3.2 Long nerve gap regeneration can be achieved with multiluminal structural support	34
2.3.3 Sustained Pleiotrophic support can entice long gap nerve regeneration and functional recovery.....	35
2.3.4 Increased axonal regeneration to distal target with BNI VEGF/PTN support	38
2.3.5 Restoration of nerve conduction in all the BNI groups	40
2.3.6 Enhanced sensory recovery across the BNI	41
2.3.7 PTN mediated motor function recovery.....	42
2.3.8 Reduced muscle weight loss in growth factor groups	42

2.4 Discussion	45
2.5 Conclusion	49
3. ELASTIC, POROUS AND TRANSPARENT NERVE GUIDES FOR EFFECTIVE MULTILUMINAL NERVE REPAIR	50
3.1 Introduction	51
3.2 Materials and Methods	53
3.2.1 CUPE nerve guide fabrication	53
3.2.2 Mechanical test of the nerve guides	55
3.2.3 CUPE Biosynthetic Nerve Implant (CUPE-BNI)	56
3.2.4 Animals	56
3.2.5 Animal Surgery	56
3.2.6 Histological tissue preparation	57
3.2.7 Immunostaining	57
3.2.8 Axonal quantification	58
3.2.9 Electrophysiology	58
3.2.10 Statistical analysis	58
3.3 Results	58
3.3.1 Translucent CUPE-NGs	58
3.3.2 Multiluminal CUPE-BNI entices functional axonal regeneration through long nerve gaps	59
3.3.3 Restricted inflammatory response elicited by CUPE revealed specific recruitment of macrophages and controlled polymer reabsorption.	65
3.4 Discussion	67
3.5 Conclusion	71
4. FUTURE DIRECTIONS	72
4.1 Additional CUPE-NG assessments for clinical applications	72
4.2 Combination of NGF/NT-3 and PTN for long gap repair	73

APPENDIX

A. GROWTH FACTOR RELEASE MODELING WITHIN NERVE GUIDES OF COMPLEX MATERIAL COMPOSITION.....	75
REFERENCES	81
BIOGRAPHICAL INFORMATION	96

LIST OF ILLUSTRATIONS

Figure	Page
1.1 Schematic representation of Chromatolysis and Wallerian degeneration post nerve injury.(A) An uninjured nerve with proper innervation to the distal muscle, (B) The cell body undergoes chromatolysis after axotomy and Wallerian degeneration initiates at the injury site leading to muscle deinnervation and (C) Regenerated Nerve reinnervates the muscle while Schwann cell aligned uniformly to form the myelin sheath.....	4
1.2 The “gold standard” for gap nerve repair. Schematic representation of a commonly used technique for nerve repairs if end-to-end repair is not possible. Mostly sural nerve is used as the donor nerve autograft in clinics.....	7
1.3 SEM images three FDA approved NGs. (A) NeuraGen (collagen);(B) Neurolac (polylactide/caprolactone);(C) Neurotube (polyglycolide).....	8
1.4 Summary of various approaches taken in basic science research to repair gap nerve injuries	13
1.5 (A) Schematic of the Biosynthetic Nerve Implant (BNI), (B) BNI fabrication method representation (i) insertion of a brush with metal fibers, (ii) the agarose inside the tube polymerizes and collagen is loaded in the well and (iii) the fibers are removed slowly and negative pressure in the microchannels help in uniform loading of the collagen, (C) Alignment of GFP+ Schwann cells and (D) growth of DRG axons inside the microchannels <i>in vitro</i>	17
1.6 Multi-luminal nerve repair through the BN across 1cm. Nerve repair 10 weeks post sciatic nerve transection by (A) autograft, (B) collagen filled empty tube, (C, E, G) collagen filled 7-channel BNI (D, F, H), collagen filled 14-channel BNI. Arrowheads indicate within the regenerating nerves and arrows indicate the outer mesenchymal membrane. Scale bars: (A) 2 mm, (E) 400 μ m	18
1.7 Cross-sectional representation of all three versions of the BNI. (A) 7 channel BNI with 5% growth area, (B) 14 channel BNI with 34% growth area and (C) the next generation 8 channel BNI with 74% growth area	20
2.1 Nanoparticle morphology and release study. Scanning electron microscope images of PLGA nanoparticles loaded with (A) PTN and (B) VEGF [scale: 5 μ m]. The cumulative release of (C) PTN and (D) VEGF from the nanoparticles over a period of 21-28 days.	27
2.2 (A) The 3cm BNI casting device along with the loading well for collagen and nanoparticle on one side and the brush on the other side, (B) An implanted 3cm BNI between a transected peroneal nerve in the rabbit; the implant is securely held by tying it to the underlying muscle. Image of a (C) simple tube filled with collagen and (D) a BNI with collagen filled microchannels.	28

2.3 Bioactivity of PTN microparticles. Ventral motor neuron cultures treated with (A) BSA and (B) PTN nanoparticles and labeled with anti- β tubulin antibody. Quantification of (C) surface area of motor neurons and (D) average axonal length when treated with PTN and BSA nanoparticles after five days in culture. This is a significant increase in the size of the cell soma as well as the axonal length in the PTN treated cultures (n=4 cultures per group; *, p< 0.005).	32
2.4 Enhanced vasculature by VEGF. P4-6 aorta explants regeneration into the microchannels in presence (a, c) and absence (b, d) of VEGF after 8 days of culture <i>in vitro</i> . Quantitative analysis DAPI-positive nuclei, confirmed a significant difference (p<0.05) in the number of cells in each group.....	33
2.5 Surgical implantation procedure of a 30 mm nerve conduit after peroneal nerve injury. (A) Incision for implantation showing Tibial (top) and Peroneal nerve (bottom), (B) the NG is first sutured to the underlying muscle (C, D) Proximal and distal stumps are sutured into the NG	34
2.6 Histological analysis six weeks post implantation. (A-D), show H & E sections and (E-H) show sections stained for Neurofilament positive axons (brown, also indicated by arrows) at six weeks post injury. Treatment groups included (A, B) simple tube (C, D) multiluminal BNI (E, F) BNI supplemented with recombinant VEGF (G, H) BNI supplemented with recombinant PTN.....	37
2.7 Myelination staining on the distal stump of the regenerated nerve in all the experimental groups. NFP 200 is used as a marker for axons and P0 is used as a marker for the myelin around these axons.	38
2.8 Total number in of myelinated axons in the complete distal segment of the regenerated peroneal nerve. Number of axons in the VEGF and PTN treated groups were comparatively higher than BNI collagen. All values are reported as mean \pm SD.	39
2.9 Diagram of terminal electrophysiology setup. Stimulating hook electrodes are used to stimulate the proximal side of the nerve implant and recording needle electrodes are placed in the tibialis anterior muscle to record CMAPs. (Adopted from Van Dyke, 2008)	40
2.10 Measurement of compound muscle action potentials (CMAPs). (A) No electrical response seen from the tibialis anterior muscle in simple tube collagen repair. (B-E) Distinct CMAP responses were observed in all the BNI groups. (F) Quantification of CMAPs across the experimental groups indicates that all BNI groups had significantly greater response as compared the simple tube control and the growth factor supplemented groups showed significantly higher CMAPs as compared to BNI without growth factors	41
2.11 Dermatome of the rabbit's feet and the formalin injection site	43
2.12 Behavioral test sensory function recovery. (A) A rabbit licking its foot after formalin injection, (B) Quantification of the number of licks for 10 minutes after injection of 10% formalin. There was a significant increase in the number of licks in all the BNI groups as compared to the simple tube collagen controls, but no significant difference was observed among the BNI groups.	43

2.13 (A) Schematic representation of the direct measurement of toe-spreading length between the first and the forth toe at the tip of nails. (B)Picture of toe-spread in a rabbit with a left peroneal nerve injury	44
2.14 Behavioral test for motor function recovery. (A) Toe spread measurement to evaluate motor functional recovery after 3 and 9 weeks of injury. (B) All the experimental groups except the simple tube collagen group had significantly greater toe spreading.....	44
2.15 Comparison of tibialis anterior muscle weight across all experimental groups. The BNI groups supplemented with pleiotrophic factor had reduced muscle loss as compared to the simple tube collagen group	45
3.1 (A) Photographs of transparent CUPE-NG of two different thicknesses (top, amber) compared to a non-biodegradable Polyurethane-NG. (bottom, clear); (B) Cross sectional view of a CUPE-NG; (C) Cross sectional view of a CUPE Multiluminal Biosynthetic Nerve Implant (CUPE-BNI), the arrow indicates agarose structure and the asterisk represents a microchannel; (D) CUPE-BNI casting device showing the metallic brush inserted in the loading well prior to collagen (top), and after fiber removal (bottom).	54
3.2 Transparency evaluation of CUPE in comparison to a transparent polymer polyurethane and the plate	55
3.3 Nerve regeneration across a 15mm long gap across a (A) CUPE-NG and (B) CUPE-BNI 8 weeks after implantation. Enhanced tissue growth is visibly observed in the multi luminal BNI as compared to the NG filled with collagen (Scale bar=2 mm).	59
3.4 Nerve tissue regeneration across a CUPE-NG and a CUPE-BNI. (A) Cross section of NFP 200 staining showed regenerated nerve tissue across a CUPE-NG (Scale bar=200 μ m); B) NFP-200 staining confirmed the multiluminal axonal regeneration across a CUPE-BNI (Scale bar=200 μ m).....	60
3.5 Representation of Image J quantification technique of counting regenerating axons. (A) A fluorescent image of NFP 200 positive regenerating axons through a CUPE-NG, (B) Image J analysis of axonal count by finding number of maxima at a noise threshold of 30.....	61
3.6 Comparison of regenerated axonal number quantification across a CUPE-NG and a CUPE-BNI indicates significant increase in the number of axons in the multi luminal BNI group (*p<0.001).....	62
3.7 (A, B) Normal fascicular nerve regeneration is demonstrated by the co-localization of Schwann cells (red labeled S-100+) wrapping regenerated axons (green label NFP+); and by (C, D) Vimentin+ fibroblast (green) regeneration in the periphery of the regenerated nerve. Vimentin+ labeling marks the formation of perineurium around each micro channel packed with a regenerated nerve fascicle (Scale bars A=5 μ m, B=1 μ m, C=50 μ m, D=20 μ m)	63
3.8 Compound muscle action potential recordings (CMAP) from the gastrocnemius muscles. All gastrocnemius muscles produced measurable signals. (A) Representation of CMAP in CUPE-NG and CUPE-BNI group (The bar indicates three stimulation peaks); (B) Comparison of CMAP between CUPE-NG (n=8) and CUPE-BNI (n=8) group showed significant increase in nerve conduction in the multiluminal BNI group (*p<0.01).....	64

3.9 ED1+ Macrophages were localized on the CUPE-NG with minimal presence in regenerated epineurium or nerve fascicles. (A, D) ED1+ cells (arrows) present in surplus on the NG (marked by the dotted lines) and sparingly inside and outside the NG; (B, E) Magnification of the region within the box outside the NG (C, F) Magnification of the region within the box inside the NG (Scale bar A, D=200 μ m; B, C, E, F=100 μ m)	65
3.10 ED-1+ cells were observed on the NG eroding the CUPE at higher magnification. (A, B) ED+1 cells on the walls of the CUPE-NG; (C) Merged image of A and B (Scale bar=5 μ m). The arrows indicate edge of the polymer being degraded; (D, E, F) Magnified images of A, B and C (Scale bar=2 μ m).	67
3.11 Scanning electron microscope (SEM) images of the CUPE-NG surface (A) before implantation and (B) 8 weeks after implantation, indicating the degradation of the NG over time (arrows point to the pores formed on the NG; Scale bar= 200 μ m). Reduction in mechanical strength of CUPE-NGs after 8 and 12 weeks of implantation according to (C) Peak stress testing (*p<0.01) and (D) Elongation at break (*p<0.01, **p<0.001).....	68
4.1 (A) DRG explants cultures from postnatal mice day 3 treated with combination of PTN and NT-3/NGF and the control group not treated with any growth factors. (B) Quantification of the axonal density from these explants cultures under the treatment of individual growth factors and combination of growth factors	74

LIST OF TABLES

Table	Page
1.1 Peripheral nerve injury classification by Seddon and Sunderland.....	3
1.2 FDA approved Nerve Guides	9
1.3 Tubularization repair of short and long (≥ 3 cm) nerve defects. * = Biodegradable	15
2.1 Growth factors used in peripheral nerve regeneration and their targets.....	23
2.2 Experimental groups for the 30 mm long gap repair study	34
3.1 Experimental groups for the CUPE based nerve repair study	56

CHAPTER 1

INTRODUCTION

How does the mechanical development of the nerve fibers occur, and wherein lies that marvelous power which enables the nerve fibers from very distant cells to make contact directly with certain other nerve cells or the mesoderm or ectoderm without going astray or taking a roundabout course?-Santiago Ramón y Cajal, 1893

1.1 Peripheral Nerve Injury

1 in every 50 people in the United States is paralyzed according to a recent survey by the Christopher & Dana Reeve Foundation. The American Paralysis Association also reported the annual cost as \$7 billion among 6 million patients. In the United States, 50,000 peripheral nerve procedures are performed every year, whereas the whole of Europe has 300,000 nerve surgeries reported in clinics per year (1, 2). Approximately 2.8% of trauma patients have peripheral nerve injuries leading to partial functional loss for life (3). Brachial plexus injury is also very common in new born as it affects every 2.9 neonatal per 1000 births in the world (4). These injuries are more common in young adults due to motorbike accidents (5). These numbers has serious implications to the country's economy as a lot of work hours are lost because of nerve injuries. Peripheral nerve reconstruction has been considered since the second century A.D, even though research advancement has been made only in the last few decades. World War I and II resulted in a lot of casualties because of nerve injuries which led to the recognition of several types of injuries with different functional prognosis (6).

1.1.1 Injury Classification

Herbert Seddon worked with traumatic open wounds suffered in World War II and initially classified the nerve injuries according to the extent of damage to axons and surrounding connective tissue (i.e. neuropraxia, axonotmesis, and neurotmesis). Neuropraxia refers to the loss of myelin due to secondary injuries such as compression injuries. Axonotmesis refers to damage to the axons but intact structure of the nerve fibers, and Neurotmesis refers to the disruption or transection of the nerves. In 1951, Sydney Sunderland modified Seddon's surgical model with one of five anatomic categories. Type 1 injury is similar to neuropraxia where there is myelin loss. He divided axonotmesis into three different categories of injuries. Type 2 corresponds to damage of axon where endoneurium, perineurium and epineurium remain intact. Type 3 injury refers to damaged axons and endoneurium with intact perineurium and epineurium. Type 4 injuries include loss of axons, endoneurium and perineurium but the epineurium stays intact. Finally type 5 injuries are categorized similar to neurotmesis where the whole nerve trunk is disrupted or transected. Complete recovery of function is possible in type 1 injury where as the recovery goes down with increase in severity of the injury and in case of type 5 injuries functional recovery is negligible (7). Despite the extensive classification, most injuries observed in the clinics are mixed nerve injuries and cannot be categorized into a single type.

Table 1.1: Peripheral nerve injury classification by Seddon and Sunderland (7)

Injury Classification		
Seddon ²	Sunderland ¹	Pathophysiologic Features
Neurapraxia	Type 1	Local myelin damage usually secondary to compression
Axonotmesis	Type 2	Loss of continuity of axons; endoneurium, perineurium, and epineurium intact
	Type 3	Loss of continuity of axons and endoneurium; perineurium and epineurium intact
	Type 4	Loss of continuity of axons, endoneurium, and perineurium; epineurium intact
Neurotmesis	Type 5	Complete physiologic disruption of entire nerve trunk

Multiple events follow after any kind of axonal injury both at the cellular and molecular level. After axotomy, one of the earliest responses is the retraction of the proximal nerve stump millimeters to centimeters (8, 9), and the resealing of cut axons. If the injury is near the soma, some neurons die as result of the injury. In the DRG approximately 10-30% of sensory neurons die post axotomy affecting more the smaller neurons (<20 um) compared to larger neurons (>20um)(10-12). In contrast, only 0-10% spinal cord motor neurons die after axotomy (13). Neuron death as a result of injury is also age dependent with more neurons affected if injured in neonatal stages(12, 14). Furthermore, neural cell death after injury increases if the axotomized axons fail to regenerate efficiently (15). In fact in chronic amputee patients, approximately 50% motor neurons have been reported to die 6 months after injury (16). Often, if the transected nerve failsto reinnervate their natural targetsthey form neuromas which is a mixture of immature axonal sprouts and loose connective tissue (17). Such neuromas are commonly painful and might induce phantom limb sensations.

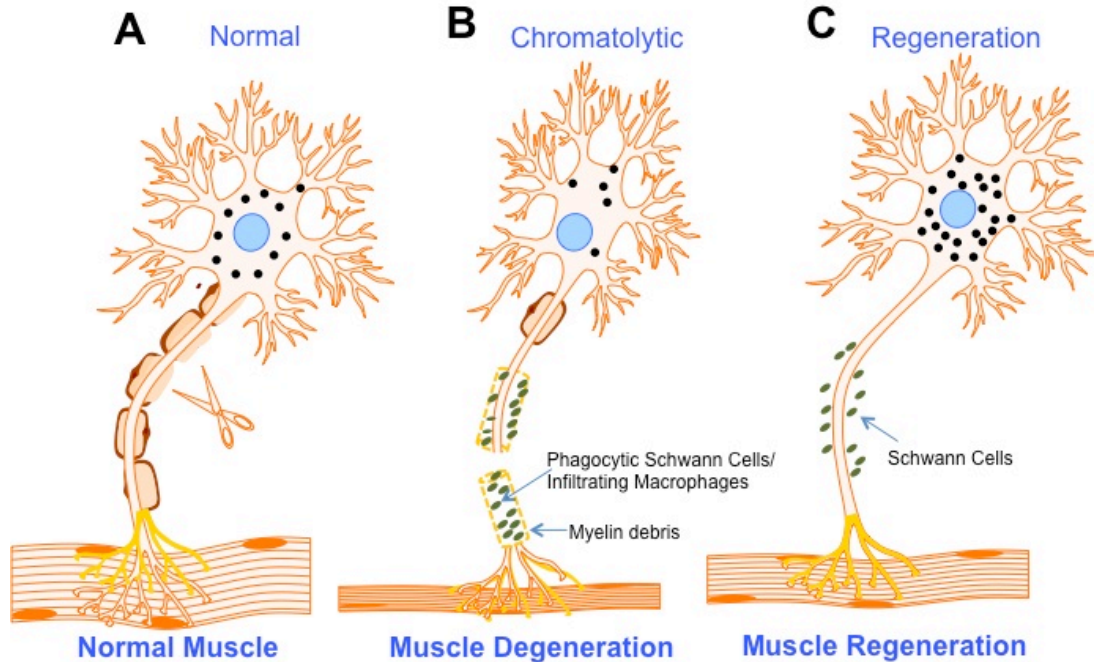


Figure 1.1: Schematic representation of Chromatolysis and Wallerian degeneration post nerve injury. (A) An uninjured nerve with proper innervation to the distal muscle, (B) The cell body undergoes chromatolysis after axotomy and Wallerian degeneration initiates at the injury site leading to muscle deinnervation and (C) Regenerated Nerve reinnervates the muscle while Schwann cell aligned uniformly to form the myelin sheath.

1.1.2 Cellular response following injury

The whole neuron undergoes massive changes after any axonal injury to the elongating distal axons. The disintegration of Nissl bodies in the neuronal soma is termed as Chromatolysis. This phenomenon is retrogradely induced after axotomy from the site of injury to the cell bodies. The morphology of the injured neuronal soma's nucleus becomes abnormal (Figure 1.1B) and the nucleolus appears prominent (18). Various events occur at the injury site level and the axonal soma level. After a peripheral nerve injury, the cell body receives a retrograde signal from the site of injury and in turn the expression levels of various transcription factors and growth factors change (19). There is an elevation of the cyclic AMP levels after injury (20). There is also activation of various pathways, which help in promoting nerve regeneration such as the MAPK, JNK and ERK pathway. Several transcriptional factors such as ATF3, c-Jun and STAT3 are

activated which help in increased actin formation and growth associated proteins (GAP 43). GAP43 helps in regeneration of the injured axons by the extension of the growth cone (21).

1.1.3 Wallerian Degeneration

Distal to the injury site, the severed axon undergoes degeneration initiated by the recruitment macrophages and Schwann cells (SCs). SCs reabsorb myelin in a what is known as Wallerian degeneration (22). Wallerian degeneration was first described by a British neurophysiologist Augustus Waller as the degeneration of the nerve fibers after injury (23). After any kind of axonal injury, the degradation process begins by the disintegration of axoplasm and axolemma which is followed by axonal and myelin debris formation (24, 25). The clearing of axonal, myelin and tissue debris is done by Schwann cells and macrophages infiltrating to the distal side of the injury (8). Schwann cells starts proliferating after injury forming a tubular structure called bands of büngner for assisting the regenerating axons to innervate their distal targets (26, 27). The time between axonal injury and degeneration of the distal stump can range from 24 hours to several days depending upon the type of injury and the animal model (28-30).

Functional impairments include the loss of movement, sensation and deinnervation of muscles leading to muscle weight loss. For decades, much effort have been placed in regenerating axons to the distal target using a variety of methods, ranging from some that rely on delivery of growth promoting molecules such as growth factors, extra cellular matrices and cell adhesion molecules for efficient neural repair (31-33) to the use of advanced scaffold for axonal guidance. Such repair strategies are detailed below.

1.2 Nerve Repair Strategies

After neurotmesis, the optimal clinical procedure for nerve repair is the surgical end-to-end re-attachment of the injured nerve, a process that is known to mediate efficient nerve regeneration and functional recovery(7). In cases in which tissue loss result in gaps that are too long for tensionless end-to-end repair, autologous nerve grafts are used as the 'gold standard' to bridge such defects(34).

1.2.1 Autografts: the current gold standard

Autografts are the preferred method for bridging gap defects if end-to-end anastomosis is not possible. Usually the sural nerve is used as the donor nerve in clinics even though the recovery of function is sub normal (Figure 1.2). The sural nerve is a sensory nerve and one of the major reasons of its failure can be attributed to the mismatch of its size while repairing a motor dominant nerve or a mixed nerve (35, 36). It has been also shown that there are two different types of Schwann cells modalities for motor and sensory neurons (37). This could also possible that there is lack of proper guidance in regeneration into the sensory nerve. There are also various other secondary reasons for failure of an autograft such as donor site morbidity, need of a second surgery, formation of neuromas at the donor site and lack of vascularization to the graft (38). However, donor site morbidity, scarce number of usable donor nerves, and suboptimal functional recovery drastically limit this alternative (18, 34).

As alternative to autografts, allogenic or xenogenic nerve grafts have been investigated. In fact, allografts are the preferred method for surgical repair of gaps longer than 5cm. However, both allografts and xenografts require immunosuppression therapy to the patient to prevent graft rejection(39). In addition, there is a risk of rejection, tumor formation and infection (40). Recently, decellularized nerve allo/xeno-grafts have also been evaluated, and while nerve regeneration was observed, the functional recovery achieved remained suboptimal (41). To eliminate the need for allografts or donor site nerves a quest for synthetic nerve guides has been sought for more than a century.

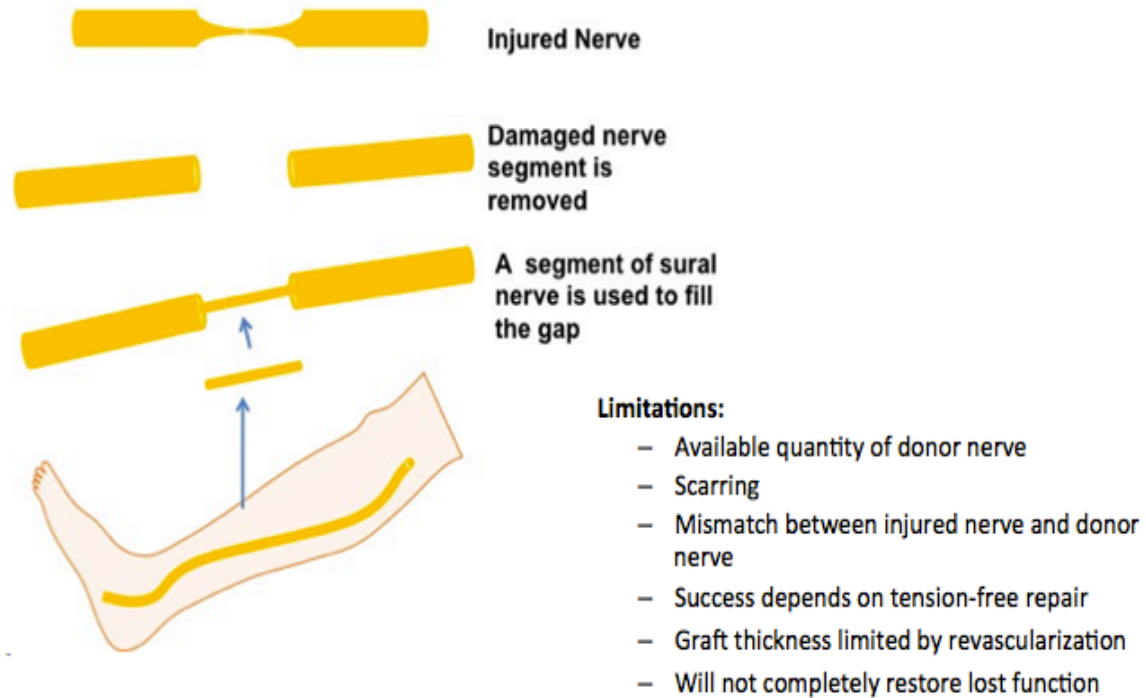


Figure 1.2: The “gold standard” for gap nerve repair. Schematic representation of a commonly used technique for nerve repairs if end-to-end repair is not possible. Mostly sural nerve is used as the donor nerve autograft in clinics.

1.2.2 Synthetic Nerve Guides

Tubular nerve guides were recognized as an alternative to autografts as they eliminate the need of morbidity of donor site, provide directionality in axonal growth, might increase the concentration of growth factors released from the support cells at the distal targets and have less chances of neuroma formation (42). Nerve guides were first proposed in 1880 by Gluck and Neuber who used a decalcified bone for nerve tissue repair using a dog sciatic nerve injury model(43). Subsequently, silicone was the first synthetic materials used as a nerve guide (NG) for repair of ulnar and median nerve in human patients(44). While partially effective, silicone tubes were discontinued in clinics because of complications that occurred due to compression injuries and fibrosis (34). Since then, a number of biodegradable materials have been demonstrated to be effective NGs for bridging gap injuries. Such materials include polylactic-co-e-copolactone, polyglycolide (PGA), polyvinyl alcohol and type I collagen. These biodegradable

NGs have been FDA approved and are commonly used for reconstruction of peripheral nerve injuries because of their convenient off-the-shelf availability. Even though, NGs has been successful in bridging short gaps, the functional recovery is not similar to autografts and hence various modifications to the internal structure of the NGs has been made and also luminal filler are evaluated for increasing neuronal growth. Extensive research is currently being done to make these simple conduits more effective for nerve repair. Those efforts include improving the porosity of the tube, adding luminal scaffold and molecular support.

Porosity of the biodegradable NGs is a vital feature for enhancing nerve regeneration through these tubes as it mediates early vascularization into the NG, better survival of the support cells inside the tube and oxygen/nutrient diffusion across the tube (35).

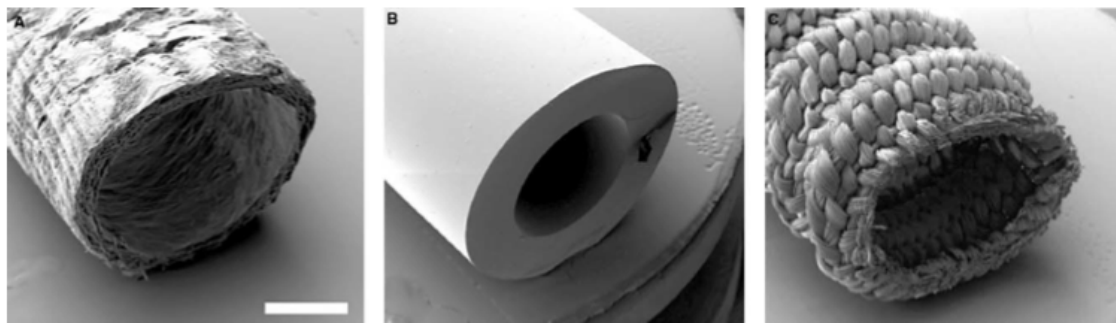


Figure 1.3: SEM images three FDA approved NGs. (A)NeuraGen (collagen);(B)Neurolac (poly lactide/caprolactone);(C)Neurotube (polyglycolide) (18)

Table 1.2: List of all the FDA approved NG (45)

PRODUCT	COMPANY	POLYMERIC MATERIAL
Neurotube	Synovis Micro Companies	Polyglycolic acid (PGA)
NeuroGen	Intergra life sciences	Type I Collagen
Neuroflex	Collagen Matrix	Type I Collagen
NeuroMatrix	Collagen Matrix	Type I Collagen
Neurolac	Polyganics Inc.	poly(DL-lactic-co-1-caprolactone) (PLCL)
Salubridge/Salutunnel	Salumedica LLC	Salubria—polyvinyl alcohol (PVA) hydrogel
AxoGuard Nerve Connector	Cook Biotech Products	Porcine small intestinal submucosa (SIS)

1.2.3 Luminal Fillers

Tubularization nerve repair methods depend on migration of fibroblasts and Schwann cells from the host proximal and distal nerve stumps into the lumen of the tubes to form a cellular scaffold supportive of neural regeneration (46). This process requires days to weeks, a time that if prolonged, encounters a decline in the ability of motoneurons to regenerate and the disappearance of the neuromuscular junctions(47). Adding autologous Schwann cells into the lumen of the conduits has a stimulatory effect on axonal regeneration(48-51), but requires harvesting and *in vitro* expanding the autologous Schwann cells. To obviate this need, some have suggested the use of multiple biodegradable fibers in the lumen of the tubes as a method to entice the regeneration of axons and non-neural cells(52, 53), while others have primarily focused in adding neural growth factors to the lumen of the tubes to enhance the regenerative response(54). This strategy is used to improve the efficacy of simple synthetic conduits and enhance nerve regeneration.

1.2.3.1 ECM proteins

In peripheral nerves, flattened, basal lamina-lined perineurial cells delineate the nerve fascicles, providing a barrier to movement of ionic compounds and macromolecules between non-neural tissues and the endoneurium. In the endoneurium fibroblasts and Schwann cells produce collagen (55). Collagen comprises of a family of proteins which share a triple helical structure in the form of an extended rod. This monomer structure is the result of a highly characteristic sequence of amino acids, with glycine in every 3rd position and a high density of proline and hydroxyproline. This structure contributes to the key functional property for structural collagens, namely aggregation into fibrils (56). Fibroblasts augment production of interstitial collagen both within a traumatized nerve segment and distal to it. This increases the tensile strength of the damaged nerve and provides the collagenous framework required for axonal regeneration (35). Collagen type IV is the principal component of basement membranes. This type of collagen has been used as nerve growth substrate as it has been shown to facilitate Schwann cell migration (36).

Neutralization of native acid soluble collagen generates a hydrogel scaffold within a few minutes by collagen fibrillogenesis. These gels represent very low density three dimensional (3D) lattices of collagen nano-fibrils (approx. 0.2 to 0.5% of wet weight) with no inherent orientation, containing a large excess (>98%) of fluid (57). This lattice also forms a substrate for cells through physical entrapment, producing a cell-seeded collagen gel scaffold. When a rectangular collagen lattice is tethered at its opposite ends the cell force generates a uniaxial strain in the gel along which cells and collagen fibrils become aligned. Such aligned, fibrillar/cellular collagen hydrogel implants have been used successfully to guide peripheral nerve repair *in vivo* (35, 36, 58).

Fibronectin is a disulfide-linked dimeric glycoprotein prominent in many extracellular matrices and present at about 300 µg/ml in plasma. Its interactions with collagen, heparin, fibrin and cell surface receptors of the integrin family are involved in many processes including cell adhesion,

morphology, migration, thrombosis and embryonic differentiation. Fibronectin is composed of tandem repeats of three distinct types (I, II and III) of individually folded modules (59). Functional fibrous fibronectin biomaterials take the form of mats or cables have been developed for use in the repair of peripheral nerves (35, 36, 60).

Laminin is the other ECM molecules that have been considered for peripheral nerve regeneration. It is a trimeric glycoprotein that has been found in the basement membranes of Schwann cells. It also is useful for Schwann cell differentiation, proliferation and migration as well as neurite outgrowth (36).

1.2.3.2 Cellular support

Schwann cells have a vital role in the restructuring and repair of peripheral nerve injuries. Schwann cells align along the fibrin matrix that is formed after a short gap injury and help in the formation of bands of Bungers (36). Hence, Schwann cells have been used to facilitate nerve regeneration inside synthetic NGs (61, 62). It has also been shown that genetically modified Schwann cells by transfection to expression CNTF can enhance peripheral nerve regeneration (63). Schwann cells also help in releasing trophic factors (NGF) and ECM molecules which assist in the repair process and myelination of the regenerating axons (64). Despite the advantages of using Schwann cells, there are some major limitations to this approach. Survival of transplanted Schwann cells is a challenge as well as the source of autologous cells. Hence, some researchers have used stem cells such as bone marrow stem cells (BMSCs) and mesenchymal stem cells (MSCs) (65, 66). This approach helps in increasing in nerve regeneration and the stem cells also transdifferentiated into Schwann cells *in vivo* (67). The stem cells also produced essential growth factors such as NGF, BDNF and CNTF which are essential for nerve growth.

1.2.3.3 Growth factors

An additional area of extensive investigation has been the incorporation of growth factors to the lumen of the nerve tubes to enhance the regenerative response including: nerve growth factor

(NGF), neurotrophin-3 (NT-3), glial cell-derived neurotrophic factor (GDNF), fibroblast growth factors (FGF), ciliary neurotrophic factor (CNTF), glial growth factor (GGF), vascular endothelial growth factor (VEGF), brain-derived neurotrophic factor (BDNF), leukemia inhibitory factor (LIF), insulin-like growth factor 1 (IGF-1), and platelet-derived growth factor (PDGF) (54, 68-74). Neurotrophins such as NGF, BDNF and NT-3, as well as GDNF a member of the transforming growth factor beta superfamily, are up-regulated in axotomized peripheral nerves, implying an important role of these molecules in axonal regeneration(54). It has been shown that NGF, BDNF and NT-3 are able to increase axonal regeneration both *in vitro* and *in vivo*(75-82). The stimulatory effect of neurotrophins is mediated through specific tyrosine receptor kinases (trk) and p75 receptors, and we have recently shown that activation of the intracellular signaling cascade mediated by the trk receptors through activation of the extracellularly regulated kinase (Erk1/2), endows peripheral neurons with enhanced regenerative capacity(83). However, when applied to the transected peripheral nerve, the beneficial effect of these growth factors is less clear. While some have observed functional regeneration by adding GDNF(84-86), others report lack of functional regeneration after BDNF or GDNF administration(87, 88). The reasons behind these contradictory results are unknown, but it might be related to differences in growth factors, specific concentration use, and/or differences in delivery methods.

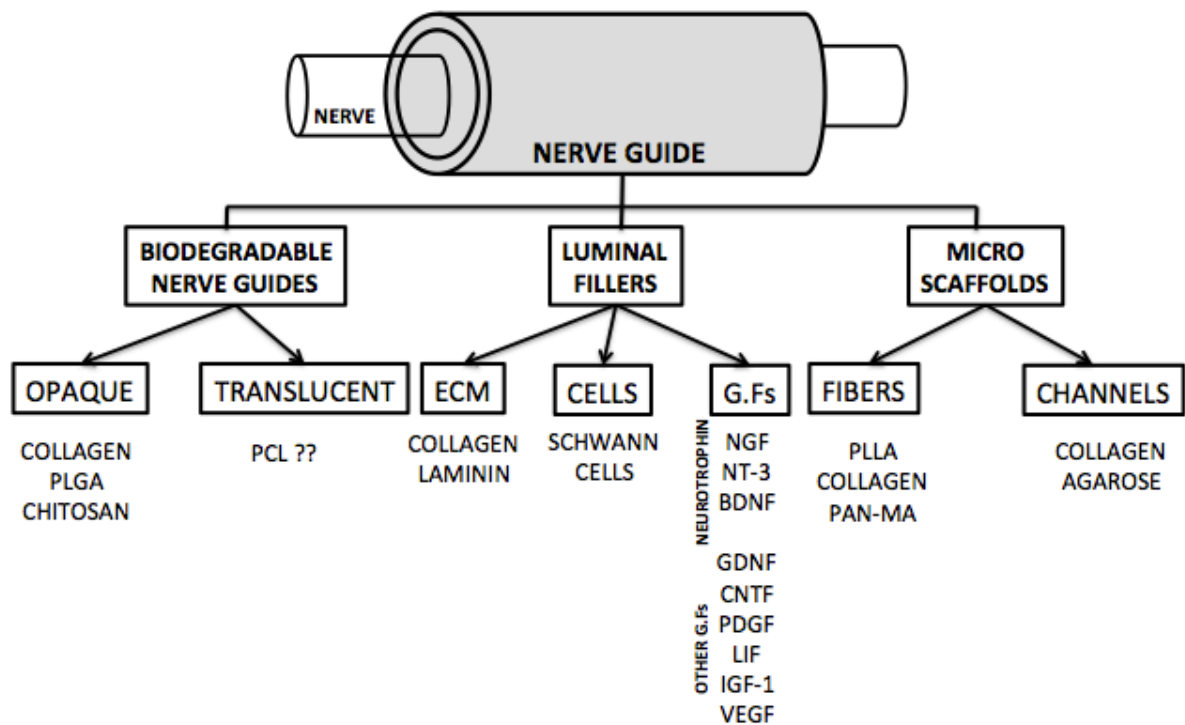


Figure 1.4: Summary of various approaches taken in basic science research to repair gap nerve injuries

1.2.4 Modified Scaffolds

Nerve regeneration using NGs have been limited to repair of short gaps and are still inferior to the gold standard autograft. Hence, emphasis has been on guiding the supporting cells and regenerating axons to their distal targets using topographical methods. Recently, it has been reported that polymeric microfibers and intraluminal microchannels assist in directed growth of axons (36, 89-92). Various approaches have been taken to modify the inner structure of the NGs to aid in robust and guided regeneration, but it can be broadly categorized into two distinct approaches, i.e. the microfibers/microfilaments and the multiluminal microchannels.

1.2.4.1 Microfibers

Different fillers such as polyamide filaments, collagen filaments, polyester filaments, Matrigel supplemented with PLA wet-spun fibers, PGA filaments and gelatin fibers have been investigated (52, 53, 89, 93-96). Cai et al showed that PLLA microfilaments inside a tube can

assist in enhancing nerve regeneration and maturation (89). Similarly, in a work reported later, it was shown that aligned fibers inside a NG could help in better Schwann cell scaffolding and hence better regeneration (90). Furthermore, the same group showed that by making sheets out of these aligned fibers also help increase regeneration (96). These approaches have shown promising results, however depending on the packing density and filament diameter, axonal regeneration might be compromised.

1.2.4.2 Microchannels

In 2000, Hadlock et al first reported the use of microchannels inside the NGs for bridging a short gap of 7mm in a rat sciatic nerve. The microchannels and the tubular construct were made of poly(lactide-co-glycolide) (PLGA). The micro architecture inside the tubes mimicked the native structure of peripheral nerves. They also reported that Schwann cell adherence was five times higher in the multiluminal tubes as compared to simple hollow tubes. However in another study, it was mentioned that the PLGA microchannels collapsed because of swelling(97, 98). Yao et al in 2010 showed that multiluminal channel inside a NG helps in controlling dispersion during axonal regeneration (91).

Our lab at UT Arlington reported the use of a multiluminal NG for repair of short gaps in a rat sciatic nerve model (92). The NG was composed of a transparent polyurethane tube and the microchannel were made out of agarose and filled with collagen and named biosynthetic nerve implant (BNI). The microfiber and the microchannel approach are to provide guidance and direction to the regenerating axons and hence enhance regeneration and function, but using the microchannels is more beneficial as it provides more surface area for axonal growth as compared to the microfibers which essentially block most of the area inside the tube and impede neuronal regeneration.

Summarizing all the approaches employed for peripheral nerve reconstruction, the bulk of studies described above have been done in a gap shorter than 20 mm which is not considered a critical gap according to the clinics. There was a single study in 2000 that reported

the repair of 80 mm gap injury in a dog peroneal nerve using laminin coated collagen microfibers inside the tube. The authors measured some nerve conduction after 3 months but no functional recovery was observed and this study has not been repeated (99). In contrast to short gap injuries (i.e., 0.5mm in mice, 10mm in rats and 20 mm in rabbits, dogs and humans), isografts achieve minimal functional recovery in longer gaps (i.e., 0.7 mm in mice, 12-20 mm in rats and ≥ 30 mm in rabbits, dogs, and humans). In fact, while clinical repair of gaps shorter than 20mm is routinely achieved using allografts, synthetic tubes, luminal cells, and/or growth factors, clinical reconstruction of motor nerve defects using NGs of ≥ 30 mm have not been achieved(100). Indeed, many of the strategies that have been found effective in mediating nerve regeneration across short nerve gaps, fail to mediate nerve repair in longer gap defects including acellular allografts(101), and luminal seeding of Schwann cells give equivocal results(101, 102). One of the major reasons for failure of long gap regeneration could be due to the lack of evident chemotaxis cues from the distal target and hence the proximal stump does not get adequate signal to regenerate towards the distal targets. The regenerative failure of peripheral nerves through long-gaps seems to be due, at least in part, to the lack of appropriate haptotaxis and chemotaxis cues such as linear growth substrate and trophic support respectively(100, 103-105). The table below represents some of the major peripheral nerve regeneration studies listing the type of polymeric nerve conduit used, the effective gap attempted to bridge and the luminal fillers.

Table 1.3: Tubularization repair of short and long (≥ 3 cm) nerve defects. * = Biodegradable

DEFECT LENGTH (cm)	TUBE MATERIAL	LUMINAL FILLER	GROWTH FACTORS	CLINICAL/ ANIMALS	AUTHORS
1.5-6	ePTFE	N	N	Human	Stanec and Stanec, 1998
2-5	Silicon	N	N	Human	Braga-Silva, 1999
1-3	PGA*	N	N	Human	Navissano, Malan et al.

					2005
2	Collagen*	N	N	Human	Ashley, Weatherly et al. 2006
2-4	PGA*	N	N	Human	Rosson, Williams et al. 2009
2	PGA*	N	N	Primate	Mackinnon and Dellon 1990
1.5	Collagen*	N	N	Primate	Archibald, Shefner et al. 1995
1	Silicone	Matrigel	VEGF	Rat	Hobson et al, 2000
1.5	EVA	N	NGF, GDNF	Rat	Fine, Valentini et al. 1991
1	PHEMA-MAA*	Collagen	NT3, BDNF	Rat	Mdha et al, 2003
1-1.8	Silicone	PLLA filaments	N	Rat	Ngo, Waggoner et al. 2003
1	Chitosan*	Laminin-1	GDNF	Rat	Patel et al, 2007
1	Silicone	N	FGF-2	Rat	Haastert et al., 2009
1	Polyurethane	Multiluminal Collagen	N	Rat	Tansey et al., 2011
1.5	CUPE*	Multiluminal Collagen	N	Rat	Dash et al., under review
3	Polyurethane	Multiluminal Collagen	PTN, VEGF	Rabbit	Dash et al., under review

1.3 Multiluminal Biosynthetic Nerve Implant (BNI) Approach

Attempts to increase the regenerative area and to direct axonal growth in peripheral nerve gap repair have included the deployment of luminal filaments or multiluminal conduits (100, 106).

We recently developed simple and reproducible method for the fabrication of multiluminal BNIs(Figure 1.5). In our design, multiple microchannels are made of 1.5% agarose inside a simple polyurethane tube and simultaneously filled with intraluminal collagen matrix to facilitate axon regeneration into, and through the microchannels (Figure 1.5 c, d). While the collagen provides a permissive intraluminal milieu within the microchannels to entice linear nerve growth, the agarose-made channels restrict the wandering of axons and prevent axonal crossing between them.

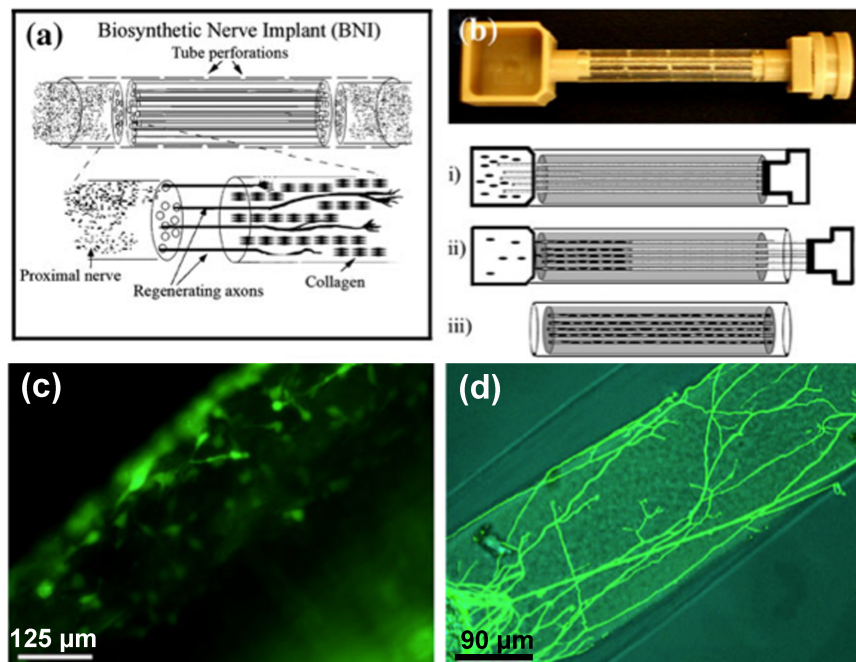
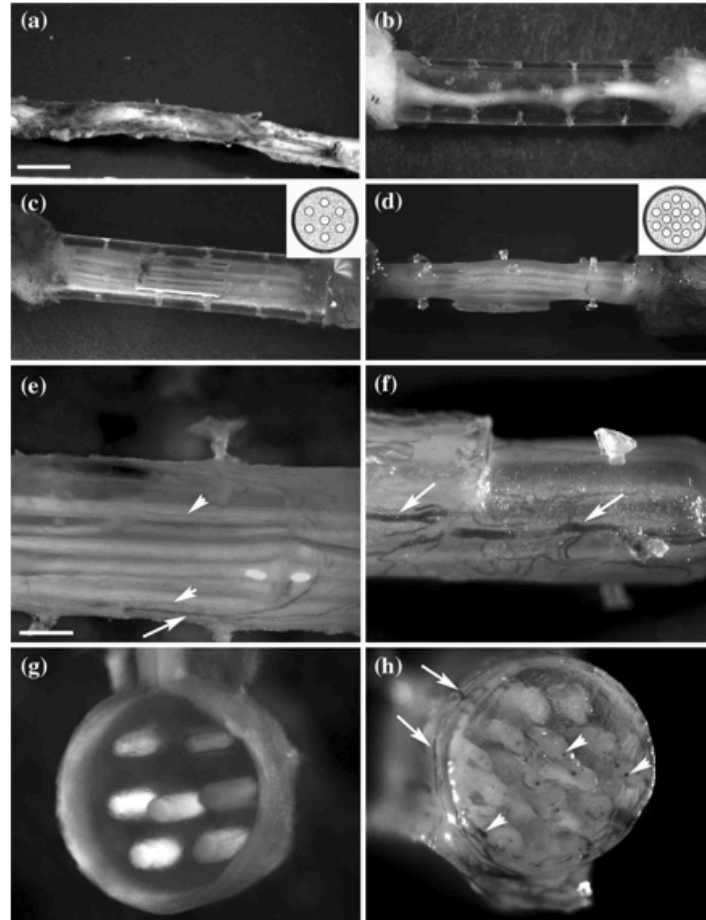


Figure 1.5:(A) Schematic of the Biosynthetic Nerve Implant (BNI), (B) BNI fabrication method representation (i) insertion of a brush with metal fibers, (ii) the agarose inside the tube polymerizes and collagen is loaded in the well and (iii) the fibers are removed slowly and negative pressure in the microchannels help in uniform loading of the collagen, (C) Alignment of GFP+ Schwann cells and (D) growth of DRG axons inside the microchannels *in vitro* (92).

This method allows the migration of Schwann cells and axonal growth (Figure 1.5 c, d), and when compared to simple tubularization repair across a 10mm rat sciatic nerve gap injury, the BNI induced fascicular- like regeneration and mediated an increase in number of myelinated axons that regenerated compared to those that were implanted with collagen filled single-lumen tube (Figure 1.6)(92).The limitation to this study is the fact that we used non-biodegradable

external tubing made of polyurethane. This approach is not amenable for clinical translation.

The other challenge is to bridge a longer and a critical gap frequently reported in clinics.



1.4 Hypothesis

The hypothesis of this dissertation is to design an advanced nerve implant with optimum growth area, biodegradable construct and effective growth factor delivery system for peripheral nerve regeneration across long critical gaps and recovery of function.

1.5 Specific Aims

Specific Aim 1: The initial aim is to improve the regeneration across the previous reported biosynthetic nerve implant by increasing the growth surface area of the multiluminal channels.

Specific Aim 2: The second aim is to test the efficacy of PTN/VEGF as potent growth factors for long gap peripheral nerve repair (a preliminary study)

Specific Aim 3: The third and major focus of this dissertation is to effectively bridge a 30 mm long gap nerve injury using a multiluminal NG loaded with nanoparticles eluding growth factors. The objective of this work is to regain motor and sensory function after traumatic peripheral nerve injury.

Specific Aim 4: The final aim is to test whether biodegradable NGs made from crosslinked urethane doped polyester elastomer (CUPE) are ideal for efficient evaluation of luminal filler prior to implantation and bridging gap injuries (107, 108).

There were two types of BNIs used in the previous explained study, i.e. one with 7 channels and the other with 14 channels. The 5 channels BNI has only 5% of the total tube's area for tissue growth and the rest was agarose while the 14 channel BNI had 34% growth area. The initial task was to maximize the growth area and hence we designed a BNI with 8 microchannels and minimal agarose. The area for growth in this BNI was 74% of the total tube area (Figure 1.7). This BNI was used for all the studies in this dissertation.

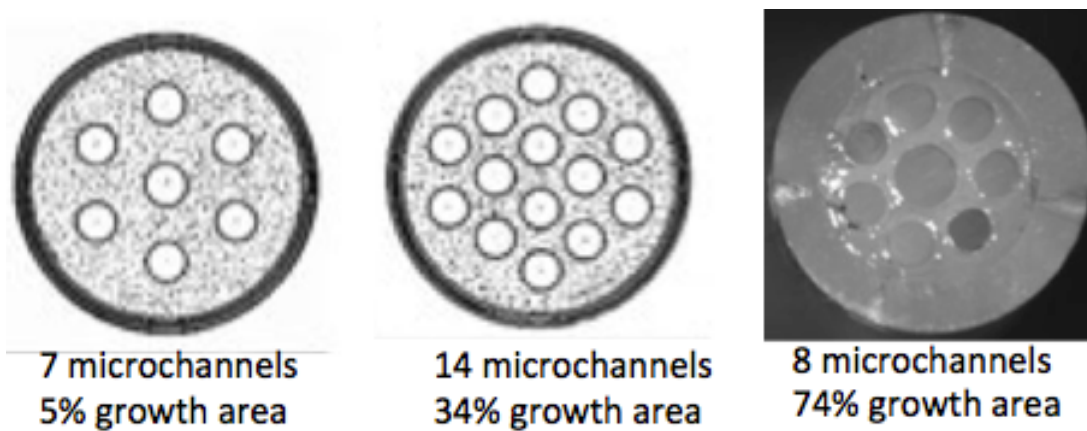


Figure 1.7: Cross-sectional representation of all three versions of the BNI. (A) 7 channel BNI with 5% growth area, (B) 14 channel BNI with 34% growth area and (C) the next generation 8 channel BNI with 74% growth area

CHAPTER 2

PLEIOTROPHIN SUPPORT IN LONG GAP PERIPHERAL NERVE REPAIR

Peripheral nerve injury gaps resulting from tissue loss after trauma or tumor resection are routinely repaired by autogenous nerve grafts. To avoid the morbidity associated with this procedure, several FDA-approved biodegradable hollow tubes (i.e., polylactic-co-e-caprolactone, polyglycolide, collagen) are currently use for the repair of short nerve gaps. However, nerve regeneration across gaps longer than 25mm often fail completely when repaired using hollow tubular scaffolds. The critical nature of such gaps seems to be due to lack of endoneural structural support and excessive dilution of endogenous growth factors. We recently developed a biosynthetic nerve implants (BNI) with linearly arranged agarose microchannels with luminal collagen that can successfully repair short nerve gaps. Based on the fact that peripheral nerve regeneration involves a complex cellular response, here we hypothesize that a broad growth factor support is necessary for successful nerve regeneration across long-gap nerve defects. Using a 30mm nerve gap in the injured rabbit common peroneal nerve, we tested the effect of vascular endothelial growth factor (VEGF) and Pleiotrophin (PTN) growth factor supplementation of the multiluminal BNI. Histological evaluation ten weeks post implantation revealed that nerve defects repaired with simple tubes failed to regenerate across the long gap, while those bridged with collagen-filled BNIs showed vascularized fascicle-like nerve regeneration through the micro-channels. The number of neurofilament-positive axons within the microchannels increased significantly in the BNIs supplemented with VEGF or PTN. Congruently, nerve conduction and functional recovery was significantly increased with growth factor support. Our study indicates that broad cellular trophic supplementation within anendoneural structured nerve guide entices nerve regeneration across critically long nerve gap defects.

2.1 Introduction

Peripheral nerve injury gaps resulting from tissue loss after trauma or tumor resection are routinely repaired by autologous nerve grafts. To avoid the morbidity associated with this procedure, several FDA-approved biodegradable hollow tubes (i.e., polylactic-co-e-caprolactone, polyglycolide, collagen) are currently used for the repair of short nerve gaps. However, nerve regeneration across gaps longer than 25mm often fail completely when repaired using hollow tubular scaffolds(35). In order to improve the efficacy of simple synthetic conduits and enhance nerve regeneration, several groups have proposed the use of luminal fillers(109), bioabsorbable filaments (52, 110), multi-luminal conduits (92, 100, 106), and electrical stimulation of the proximal stump (111). These strategies have resulted in promising but modest improvements on nerve regeneration and functional recovery (112, 113). We recently demonstrated that linearly restricting the regeneration pathway within a biosynthetic nerve implant (BNI) through multiple longitudinally oriented collagen-filled microchannels, the regenerative process and the recovery of function could be enhanced over a short (i.e., 10 mm) nerve gap defect (92). However, our preliminary data in the use of the BNI to repair critically long gap injuries, also suggest that linear scaffolding, while helpful in directing axonal growth, it may not be sufficient to entice nerve regeneration across critically long gaps.

It has been shown that Schwann cells in the distal nerve stump secrete a number of growth factors including neurotrophins such as NGF, BDNF, and NT-3, as well as GDNF a member of the transforming growth factor beta super family (6, 54, 114). Indeed, adding prolonged release of NGF and GDNF to simple nerve guides has been shown to increase axonal regeneration across a 13-15 mm gap in a rat model (82, 115-117). However, the beneficial effect of these growthfactors have been controversial. While some have observed functional regeneration by adding GDNF(84, 85)others have not seen a superlative functional regeneration after BDNF or GDNF administration (32). The reason behind these contradictory

results is unknown, but it might be related to differences in growth factor concentration and delivery methods.

Table 2.1: Growth factors used in peripheral nerve regeneration and their targets (118)

Growth factor	Major target*	Reference
NGF: nerve growth factor	Sensory neurons, small axons	<i>Lee et al. (2006)</i>
NT-3: neurotrophin 3	Sensory neurons, small- and medium-size axons	<i>Midha et al. (2003)</i>
BDNF: brain-derived neurotrophic factor	Sensory neurons, large axons	<i>Terris et al. (2001)</i>
GDNF: glial-derived neurotrophic factor	Motor neurons	<i>Barras et al. (2002)</i>
FGF-1: fibroblast growth factor 1 (acidic fibroblast growth factor)	Vascular endothelial cells	<i>Cordeiro et al. (1989)</i>
FGF-2: fibroblast growth factor 2 (basic fibroblast growth factor)		<i>Ohta et al. (2004)</i>
GGF: glial growth factor	Schwann cells	<i>Mohanna et al. (2005)</i>
PDGF: platelet-derived growth factor	Schwann cells	<i>Wells et al. (1997)</i>
CNTF: ciliary neurotrophic factor	Schwann cells (injury factor)	<i>Ho et al. (1998)</i>
VEGF: vascular endothelial growth factor	Vascular endothelial cells	<i>Hobson (2002)</i>
IGF-1: insulin-like growth factor I	Inflammatory cells (anti-inflammatory)	<i>Fansa et al. (2002)</i>
LIF: leukemia inhibitory factor	Neurons (injury factor)	<i>McKay Hart et al. (2003)</i>

*Many growth factors are pleiotropic and act on a variety of cells. Here, however, we indicated only the putatively most important targets for peripheral nerve regeneration.

Peripheral nerve regeneration involves a complex combination of nerve growth, fibroblast proliferation and differentiation and blood vessel growth. In fact, nerve regeneration requires a complex interplay between cells, extracellular matrix, and growth factors. Several growth factors such as insulin-like growth factor (IGF-1), basic fibroblast growth factors (FGF1 and 2), vascular endothelial growth factor (VEGF) and pleiotrophin (PTN), have trophic effects on multiple cell types. When applied to peripheral nerve regeneration IGF-1 has been shown to promote nerve elongation, muscle cell proliferation and angiogenesis in regenerating skeletal muscle(119, 120). Fibroblast growth factors (FGFs) are mitogenic for endothelial cells, fibroblasts, and Schwann cells, and both FGF-1 and FGF-2 provide support for peripheral nerve regeneration(50, 80, 121).

Pleiotrophins such as VEGF and PTN have been used in nerve repair across 10-13mm gaps because of their role in neuroprotection (122-124). PTN has been shown to convey neurotrophic support for motor neurons (124). VEGF is a known angiogenic factor that binds to VEGFR-1, VEGFR-2, VEGFR-3, receptors and neuropilin-1 (NRP1) and neuropilin-2 (NRP2) co-

receptors, some of which are expressed in the injured peripheral nerves (125) and have demonstrated nerve regeneration functions (126). In addition to the neurotrophic role of PTN, they have mitogenic effect on the supporting cells such as Schwann cells, macrophages, fibroblast and endothelial cells which are essential for the reconstruction nerve tissue after injury(127-129). Also, VEGF would provide adequate migration of vasculature into the scaffold for efficient nerve regeneration along with its neurotrophic properties.

Here we hypothesize that the broad cellular effect of PTN and VEGF in attracting multiple cells in the injured peripheral nerves, if provided in the lumen of a multiluminal scaffold, would entice axonal regeneration across a critically long gap and mediate functional recovery. In this chapter I describe the experiments designed to evaluate whether delivering PTN and VEGF in a multiluminal biosynthetic nerve implant (BNI) would enhance axonal regeneration across long gaps and regain motor and sensory function. Using a 30 mm injured common peroneal nerve gap model in rabbits we demonstrated the importance of the luminal physical guidance for long-gap nerve repair and the significant increase in nerve regeneration and functional recovery by supplementing it with pleiotrophic growth factor support. Specifically, in sharp contrast to the total failure in nerve repair observed with collagen-filled tubes, those with multiple linear microchannels filled with collagen and particularly those supplemented with VEGF or PTN showed robust nerve regeneration across the long critical gap. The successful nerve repair was indicated by numerous neurofilament-positive axons observed within the regenerated microfascicles, and the recovery of compound muscle action potentials, as well as motor and sensory function. Our study indicates that designed linear microenvironments supplemented with pleiotrophic factors effectively stimulate nerve regeneration across long-gap peripheral nerve defects.

2.2 Materials and Methods

2.2.1 Animals

Forty-one New Zealand white rabbits (Myrtle Rabbitry, TN) of 1.5-1.8 kilograms were used in this study. The animals were divided into five experimental groups for nerve repair: 1) simple tube filled with collagen, 2) BNI with luminal collagen, and BNI with luminal collagen supplemented with either 3) PTN, 4) VEGF or 5) PTN/VEGF combination (Table 2.2). The animals were also divided in two separate time groups: a small cohort was evaluated at 6 weeks (n=8) and a second analyzed for 10 weeks after implantation (n=33).

2.2.2 BNI Nerve guides with multiluminal pleiotrophin support

The nerve conduits consisted in a transparent polyurethane tube (Micro-Renathane®; Braintree Scientific, Inc; OD 3 mm, ID 1.75 mm, and length of 30 mm) filled with atelomeric chicken collagen (85 % type I, 15 % type II; Millipore). As previously reported, the BNI mediates fascicular-like growth after peripheral nerve gap repair by directing the growth of the regenerating axons through multiple agarose microchannels filled with collagen. The BNIs were reproducibly prepared by a casting device that aligns metal fibers (250 and 350 μm) was inserted through the tubes. A 1.5% agarose solution was then injected in to the tube, filling the lumen and allowed to polymerize. Before removing the fibers from the agarose either a suspension of recombinant VEGF or PTN mixed with collagen (2.5 $\mu\text{g}/\text{ml}$), or a suspension of PLGA nanoparticles with the encapsulated growth factors were placed into a well of the BNI casting device and loaded into the microchannels by the negative pressure formed in after removal of the embedded fibers as previously reported (Figure 2.2)(130). Approximately a 0.5 mg of nanoparticles containing 92ng of VEGF and PTN was added in each BNI. According to our release study, it can be estimated that 46 ng of the growth factor was released during the first 24 hr and the rest gradually released during the 3 months. This amount falls within the physiological range (10-100ng/ml) of PTN and VEGF(124, 126). In order to test whether a combination of VEGF and PTN would elicit a synergistic effect we decide to have a group with

half the concentration of each of these growth factors in order to maintain the same amount of nanoparticles in the microchannels.

2.2.3 BNI Nerve Repair

The rabbits were anaesthetized with ketamine (35mg/kg) / xylazine (5mg/kg) intramuscular injection, and maintained under 1-3% isoflurane and oxygen. The hind limb was shaved and disinfected with ethanol and betadine and the animal placed on a heating pad to maintain at 37°C. The left peroneal nerve was exposed by spreading the abductor cruris cranialis muscle and the biceps femoris muscle of the left thigh. The peroneal nerve bisected and the BNI was placed in between the two ends. The BNI was tied to the underlying muscle using a 3-0 chromic gut suture and the nerve ends were inserted 1mm inside the tube and secured by 9-0 monofilament suture. Using a 3-0 suture, the muscles closed followed by stapling the skin. Triple antibiotic ointment and bandages were applied to the wound (Figure 2.5). The animals were given 40 mg of sulfamethoxazole, 8 mg of trimethoprim orally and 1 mg of buprenorphine subcutaneously daily for a week after surgery. The animals were maintained under conditions of controlled light and temperature with food and water ad libitum.

At the end of the experimental phase, the animals were euthanized with sodium pentobarbital, 120 mg/kg, intravenously and perfused transcardially with 0.9% normal saline, followed by pre cooled 4% Paraformaldehyde (PFA). The control non-injured nerves and the BNI repair common peroneal nerves were dissected and post fixed in 4% PFA. The study had a double blind design (i.e., the surgeon was blind to the type of implant, and evaluators were blind to treatment as the animals were randomized for further testing and coded after the surgery). All procedures were in accordance with the Institutional Animal Care and Use Committee (IACUC) at the University of Texas at Arlington.

2.2.4 Nanoparticle fabrication

Poly (lactide-co-glycolide) acid (PLGA) micro spheres were synthesized using the double emulsion evaporation method as reported elsewhere (131). Briefly, PLGA (Lakeshore

Biomaterials, Birmingham, AL) was dissolved in dichloromethane (DCM; Sigma-Aldrich, St. Louis, MO) at a concentration of 200 mg/ml; mixed with aqueous solutions of BSA (10 μ g/ml; Sigma-Aldrich, St. Louis, MO), PTN (10 μ g/ml; PeproTech Inc., Rocky Hill, NJ) and VEGF (10 μ g/ml; Invitrogen, Carlsbad, CA) and sonicated. After DCM evaporation and centrifugation, the particles were suspended in PBS and freeze dried. The particles were characterized by Scanning Electron Microscopy (Hitachi S-3000N Variable Pressure SEM; Fig. 2.1 A, B); the particle size distribution was measured with a Zeta Potential particle size analyzer, and the release profile determined by protein assay and ELISA (Fig. 2.1 C, D). Drug release kinetics determined by protein content using via 540nm spectrophotometry and PTN and VEGF ELISA quantification (Invitrogen, Carlsbad, CA), confirmed low-burst and sustained release profile over several weeks(Figure 2.1).

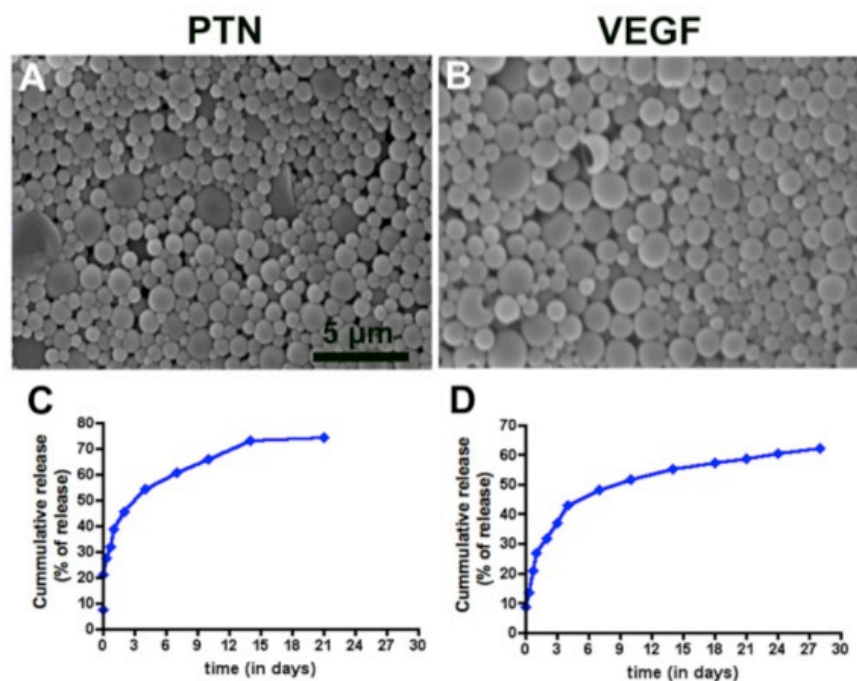


Figure 2.1: Nanoparticle morphology and release study. Scanning electron microscope images of PLGA nanoparticles loaded with (A) PTN and (B) VEGF [scale: 5 μ m]. The cumulative release of (C) PTN and (D) VEGF from the nanoparticles over a period of 21-28 days.

2.2.5 Bioactivity evaluation of nanoparticle encapsulation of PTN and VEGF

PTN: To examine the biological activity of the PTN nanoparticles, we added the nanoparticles directly to dissociated spinal cord neurons isolated from the murine ventral spinal cord at post-natal day 3. The neurons were cultured in Neurobasal medium supplemented with L-glutamine (Gibco Invitrogen), B-27, and penicillin/streptomycin (Gibco Invitrogen, Carlsbad, CA). BSA (control) or PTN nanoparticles were added to the cultures 24hrs after seeding. Five days after adding either BSA or PTN nanoparticles, the cultures were fixed with 4% PFA. The cells were then immunostained for b-tubulin for quantification of the cell soma size and axon length. The quantification of axons length was performed using the Image J and statistical analysis was done using students t-test (Figure 2.3).

VEGF: As previously reported, VEGF PLGA nanoparticles mixed and suspended in collagen, once loaded into the lumen of the multi-channel hydrogels significantly increased the proliferation of the endothelial cells seeded compared to those with BSA nanoparticle controls from the aortic explants (Figure 2.4) (130).

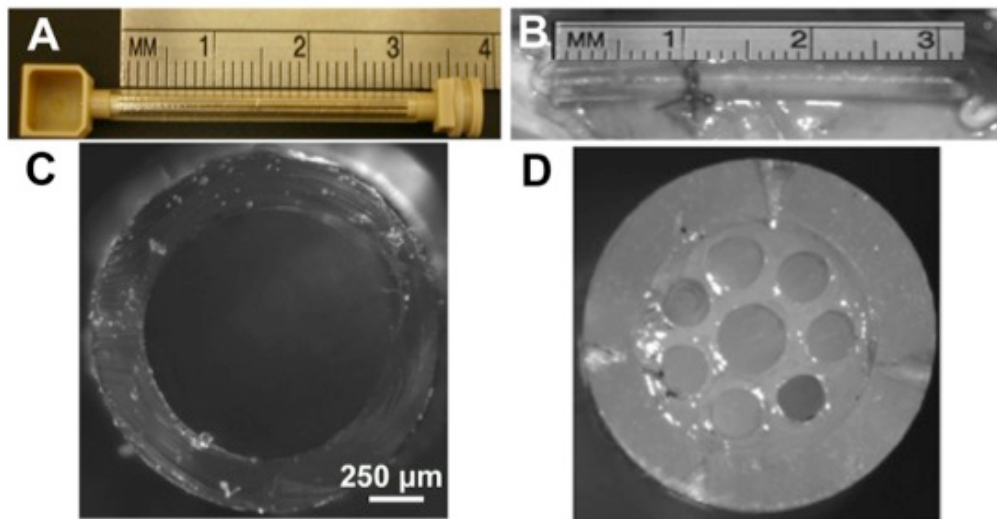


Figure 2.2: (A) The 3cm BNI casting device along with the loading well for collagen and nanoparticle on one side and the brush on the other side, (B) An implanted 3cm BNI between a transected peroneal nerve in the rabbit; the implant is securely held by tying it to the underlying muscle. Image of a (C) simple tube filled with collagen and (D) a BNI with collagen filled microchannels.

2.2.6 Immunocytochemistry

Culture cells were washed 3 times in PBS, permeabilized in 0.5% triton-X and incubated in 4% normal goat serum in 0.5% triton-X to reduce non-specific binding. Neuronal cell bodies and the axons were labeled mouse anti- β -tubulin (1:500; Sigma, St. Louis, MO). Cy3 Goat anti-Mouse, (1:400, R & D Systems) was used to visualize the labeled cell bodies and axons. The immunofluorescence staining was then evaluated using a confocal microscope at 20X magnification (Carl Zeiss LSM 510). Quantification metrics included total axonal length and average cell body surface area.

Tissue sections: The BNIs were carefully cleaned and the outer micro-renathane tubing was cut away. The nerve sample was then blocked into proximal, middle and distal. The tissues were the dehydrated alcohol and embedded in paraffin. The tissue was then cut into 10 μm slices using a microtome. The tissue was dried and deparaffinized in xylene. The tissues were stained overnight at 4 C with primary antibodies mouse anti-neurofilament protein (1:200, Sigma) for labeling axons and chicken anti P0 (1:200, Millipore) as a marker for myelin. After three washes with 0.5% triton X solution, the secondary antibodies, goat anti-mouse Cy2 and goat anti chicken Cy3 (1:400, Jacksonimmuno research) were used for 1hour at room temperature and the glass slides were further washed three times with 1X PBS. Samples were coverslipped and stored at 4°C for evaluation. The staining was evaluated using confocal microscopy (Carl Zeiss LSM 510 Meta).

2.2.7 Myelinated axon quantification

The confocal images were taken using a 63X oil objective. 4-6 images were captured for each sample and myelinated axons were manually quantified by counting the number of complete P0 positive circles (red) over NFP+ axons (green) in a 100 μm^2 area. The total area of the distal stump of the peroneal nerve is measured using Image J pixel intensity quantification based on a known surface area. These numbers were used to extrapolate the total axonal count on the

distal stump. The plotted graph indicates the total number of myelinated axons on the distal stump.

2.2.8 Electrophysiology

The peroneal nerve was exposed; the nerve was separated from the fascia and warm mineral oil added to insulate the nerve from the surrounding tissue. Needle electrodes were used to stimulate the proximal part of the implant. According to published methods, a CadwellCascade™ system was used to evoke three pulses of 50µs duration were applied with increasing amplitudes from 2 to 6 volts(132). The compound muscle action potential (CMAP) was recorded from the tibialis anterior muscle by placing the active electrode under the fascia of the muscle (Figure 2.9, 2.10).

2.2.9 Behavioral function Recovery

Toe spread index (motor): Toe spread Index (TSI) was done evaluate functional recovery after peripheral nerve injury. The toe spread measurements were taken every week starting 3rd week of nerve injury. The animals were held by the scruff of their neck and suddenly lowered in order to measure the distance between their first and fourth toe created by the startle response. The toe nails were painted with different colors in order to facilitate the measurements.

Formalin (sensory): In rodents, sensory testing after nerve injury routinely uses 5% formalin injected subcutaneous on the dorsal side of the injured foot (133). However, no sensory test for peripheral nerve injury has been previously reported for rabbits. Given that the common peroneal nerve has well defined dermatomes (134), we reasoned that the formalin test would be also effective in evaluating sensory function in the rabbit foot after 5 and 7 weeks post implantation of the BNI. We delivered formalin subdermally at different concentrations to test the effectiveness of this test. The concentration of formalin used in a trial test was 1, 5 and 10% on three uninjured rabbits. 10% formalin injection resulted in eliciting pain and the animals licked the site of injection while 1% and 5% did not result in licking of these animals. Hence, the formalin test in the rabbits consisted of a 0.1 ml subcutaneous injection of 10% formalin on the

dorsal part of the injured foot between the two inner most toes, at 1 cm from the foot edge. The animals were then videotaped for 10minutes after formalin injection and the number of licks was counted.

2.2.10 Statistical analysis

GraphPad Prism software was used to perform all the statistical analysis. All the data are represented as the average \pm standard deviation unless otherwise mentioned. One-way ANOVA with post hoc Neuman-Keuls multiple comparison tests was performed to analyze statistical difference. When $p < 0.05$, the difference between groups was considered significant.

2.3 Results

2.3.1 Sustained release of biologically active VEGF or PTN within agarose microchannels

Particle size analysis confirmed that 50-70% of the particles were smaller than 500 nm. The ELISA quantification of both VEGF and PTN release shows an initial burst release of protein within the first 24 hrs. By day 5 about 40-55 % of the growth factor was released followed by 50-70 % of the release after the first month. The biological activity of PTN was confirmed in dissociated spinal cord neurons. The average axon length of motor neurons was $210 \pm 78 \mu\text{m}$ when treated with PTN nanoparticles, whereas it was $56 \pm 21 \mu\text{m}$ in BSA controls. Hence, PTN nanoparticles significantly enticed longer axons compared to those exposed to BSA-releasing nanoparticles. In addition to the noted effect of PTN on the total axonal length, the average surface area of the cell bodies in the PTN treated cultures was also significantly higher compared to those in BSA treated cultures. The average cell soma area in the BSA controls was $45 \pm 21 \mu\text{m}^2$ whereas in the PTN treated groups it was $307 \pm 74 \mu\text{m}^2$ (Figure 2.3).

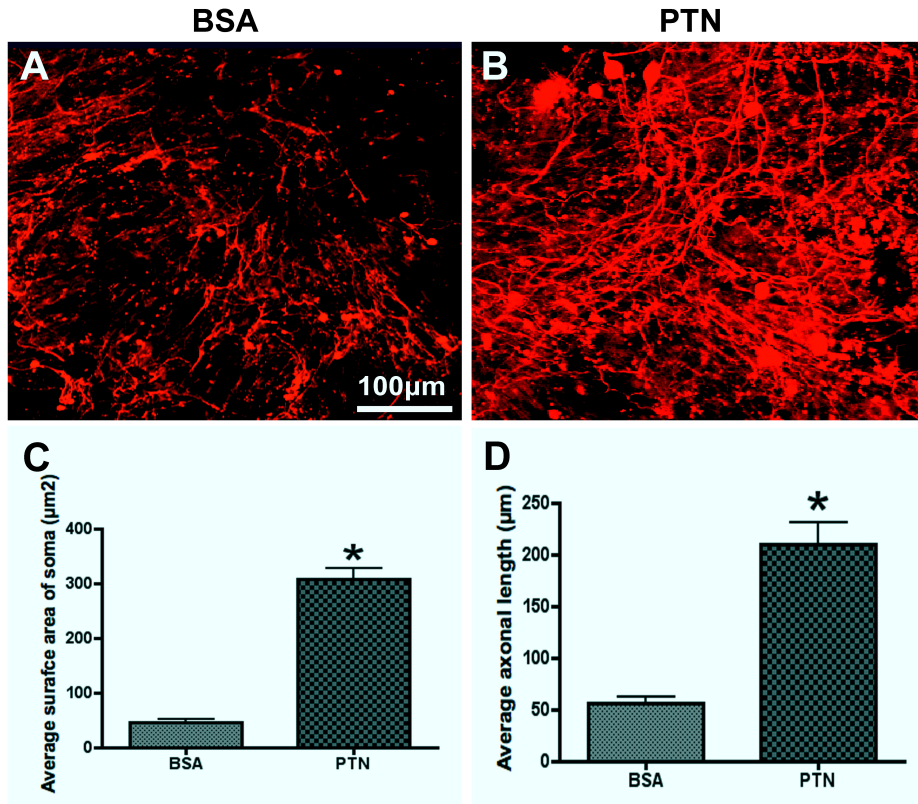


Figure 2.3: Bioactivity of PTN microparticles. Ventral motor neuron cultures treated with (A) BSA and (B) PTN nanoparticles and labeled with anti-β tubulin antibody. Quantification of (C) surface area of motor neurons and (D) average axonal length when treated with PTN and BSA nanoparticles after five days in culture. This is a significant increase in the size of the cell soma as well as the axonal length in the PTN treated cultures (n=4 cultures per group; *, p < 0.005).

As previously reported (130), encapsulated VEGF in PLGA nanoparticles suspended in collagen and loaded in the agarose microchannels induced prolonged trophic effect from adult aortic explants, with endothelial cell migration and proliferation extending for up to two weeks (Figure 2.4). While VEGF-supplemented P4-6 aortic explants showed a substantial number of cells inside the microchannels (390 ± 57 ; $n = 19$), those lacking growth factor support recruited significantly fewer cells (212 ± 48 ; $n = 10$). (Figure 2.4)

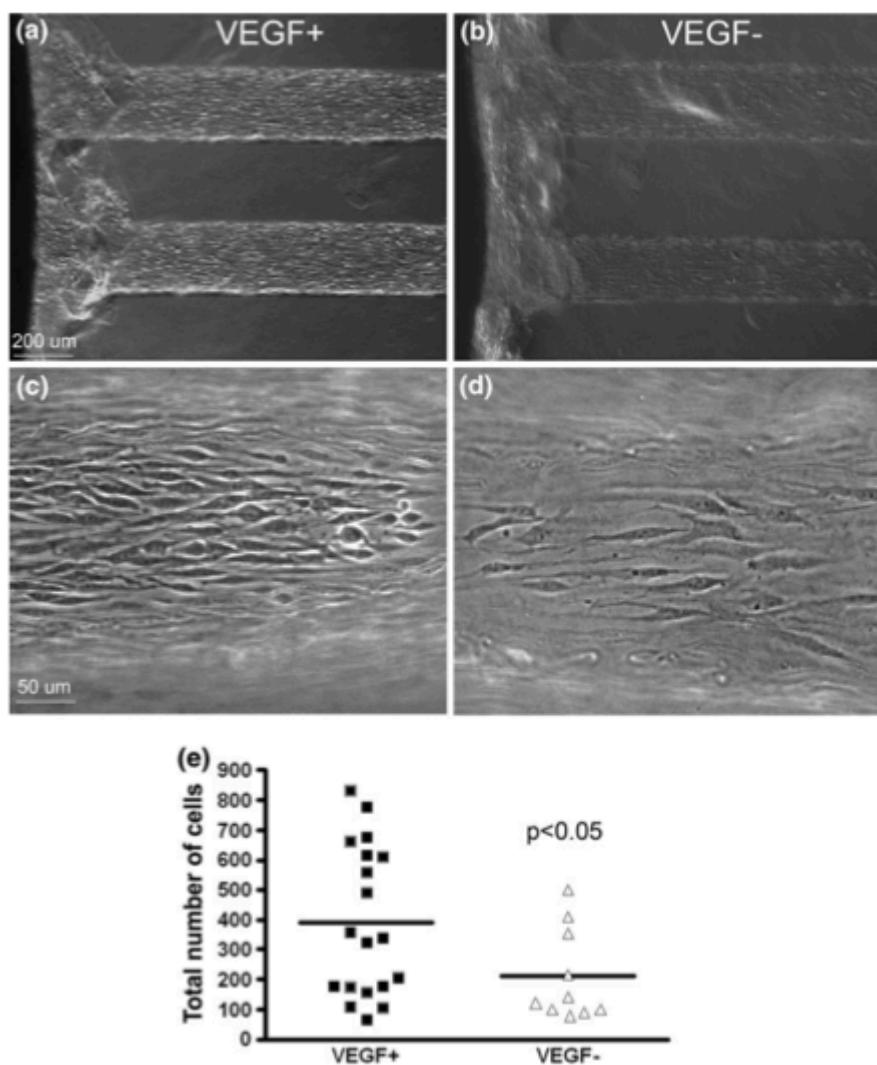


Figure 2.4: Enhanced vasculature by VEGF. P4-6 aorta explants regeneration into the microchannels in presence (a, c) and absence (b, d) of VEGF after 8 days of culture *in vitro*. Quantitative analysis DAPI-positive nuclei, confirmed a significant difference ($p < 0.05$) in the number of cells in each group (130).

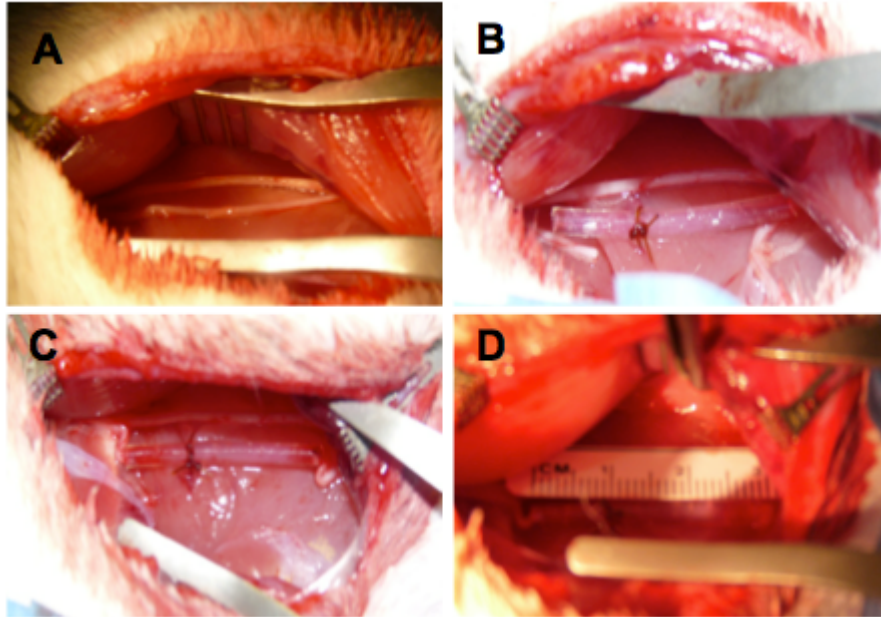


Figure 2.5: Surgical implantation procedure of a 30 mm nerve conduit after peroneal nerve injury. (A) Incision for implantation showing Tibial (top) and Peroneal nerve (bottom), (B) the NG is first sutured to the underlying muscle (C, D) Proximal and distal stumps are sutured into the NG.

2.3.2 Long nerve gap regeneration can be achieved with multiluminal structural support

Gross evaluation of the nerves within the simplenerve guide filled with collagen taken at six and ten weeks post implantation failed to show nerve regeneration in all animals tested. In contrast, multiluminal nerve regeneration was observed in all the injured animals repaired with BNIs. Also we observed proper vascularization of the regenerated nerve fibers in the BNI microchannels. These results were confirmed by immunohistochemical characterization.

Table 2.2: Experimental groups for the 30mm long gap peroneal nerve repair study

Groups	No. of rabbits
Simple Tube, 6 weeks	2
BNI, 6 weeks	2
BNI+VEGF(rc), 6 weeks	2
BNI+PTN(rc), 6 weeks	2
Simple Tube, 10 weeks	7
BNI, 10 weeks	7
BNI+VEGF, 10 weeks	7
BNI+PTN, 10 weeks	7
BNI+PTN+VEGF, 10 weeks	5

In an initial test, VEGF or PTN (1µg/ml each) were mixed with the collagen and loaded in the BNI prior to implantation and evaluated 6 weeks post nerve repair. Cross sections of the nerve were taken in the proximal third section of the regenerated nerve (Figure 2.6). Histological evaluation showed aneurofilament-positive immunofluorescence staining in all the BNI implanted groups, but none in animals grafted with simple tubes. Groups of NFP positive axons were encapsulated by a perineurium and a distinct epineurium, resembling the normal anatomy of a nerve fascicle. This result demonstrated the specific benefit of the multiluminal design over the simple tubularization repair method. Moreover, the initial group of animals that received recombinant VEGF or PTN (1µg/ml each) directly mixed with the collagen and loaded in the BNI prior to implantation, showed an apparent increase of NFP+ axons compared to the BNI-collagen only groups. This results, give us confidence on the biological benefit of adding PTN/VEGF to entice long gap nerve repair. However, recombinant proteins mixed with collagen are expected to provide only acute support, not likely sufficient for sustaining axonal growth for long distances. Considering that regenerating axons grow at a 1-2 mm/day rate(135), crossing a 30 mm gap will demand trophic support from 15-30 days. In that light we envisioned the need of providing sustain growth factor release of PTN and VEGF in order to maximize the trophic support, nerve regeneration and functional recovery.

In our 6 week pilot study, we observe an increased number of axons regenerating through the multiluminal BNI at the proximal third section as compared to the simple tube controls. Also, the number of regenerated axonal profiles was higher by threefold in the BNI groups which were supplemented by recombinant VEGF and PTN (Figure 2.6)

2.3.3 Sustained Pleiotrophic support can entice long gap nerve regeneration and functional recovery.

The local presence of growth factors plays an important role in controlling survival, migration, proliferation, and differentiation of the various cell types involved in nerve regeneration(136).

Therefore, therapies with relevant growth factors received increasing attention in recent years. However, growth factor therapy is a difficult task because of the high biological activity (in pico- to nanomolar range), pleiotropic effects (acting on variety of targets), and short biological half-life (few minutes to hours)(137)of these proteins (118). The half-life of growth factors demands for a delivery system that protects and slowly releases locally the protein over a prolonged period of time. Therefore, growth factor delivery for peripheral nerve regeneration may be ideally combined with an NG.

Growth factors have been loaded into the lumen of an NG to prolong localized drug availability. Studies using NGF (138),BDNF (80, 139), NT-3(80), fibroblast growth factor (FGF)-2(140), VEGF(122, 141), platelet-derived growth factor (PDGF)(142), glial growth factor (GGF) (1, 143) and leukemia inhibitory factor (LIF) (144) have been mixed with hydrogel-forming collagen,laminin, alginate, heparin, and heparin sulfate. These methods while useful for growth factor delivery over a period of days, but failed to provide long term controlled release (118). Biodegradable, polymeric microspheres havebeen considered for the delivery of neuronal growthfactors in the context of both the implantation in thebrain (145, 146) and thecombination with NGs for peripheral nerve repair. In fact NGF releasing microspheres implanted in a rat sciatic nervegap of 10 mm showed significantly more fibers and a higher fiber densitythan the control groups(147). However, attempts to engineer NGs with controlled growthfactor release kinetics are relatively scarce. Our lab developed a computer model to simulate growth factor release into the multiluminal BNI compared to the collagen filled empty tube (Figure in Appendix A). That analysis suggested the benefit of using nanoparticle growth factor release compared to that suspended in collagen.

In that light, poly (lactide-co-glycolide) acid (PLGA) nanospheres were synthesized, and a second cohort of rabbits undergo 30 mm gap repair of the peroneal nerve defect. For this experiment,we repeated the initial experiment but implemented a controlled growth factor release method into the BNI using PLGA nanoparticles, and evaluated the functional recovery

using electrophysiology and behavioral tests. In this study, VEGF and PTN were encapsulated in PLGA nanoparticles at a 66% efficacy, and their release profile quantified by ELISA over 30 days at 37°C (Figure 2.1 C, D).

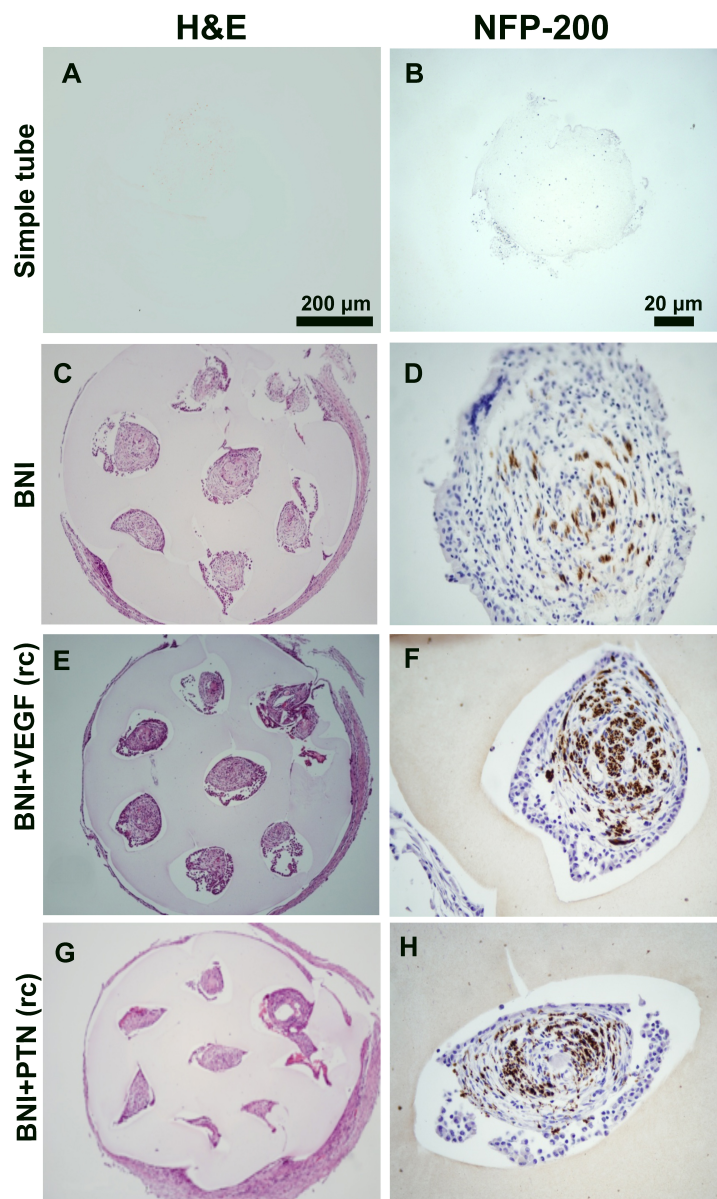


Figure 2.6: Histological analysis six weeks post-implantation. (A-D), show H & E sections and (E-H) show sections stained for Neurofilament positive axons (brown, also indicated by arrows) at six weeks post-injury. Treatment groups included (A, B) simple tube (C, D) multiluminal BNI (E, F) BNI supplemented with recombinant VEGF (G, H) BNI supplemented with recombinant PTN.

2.3.4 Increased axonal regeneration to distal target with BNI VEGF/PTN support

In our 6 week pilot study, we observe an increased number of axons regenerating through the multiluminal BNI at the middle section as compared to the simple tube controls. Also, the number of regenerated axonal profiles was higher by threefold in the BNI groups which were supplemented by recombinant VEGF and PTN.

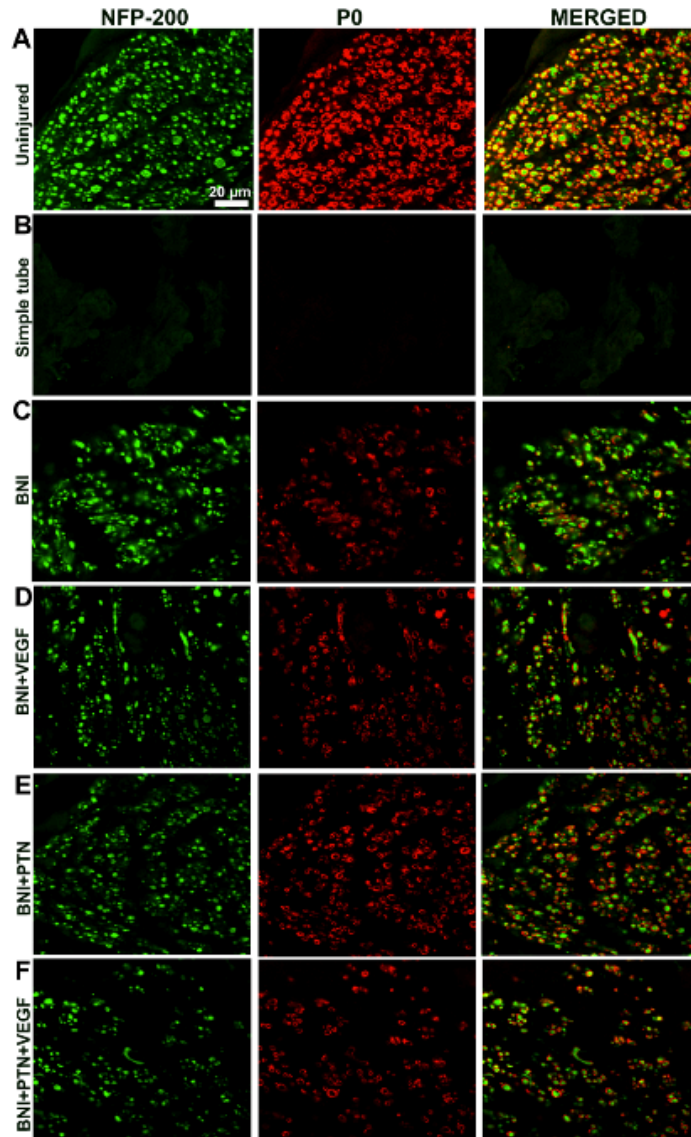


Figure 2.7: Myelination staining on the distal stump of the regenerated nerve in all the experimental groups. NFP 200 is used as a marker for axons and P0 is used as a marker for the myelin around these axons.

We followed with a complete ten week study employing release of pleiotropic factors by nanoparticles and added an additional group with combination of VEGF and PTN nanoparticles. We observed similar results for number of axonal profiles in the midsection of the tube. Also, the number of myelinated axons 5-8 mm into the distal stump was evaluated. We found that all the BNI treated animals had myelinated axons in the distal stumps and the numbers were significantly higher in all the growth factor supported groups but were threefold lower than the numbers found in uninjured controls. The number of myelinated axons in an uninjured peroneal nerve was 145 ± 16.5 per $100 \mu\text{m}^2$ while there were no myelinated axons in the simple tube group. It was 10.75 ± 7 in the BNI group, 42 ± 8.5 in the BNI VEGF, 49 ± 8.5 in the BNI PTN group and 37.5 ± 6.3 in the combination of BNI VEGF/PTN group.

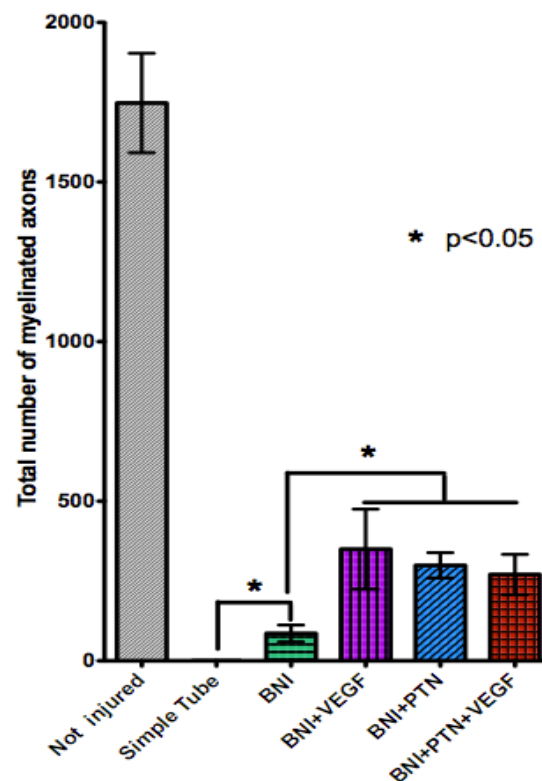


Figure 2.8: Total number in of myelinated axons in the complete distal segment of the regenerated peroneal nerve. Number of axons in the VEGF and PTN treated groups were comparatively higher than BNI collagen. All values are reported as mean \pm SD.

2.3.5 Restoration of nerve conduction in all the BNI groups

CMAPs were measured from the anterior tibialis anterior muscle after stimulation of the proximal side of the implant. It was only done in three animals from each group. We did not visualize any muscle contraction in the simple tube group whereas we saw muscle twitching in all the BNI groups after stimulation on the proximal side. The multiluminal BNI yielded significantly higher CMAPs in comparison to the simple tube controls. The BNI groups supplemented with growth factors had significantly higher CMAPs as compared to the BNI only group but there was no significant difference observed among the growth factor aided groups.

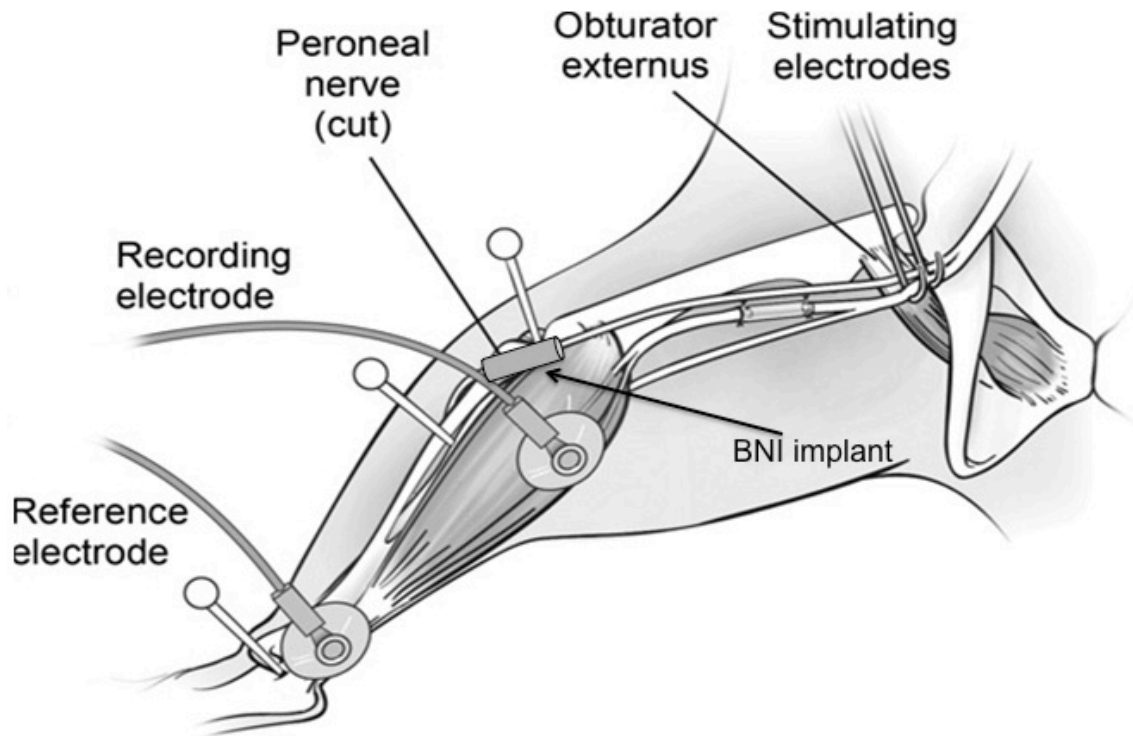


Figure 2.9: Diagram of terminal electrophysiology setup. Stimulating hook electrodes are used to stimulate the proximal side of the nerve implant and recording needle electrodes are placed in the tibialis anterior muscle to record CMAPs. (Adopted from Van Dyke, 2008) (148)

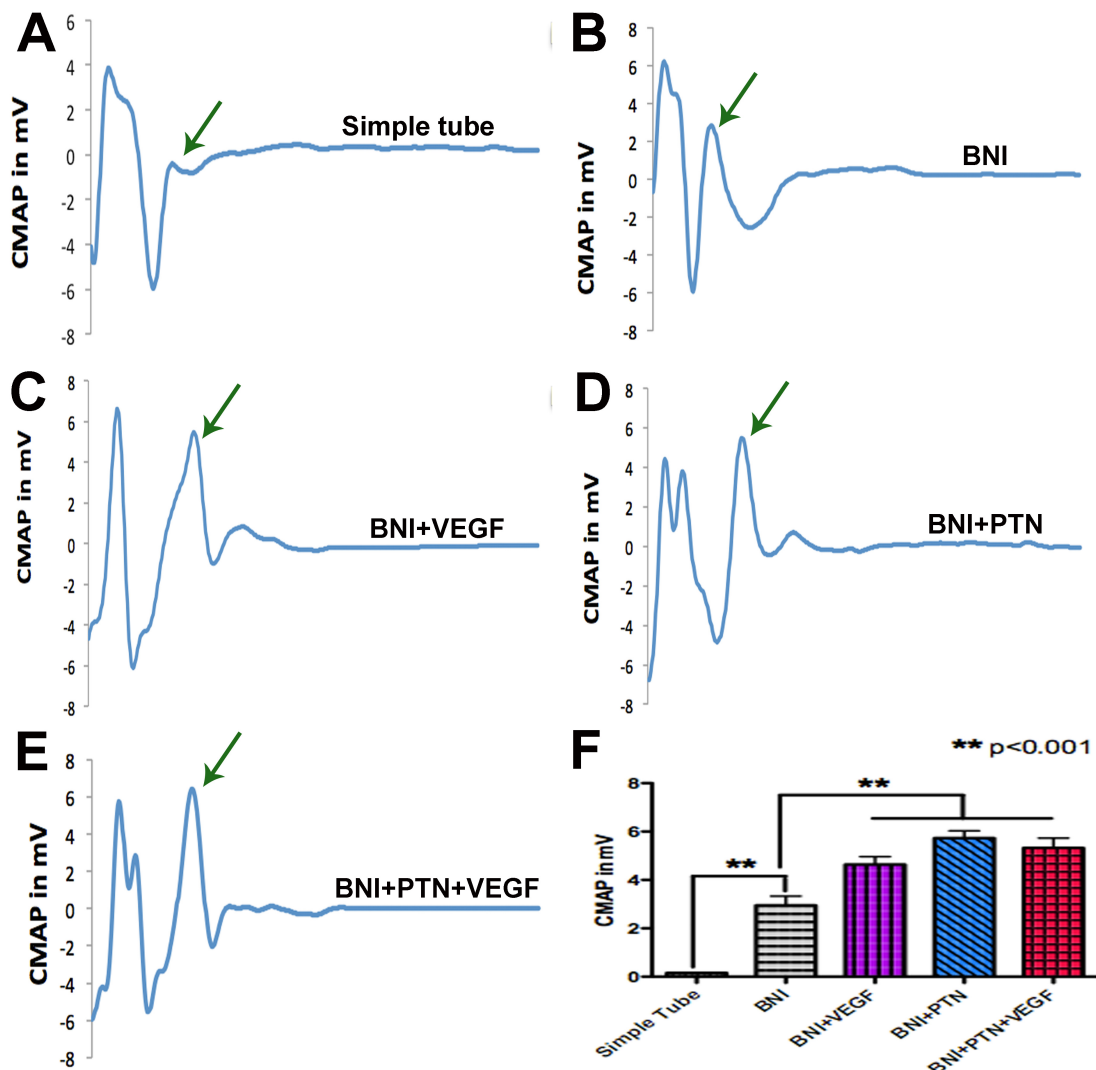


Figure 2.10: Measurement of compound muscle action potentials (CMAPs). (A) No electrical response seen from the tibialis anterior muscle in simple tube collagen repair. (B-E) Distinct CMAP responses were observed in all the BNI groups. (F) Quantification of CMAPs across the experimental groups indicates that all BNI groups had significantly greater response as compared the simple tube control and the growth factor supplemented groups showed significantly higher CMAPs as compared to BNI without growth factors.

2.3.6 Enhanced sensory recovery across the BNI

We conducted a sensory response test by injection of formalin subcutaneously on the dorsal side of the rabbit feet to induce pain. Induction of pain leads to the rabbit licking its feet. The dorsal side of rabbit feet is innervated by superficial branch of common peroneal nerve (149). After the injection, the animals were observed for the first 10 minutes and then the numbers of

licks were counted. We observed a significant recovery of sensory function in all the BNI groups as compared to tube collagen group. Interestingly, we did not see any significant recovery of sensory functions among all the three BNI groups with PTN and VEGF as observed in the motor function recovery (Figure 2.12).

2.3.7 PTN mediated motor function recovery

Several nerve regeneration studies have focused on electrophysiological and morphological test for evaluation but assessment of function is essential as well. The toe spreading index measurement in a rabbit is an ideal and extremely sensitive method to evaluate the onset of motor function recovery after peroneal nerve injury. The peroneal II, III and IV muscles are involved in this reflex toe spread behavior of the rabbit (150). Each animal was tested for functional recovery by the effectiveness of its toe spread once a week after the 3rd week of implantation. No difference in the toe spreading index was observed at the 4th week time point among all the groups. By the 7th week, all the BNI group animals as well as the BNI supplement with growth factors groups had significantly wider toe spread as compared to the animals having simple tubes. At the end of the 10th week study point, BNI-PTN group had the maximum spread with TSI values at 0.85 ± 0.10 units, whereas the simple tube implanted animals had 0.62 ± 0.061 TSI. This result clearly indicates that there was a significant increase in motor function in all the BNI groups. Also, BNI-PTN group had the best motor function recovery (Figure 2.14).

2.3.8 Reduced muscle weight loss in growth factor groups

After the CMAPs recording from the tibialis anterior muscle, that muscle from the injured side and the uninjured side are collected and weighed. The weight of the tibialis anterior muscle of the injured and the contralateral sides were measured. It was observed that there were no significant differences in the contralateral muscle mass among all the groups where as on the injured side the simple tube collagen group had significant muscle mass loss as compared to the PTN supplemented BNI groups (Figure 2.15).

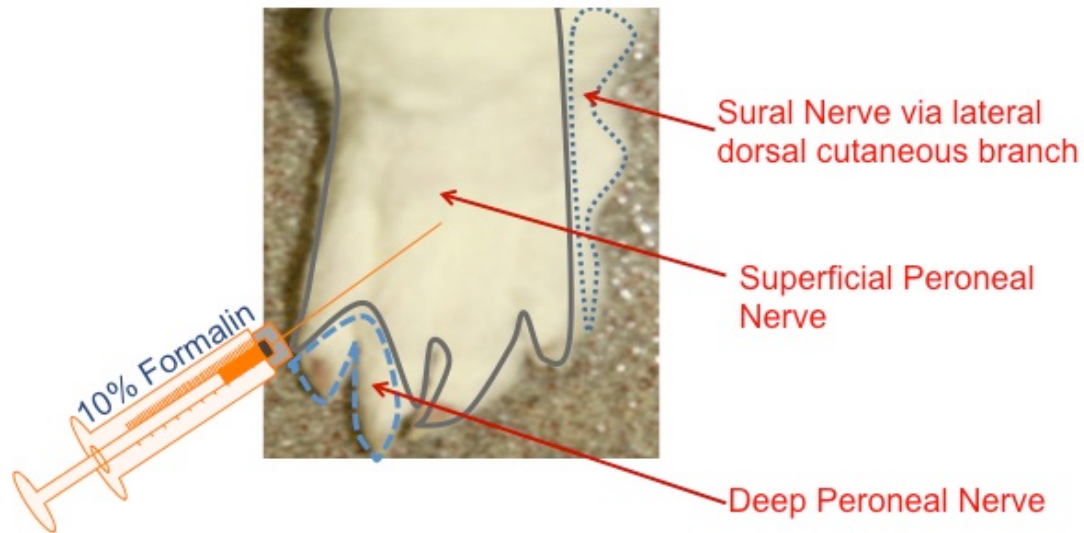


Figure 2.11: Dermatome of the rabbit's feet and the formalin injection site

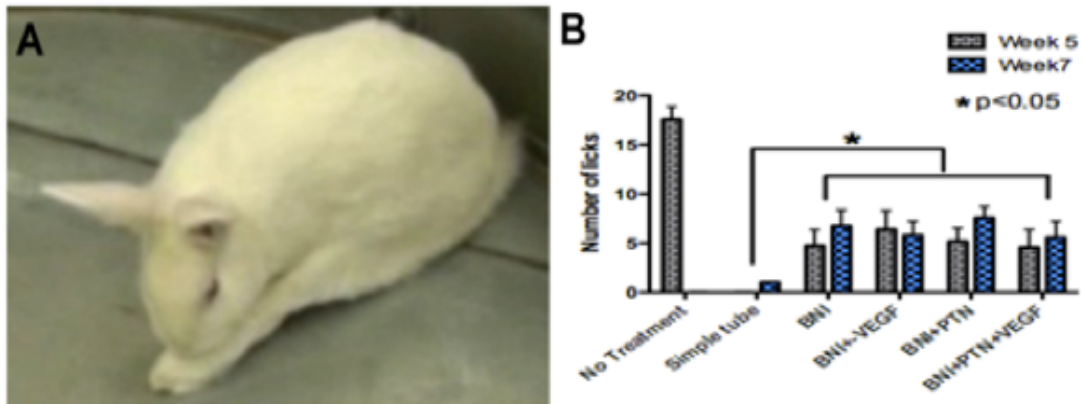


Figure 2.12: Behavioral test for sensory function recovery. (A) A rabbit licking its foot after formalin injection, (B) Quantification of the number of licks for 10 minutes after injection of 10% formalin. There was a significant increase in the number of licks in all the BNI groups as compared to the simple tube collagen controls, but no significant difference was observed among the BNI groups.

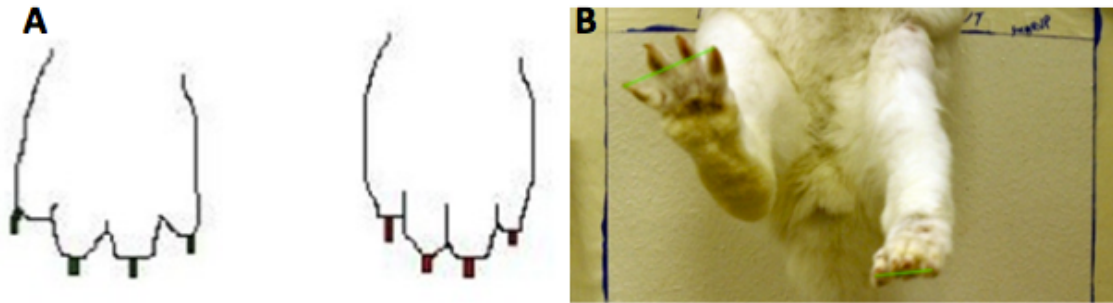


Figure 2.13: (A) Schematic representation of the direct measurement of toe-spreading length between the first and the fourth toe at the tip of nails. (B) Picture of toe-spread in a rabbit with a left peroneal nerve injury

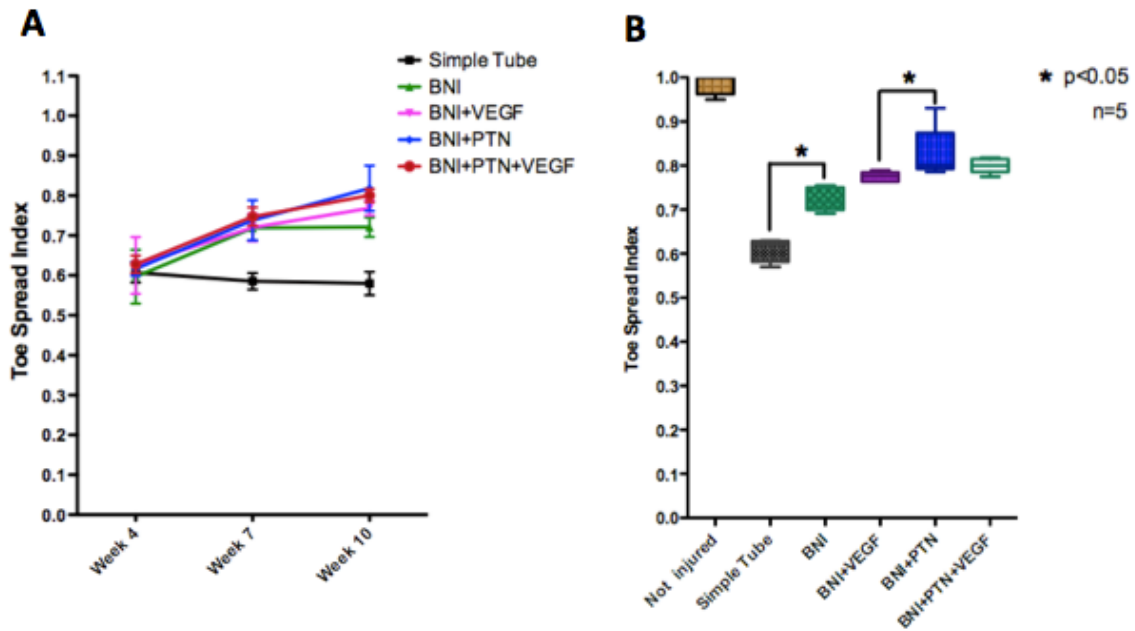


Figure 2.14: Behavioral test for motor function recovery. (A) Toe spread measurement over the length of the study at week 4, 7 and 10 post injury. (B) Toe spread measurement at the end of the study. All the experimental groups except the simple tube collagen group had significantly greater toe spreading. The BNI group supplemented with PTN had the maximum toe spread ($p < 0.05$).

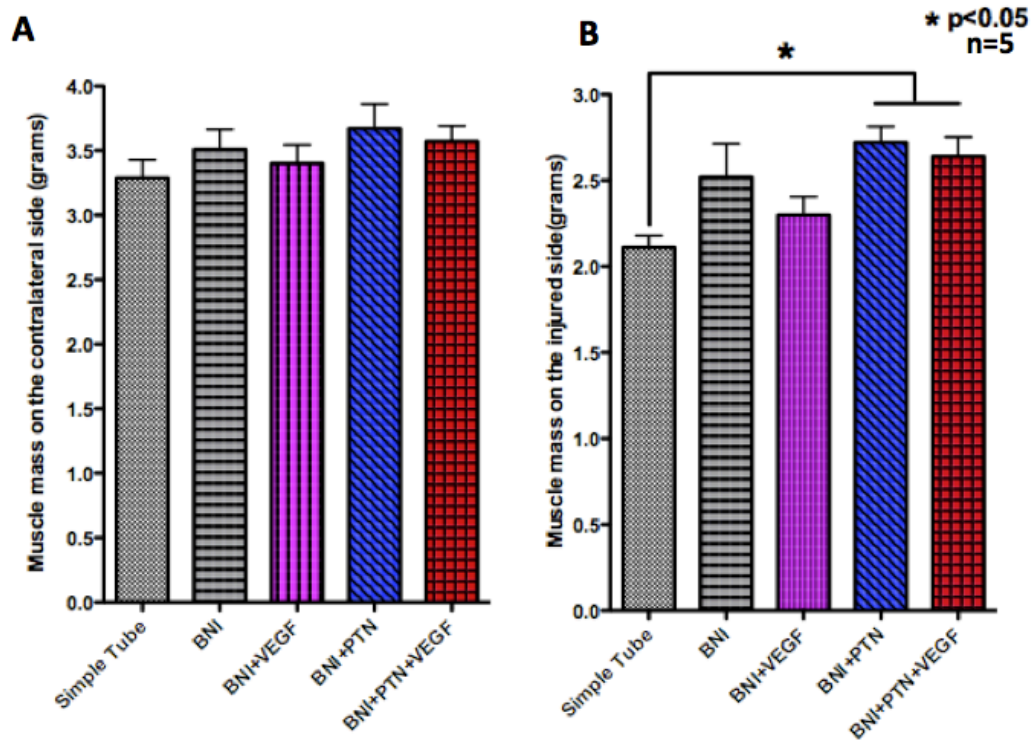


Figure 2.15: Comparison of tibialis anterior muscle weight across all experimental groups. (A) Muscle weight on the contralateral side (B) muscle weight on the injured side. There was no significant difference observed across all groups on the contralateral side but on the injured side the BNI groups supplemented with PTN or PTN/VEGF had reduced muscle loss as compared to the simple tube group ($p < 0.05$, $n = 5$).

2.4 Discussion

Several synthetic nerve guides have been proposed to achieve nerve regeneration across long gap nerve injuries. Such tubularization techniques depend on migration of fibroblasts and Schwann cells from the host proximal and distal nerve stumps into the lumen of the tubes to form a cellular scaffold supportive of neural regeneration (90). We demonstrated that a biosynthetic nerve implants (BNI) with linearly arranged agarose microchannels with luminal collagen can bridge a 30 mm critical gap in the rabbit common peroneal nerve. While incorporation of orientated microchannels within the lumen of the conduits has previously shown to substantially influence the rate and direction of regenerative events through short gaps (52, 92, 109, 110, 151, 152). This study is first to report that such structure in itself can provide nerve growth over critical long gaps bridged with collagen-filled BNIs as vascularized fascicle-like

nerve regeneration was confirmed through the micro-channels. This result is in agreement with the known stimulatory effect of collagen on axonal regeneration, myelination, and vascularization when compared to empty silicone-based conduits, presumably by stimulating early vascularization of the regenerated nerve (46), and underlies the importance of incorporating cell matrix molecules as part of the regenerative environment for nerve gap repair. Luminal collagen has been previously shown to promote nerve regeneration (153-155). Specifically, the incorporation of collagen microfibers have been reported to bridge an 8 cm gaps of canine peroneal nerves over a long time (10–12 months), with numerous myelinated axons of a range of diameter. However, in that study myelination were less well developed than in the contralateral unoperated peroneal nerve and there was no recovery of function 12 months post injury.

Others have used hollow conduits filled with collagen gel alone or supplemented with neurotrophin-3(NT-3), BDNF or acidic fibroblast growth factor (aFGF) enhance nerve regeneration across non critical gaps (80). Many growth factors have been identified that influence nerve regeneration (see table 2.1).While the inclusion of single growth factors some functional recovery in short gap repairs the failed to repair gap injuries longer than 2.5 cm. The failure of single growth factor delivery may be attributed to narrow cellular specificity of most common neural growth factors. Indeed, each family of growth factors has distinct functional characteristics. As such, NGF stimulates trkA bearing nociceptive sensory neurons; BDNF stimulates trkB positive CNS neurons, NT-3 mostly attracts trkC positive proprioceptive sensory fibers (156) whereas GDNF mainly stimulates RET expressing dopaminergic and motoneurons(157). Knowing the narrow cellular effect of most growth factors, some have proposed to combined them in an attempt to enhance nerve repair. Indeed, co-delivery of both NGF and GDNF, and BDNF with ciliaryneurotrophic factor (CNTF) seems to increase functional regeneration by attracting different neuronal subpopulations (both motor and sensory) (158). However, this effort also is restricted as it focused only in the neural populations, while lacking

support for other cell types such as fibroblasts and perineurial, endothelial cells and Schwann cells which must be recruited from the severed peripheral nerve stumps to assist in axonal regeneration (159).

In this study we demonstrated a stimulatory effect of PTN and VEGF supplementation of the multiluminal BNI in mediating nerve repair and functional regeneration. In contrast to the catastrophic failure observed using simple tubes with luminal collagen, and the reduce growth provided by the multiluminal support, BNIs supplemented with PTN or VEGF showed a significantly increased number of neurofilament-positive axons within the microchannels, with congruent nerve conduction and functional recovery.

Blondet et al reported increase in levels of PTN after the first week of sciatic nerve crush injury (160) and PTN was also upregulated in the surrounding support cells (Schwann cells, macrophages, and endothelial cells) on the distal stump of the injured nerve (161). Also it has been reported that PTN mRNA is highly expressed in a motor nerves as compared to sensory fibers. PTN have been found to promote outgrowth in neurons, glial progenitor cells and oligodendrocyte progenitors (162) and is a mitogen for endothelial cells, epithelial cells, fibroblasts, and has demonstrated neurotrophic effect in motor neurons (129, 163-166). There are four receptors for PTN: receptor protein tyrosine phosphatase (RPTP) β/ζ , anaplastic lymphoma kinase (ALK), N-syndecan, and low-density lipoprotein receptor-related protein-5 (162). Mi et al reported for the first time that PTN is a neurotrophic factor for motor neurons (124).

Similarly, VEGF significantly increased blood vessel penetration and Schwann cell migration, and has recently been shown to influence neuronal growth, differentiation, and survival (167). The major role of VEGF is to promote angiogenesis in the nerve conduit and also help in axonal regeneration (168, 169). It have been shown that VEGF increases Schwann cell proliferation and migration along with increased vascularization of the transected nerve (169). A study reported significant increase in myelinated axons and motor function recovery when

matrigel with VEGF was added to the silicone chambers (141). In another study, application of VEGF to the acellular peripheral nerve grafts resulted in significant increase in axonal sprouting (168). Recently, a study also showed better and efficient innervation of musculocutaneous nerve stumps after transfection with VEGF plasmid (170). While the precise cellular and molecular mechanism for the neurotrophic effect of VEGF is unknown, it likely involves the recruitment and stimulation of Schwann cells, as these cells upregulate VEGF expression secondary to nerve injury (171). Moreover, exogenous VEGF has been shown to stimulate the proliferation and migration of Schwann cells (172), and to significantly increase the total number of regenerating axons through a 20 mm gap injury when combined with acellular peripheral nerve isografts(141).

In accordance to the mild functional regeneration observed in the BNI with multiluminal collagen group, as indicated by TSI and CMAP values, a significantly higher number of axons were observed in the VEGF, PTN and combinatorial treatment groups, which closely correlated with the functional reinnervation parameters. The VEGF treated groups exhibited slightly increased CMAP and TSI values compared to the BNI only group, indicating that stimulation of vascularization and nerve regeneration are critical for long gap peripheral nerve repair. In turn, animals in the PTN treated groups elicited the highest CMAP amplitudes and toe spread index values among all groups, which suggest the support of motor nerve regeneration. The combination of PTN and VEGF has similar CMAPs and number of regenerating axons as the individual growth factor growth indicating no additional effects. These results are also supported by the regain in muscle weight of the anterior tibialis muscle compared to that observed in the BNI control. The formalin test for the sensory response also suggests that all the BNI treated animals had recovery of nociception when compared to the control group with simple tubes. Combined, these results indicate the essential role of the BNI for unidirectional axonal growth along with pleiotropic supplements for effective recovery after long gap nerve defects.

2.5 Conclusion

Our finding shows that multiluminal design of the BNI is critical to bridge a gap of 30mm long peripheral nerve repair. The micro channels provide proper topographical cues for the regenerating axons to grow towards the distal nerve stump. Also, the micro channels help in unidirectional growth of the axonal fibers and mimics fasciculation. Sustained delivery of PTN also showed better motor function recovery among all the BNI groups. Also, the BNI groups have sensory function recovery as compared to the empty tube collagen group.

CHAPTER 3

ELASTIC, POROUS AND TRANSPARENT NERVE GUIDES FOR EFFECTIVE MULTILUMINAL NERVE REPAIR

Tubularization of peripheral nerve gap injuries has been proposed as a viable alternative to autograft repair. Recent progress in luminal fillers and multi-luminal designs has demonstrated promising results in mediating axonal regeneration and functional recovery across nerve gap injuries. However, most biodegradable materials used for nerve guide fabrication such as collagen or poly-lactic acid are opaque and prevent the evaluation of luminal fillers in the nerve conduit prior to surgery. This is important as discontinuous filler defects may compromise nerve regeneration. To address this limitation, we report the use of crosslinked urethane-doped polyester elastomer (CUPE), for the fabrication a translucent biodegradable nerve guide, which allows the inspection of the luminal fillers in the nerve guide prior to implantation. The CUPE polymer is strong and elastic with an estimated peak stress of 23 MPa and 135% elongation at break. Here we demonstrate that CUPE nerve guides can be used to repair a 15 mm nerve gap in the rat sciatic nerve, eliciting a restrictive foreign body response. Activated ED-1 expressing macrophages were observed to mediate CUPE reabsorption, sparing the regenerated tissue. Morphological and electrophysiological evidence demonstrated successfully nerve regeneration across long nerve gaps using the multiluminal nerve conduits made of CUPE, further supporting its use as a viable method for peripheral nerve gap repair, allowing pre and post-surgery evaluation of luminal fillers.

3.1 Introduction

Tubularization of peripheral nerve gap injuries with biodegradable nerve guides has been proposed as a viable alternative to autograft repair. Various reabsorbable polyesters including polylactide(173), poly (L-lactide-co-glycolide)(174), poly (L-lactide-co- ϵ -caprolactone) (175), poly (D, L-lactide-co-glycolide) (176), trimethylene carbonate-caprolactone block copolymer (177), and methoxy poly (ethylene glycol)-*b*-poly (D, L-lactide) diblock copolymer(178). Several tubular scaffolds are currently FDA-approved such as those made with collagen [NeuraGen; Integra Sciences] (35, 179, 180), polyglycolic acid (PGA) [Neurotube; Synovis] (181, 182), and poly(dl-lactide- ϵ -caprolactone) [Neurolac; Ascension] (35). However, these conventional polyesters polymers have low mechanical strength, are not elastic and have limited porosity. These limitations have direct effects in nerve regeneration, as ideal nerve guides should match the properties of the elastic nature of the nerve (i.e., in situ strain approximates 11%) (183), while maintaining sufficient mechanical strength to support surgical handling. This is particularly important when fragile luminal fillers such as ECM or agarose hydrogels are used to create microchannels.

While several elastomers can match the elongation capacity of the nerve (i.e., 2-12 MPa), including those made of poly(diols citrates) and poly(glycerol sebacate (0.5-11MPa), if used to fabricate porous scaffolds, they lose mechanical strength significantly. For example, peak stress of poly(1,8-octanediol citrate) decreases from 3 to 0.3 MPa upon scaffold fabrication (184). Recently, a cross-linked urethane-containing polyester (CUPE) was demonstrated as soft, elastic (200-350 elongation at break), strong (20-40 MPa peak stress), and biocompatible material with reduced foreign body reaction compared to PLLA (Day et al., 2008). The CUPE scaffolds are fabricated by salt-leaching method and thus are highly porous (50-200 μ m porous size).

Several studies have suggested the incorporation of biomimetic luminal fillers such as collagen matrix and growth factors as mechanisms to enhance nerve regeneration across a gap injury.

Furthermore, aligned fibers, microfilaments and microchannels have been reported to linearly guide the growth of regenerated axons through the nerve gap, potentially reducing re-innervation errors distal to the repair site (35, 89, 90, 97). In such biosynthetic nerves, it is of critical importance to ascertain the nature of the filler content, such as the linearity of the guidance cues, and the even distribution of the extracellular matrix and growth factors, prior to grafting. Of equal importance is the need of evaluating possible luminal fabrication defects, such as discontinuous fillers or contamination that may in turn compromise nerve regeneration. However, most other polymers currently used for nerve repair such as collagen or poly-lactic acid, are opaque and prevent the evaluation of luminal fillers in the nerve conduit prior to surgery. In addition to the elasticity and mechanical strength, the CUPE polymer is translucent, and thus can be used to fabricate NGs that allow the visualization of possible fabrication defects in the luminal fillers and will assist the surgeon in suturing the nerves to the BNI without damaging the multiluminal scaffold. We recently reported the use of transparent polyurethane tubing as a nerve guide material with multiple collagen-filled agarose microchannels as luminal filler in the repair of short nerve injury gaps (92). In that study, the transparency of the polyurethane tube also assisted in the visualization of nerve stumps inside the nerve guide and facilitated their placement into the tubing without disrupting the luminal filler. However, polyurethane is non-biodegradable and thus, not an optimal material for nerve repair.

While the CUPE scaffolds seem a natural better choice for the fabrication of the external NG in multiluminal nerve implants, it has long degradation rates *in vitro* (i.e., 8-16% mass loss over 60 days), but they can be properly shortened by the choice of diol used in the synthesis, the isocyanate content, and the post-polymerization conditions (Day et al., 2008). Here we hypothesized that CUPE can be used to make a BNI with optimal biodegradability designed with strength to protect the soft agarose made microchannels, yet elastic and porous to favor cellular migration and nerve repair. This study demonstrates that CUPE-BNIs can be used to repair a critical 15 mm nerve gap in the rat sciatic nerve.

3.2 Materials and Method

3.2.1 CUPE Nerve Guide Fabrication

CUPE pre-polymers were synthesized as previously reported (107, 108). A poly-octamethylene citrate (POC) pre-polymer was first synthesized by reacting 1:1.1 monomer ratio of citric acid and 1,8-octanediol under constant nitrogen flow, mixed at 100rpm for 2 hours at 140°C. The pre-polymer was then dissolved in 1,4-dioxane and purified by drop precipitation in deionized water. Finally, the precipitate was collected and lyophilized for 2 days. Pre-POC was dissolved in 1, 4-dioxane to make a 3 wt.-% solution. To synthesize cross linked urethane-doped polyester (CUPE), pre-POC was reacted with HDI in a 1:1.2 molar ratio. HDI and stannous octoate were added to the POC solution and allowed to react for 7 days at 55°C. 1.5 × 90 mm glass capillary tubes were dip coated with CUPE until a wall thickness of 250 μm was achieved. The CUPE coated conduits were cross linked at 80°C for 4 days and at 120°C for 1 day. The conduits were swollen in 50% ethanol to remove the guides and lyophilized for 1 day. All chemicals were purchased from Sigma Aldrich (Milwaukee, WI).

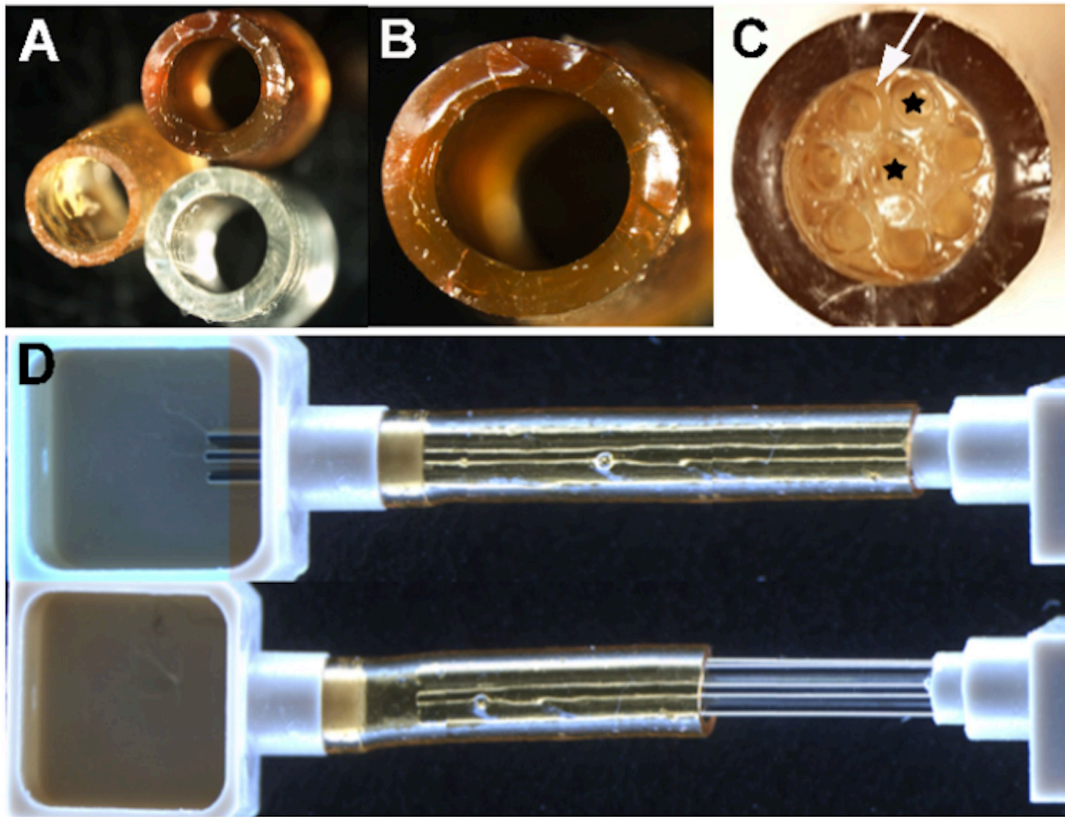


Figure 3.1: (A) Photographs of transparent CUPE-NG of two different thicknesses (top, amber) compared to a non-biodegradable Polyurethane-NG. (bottom, clear); (B) Cross sectional view of a CUPE-NG; (C) Cross sectional view of a CUPE Multiluminal Biosynthetic Nerve Implant (CUPE-BNI), the arrow indicates agarose structure and the asterisk represents a microchannel; (D) CUPE-BNI casting device showing the metallic brush inserted in the loading well prior to collagen (top), and after fiber removal (bottom).

3.2.2 Mechanical Test of the Nerve Guides

Strains were measured using a laser extensometer (MTS, Insight Eden Prairie, MN). Conduits were pulled at a rate of 500 mm/min until failure using a 500 N load cell. Values were converted to a stress vs. strain curve. The Initial modulus was recorded at 0-10% strain.

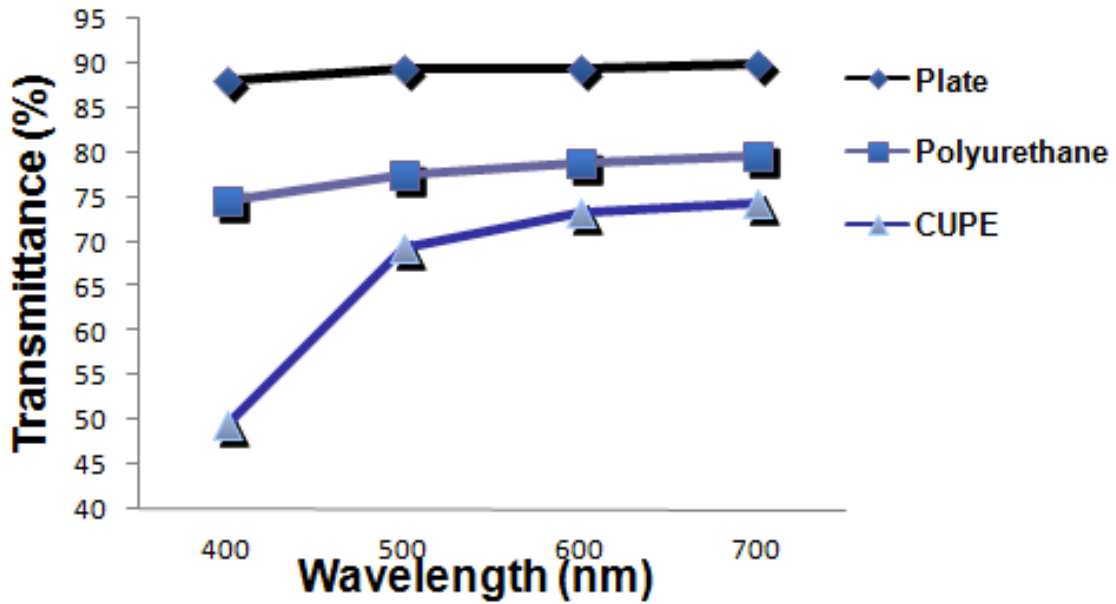


Figure 3.2: Transparency evaluation of CUPE in comparison to a transparent polymer polyurethane and the plate

3.2.3 CUPE Biosynthetic Nerve Implant (CUPE-BNI)

The CUPE-BNI was fabricated as previously reported (92). Briefly, a casting device was used which comprises of a loading well, a brush with titanium fibers (250µm and 500 µm) and the perforated CUPE-NG (Fig 3.1). The CUPE-BNI has a center micro channel with 500µm diameter and seven smaller micro channels on the periphery with 250µm diameter. A 1.5% agarose solution was injected into the CUPE-NG and the agarose was allowed to polymerize. The well was loaded with collagen IV (Millipore, USA) and then fibers were carefully pulled out of the casting device inducing a negative pressure in the wells and allowing the collagen to fill the micro channels uniformly. The CUPE-BNI was designed to linearly guide the regenerating axons across nerve gap lesions through the agarose micro channels filled with collagen.

Table 3.1: Experimental groups for the CUPE based nerve repair study

Groups	No. of rats
CUPE-NG, 8 weeks	8
CUPE-BNI, 8 weeks	8
CUPE-NG, 12 weeks	8
CUPE-BNI, 12 weeks	8

3.2.4 Animals

32 female Lewis rats (Charles River, MA) weighing between 275-300 grams were used for this study. The animals were divided equally into two groups: 1) Collagen filled CUPE single nerve guide (CUPE-NG) and 2) Collagen filled CUPE multiluminal BNI (CUPE-BNI), each group having a subset of two evaluation time points, 8 and 12 weeks. The animals were maintained under conditions of controlled light and temperature. Food and water were available ad libitum.

3.2.5 Animal Surgery

In deeply anesthetized animals (60mg/kg sodium pentobarbitol intraperitoneally) the left thigh was shaven and disinfected with povidone-iodine. The animal was then placed on a heating pad and the body temperature maintained at 37°C. The left sciatic nerve was exposed through a

dorsolateral gluteal-muscle splitting incision, and a 5 mm segment was excised proximal to the branching of the sciatic nerve. A 15 mm gap was created by attaching 1 mm of the proximal and distal ends of the transected nerve into a 17 mm CUPE-NG or CUPE-BNI tube using 9-0 nylon sutures (Arosurgical, Newport Beach, CA). The muscle was closed using chromic gut 3-0 sutures (Ethicon, San Angelo, Texas), and the overlying skin was stapled. Pain was alleviated with buprenorphine hydrochloride (Hospira) 1mg/kg subcutaneously for a week after surgery. All procedures involving animal surgery and care were performed in accordance with the Institutional Animal Care and Use Committee (IACUC) at the University of Texas at Arlington.

3.2.6 Histological tissue preparation

At 8 and 12 weeks post implantation the animals were sacrificed via overdose of sodium pentobarbital (120mg/kg) and perfused transcardially with 0.9% buffered saline followed by 4% paraformaldehyde (PFA). The implanted nerve guides were harvested, post-fixed in 4% PFA at 4°C overnight and then transferred to PBS. The regenerated tissue was isolated from the tubing and processed for paraffin embedding, and sectioning at 8 µm on a microtome (Leica 2145).

3.2.7 Immunostaining

Sections from each group were immunostained using a mouse anti-neurofilament protein 200 antibody (1:200, Sigma, Saint Louis, Missouri, USA) to label regenerating axons. Also, rabbit anti-S-100 (1:200) and mouse anti-vimentin(1:200) antibodies (Sigma, Saint Louis, Missouri, USA) were used to label Schwann cells and the perineurium respectively. Adjacent sections were labeled using a mouse anti-ED-1 (1mg/ml, Chemicon), a marker for macrophages and monocytes. The antibodies were diluted with blocking solution (4% normal goat serum in 0.5% Triton X in PBS) and incubated at 4°C overnight followed by extensive rinsing in PBS. Fluorochrome-labeled secondary antibodies (Cy2 and Cy3; 1:400; Jackson Immuno Research Laboratories, West Grove, PA; diluted with 0.5% Triton X in PBS) were incubated at room temperature in the dark for 1 hour. After rinsing in PBS, Fluoromount (Thermo Scientific, USA) was used to coverslip the tissue. The staining was evaluated using a confocal microscopy.

3.2.8 Axonal quantification

The NFP positive staining was imaged using a confocal microscope (LSM 510 meta) at 20X magnification. Cross sectional NFP 200 labeling axons were quantified in both the groups. Four slides from each nerve tissue section were used for quantification. In the CUPE-NG and the CUPE-BNI group, the total numbers of individual axons on each tissue section was counted using Image J find fluorescence maxima method by setting an appropriate noise threshold (Figure 3.5). In the CUPE-BNI group, we observed axonal growth in between the tube and the agarose walls and these numbers were also added to the total axonal count. The data was analyzed as the mean \pm standard deviation.

3.2.9 Electrophysiology

At the end of the eighth week, the animals were anesthetized by injecting 60mg/kg sodium pentobarbital and an incision was made over the implantation site. The sciatic nerve was re-exposed and covered with mineral oil (37°C) and stimulated through a bipolar needle electrode proximal to the implant. The compound muscle action potential (CMAP) was recorded from the gastrocnemius muscle with a needle electrode. A Cadwell Cascade™ system was used to stimulate a train of three pulses of 50 μ s duration and 2 to 4 volts to evoke a maximal response.

3.2.10 Statistical Analysis

The data is presented as average with the standard deviation of the mean. All statistical analysis was performed using one way-ANOVA with post hoc Newman-Keuls testing. A p-value of 0.05 or less was considered statistically significant.

3.3 Results

3.3.1 Translucent CUPE-NGs

Conduits made with CUPE were fabricated with a wall thickness of 250 μ m. Compared to the transparent non-biodegradable polyurethane tubes; those made of biodegradable CUPE elastomer were translucent with a slight amber color (Figure 3.1). Light transmittance through

the CUPE was estimated to be 73% using a spectrophotometer under visible spectrum while the polyurethane had 80% light transmittance and the polypropylene 96well plate has close to 90% transmittance. This allowed the visualization of fibers through the CUPE tubes, and assisted the fabrication of multiluminal biosynthetic nerve implants (Fig. 3.1D). The translucency of the CUPE material allowed the inspection of luminal fillers as well as evaluation of the integrity of the micro channels. Fabrication defects such as hydrogel braking, discontinuous luminal collagen, bubbles, or contamination were clearly identified prior to implantation. This ensured that only those without fabrication defects were used for animal implantation.

3.3.2 Multiluminal CUPE-BNI entices functional axonal regeneration through long nerve gaps
To evaluate whether CUPE is permissive for nerve grafting we compared simple tubularization repair (CUPE-NG) to those containing multiluminal collagen-filled microchannels (CUPE-BNI), in bridging 15 mm gap defects in the rat sciatic nerve. At eight weeks post implantation, fibrotic tissue covered the CUPE tube to an extent similar to that previously reported with the use of polyurethane tubing (108). This indicates that the material did not induced additional immune response to the CUPE implant rather there was a nice wrapping of a connective tissue around the CUPE as seen in silicone and polyurethane tubes. Also, vascularization was observed inside the implants as many blood vessels were entering through the porous tube towards the regenerating axons.

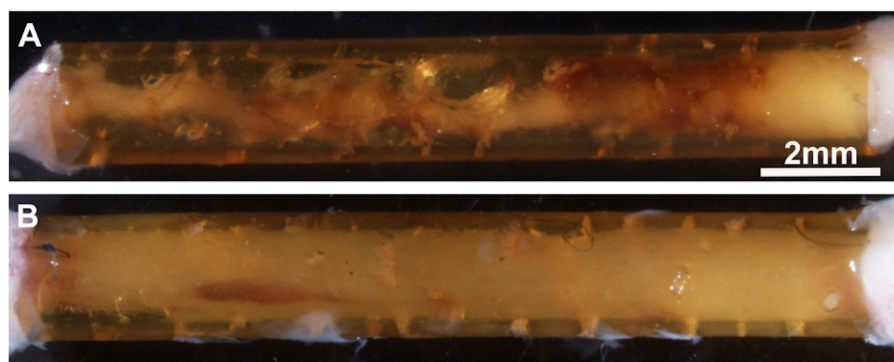


Figure 3.3: Nerve regeneration across a 15mm long gap across a (A) CUPE-NG and (B) CUPE-BNI 8 weeks after implantation. Enhanced tissue growth is visibly observed in the multi luminal BNI as compared to the NG filled with collagen (Scale bar=2 mm).

In the simple collagen filled NG a nerve cable was clearly observed to regenerate through the complete length of the tube in all animals repaired with the CUPE-NG (Figure 3.3 A), while as expected, multiple nerve fascicles were observed to fill all available microchannels in animals repaired with the CUPE-BNIs (Figure. 3.3 B). The simple tube had a single thin nerve cable growing while the multiluminal BNI tube was packed with nerve fibers.

Axonal regeneration was visualized by immunolabeling of neurofilament peptide 200kD (NFP 200), and confirmed in both the simple tubularization (Figure 3.4 A, B), and across the CUPE-BNI microchannels (Figure 3.4 C, D). NFP positive nerve fibers towards the distal end of the implants were imaged with a 20X objective using a confocal microscope. Figure 3.4 A, C shows the orientation of the regenerating axons right before innervating the distal stump of the injured nerve. Figure 3.4 B, D are the magnified images of figure 3.4 A, C showing the regenerating axons across a simple collagen filled CUPE-NG and a CUPE-BNI respectively. The regenerating axons were quantified to evaluate and compare the amount of regeneration in the two different groups and indicate the role of multiluminal scaffold for enhanced growth.

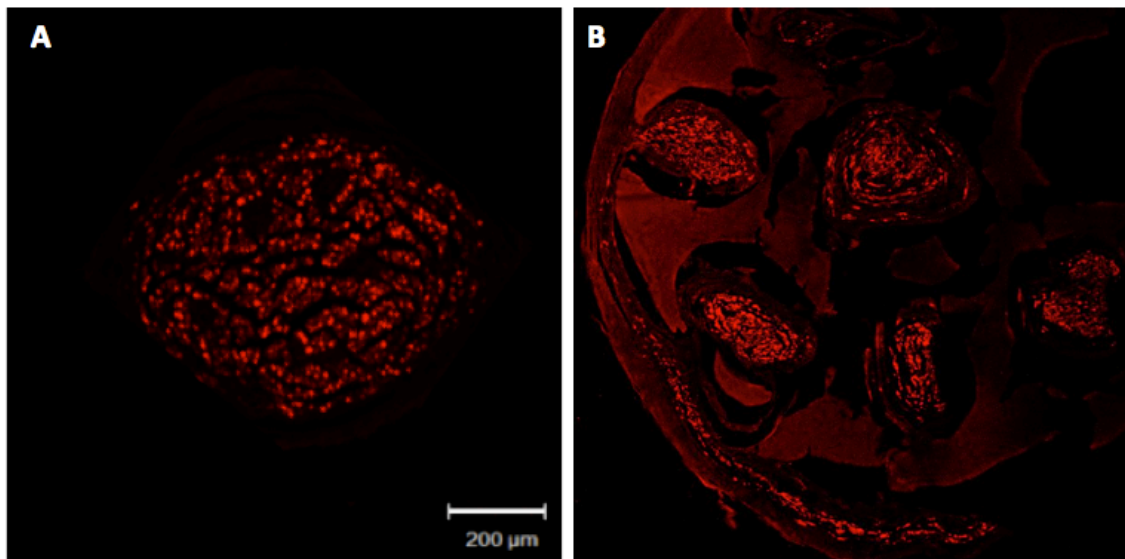


Figure 3.4: Nerve tissue regeneration across a CUPE-NG and a CUPE-BNI. (A) Cross section of NFP 200 staining showed regenerated nerve tissue across a CUPE-NG (Scale bar=200 µm); (B) NFP-200 staining confirmed the multiluminal axonal regeneration across a CUPE-BNI (Scale bar=200 µm).

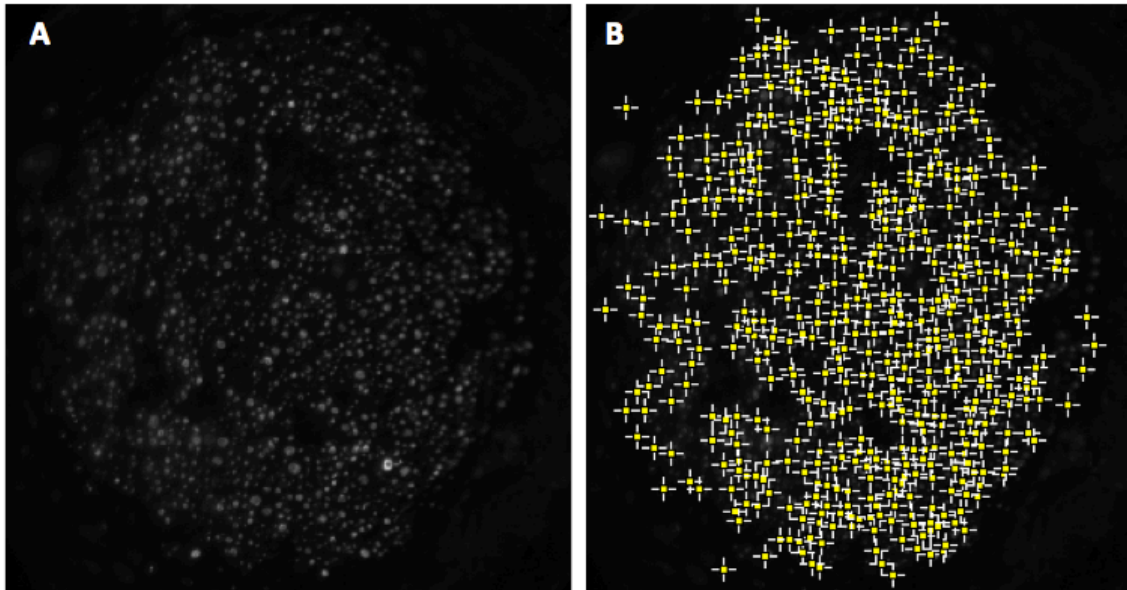


Figure 3.5 Representation of Image J quantification technique of counting regenerating axons. (A) A fluorescent image of NFP 200 positive regenerating axons through a CUPE-NG, (B) Image J analysis of axonal count by finding number of maxima at a noise threshold of 30

Quantitative analysis of axonal regeneration density at the distal end of the implants (i.e., 12-14 mm from the proximal end) revealed a highly significant ($*p < 0.001$) 3.5 fold increase in the number of regenerated axons through the CUPE-BNI (2757 ± 658.5) compared to that in the CUPE-NG (671.6 ± 168.1 ; Fig. 3.5). This quantification was done by manually counting the number of axons in the simple tube and in the small microchannels. The small acidic protein S-100 immunoreactivity in myelinated fibres appeared to correlate directly with the thickness of the myelin sheath formed by the Schwann cell. We evaluated myelination across the implants by immunolabeling of NF-200/S-100, and observed Schwann wrapping around the axons indicating normal myelination (Fig 3.6 A, B).

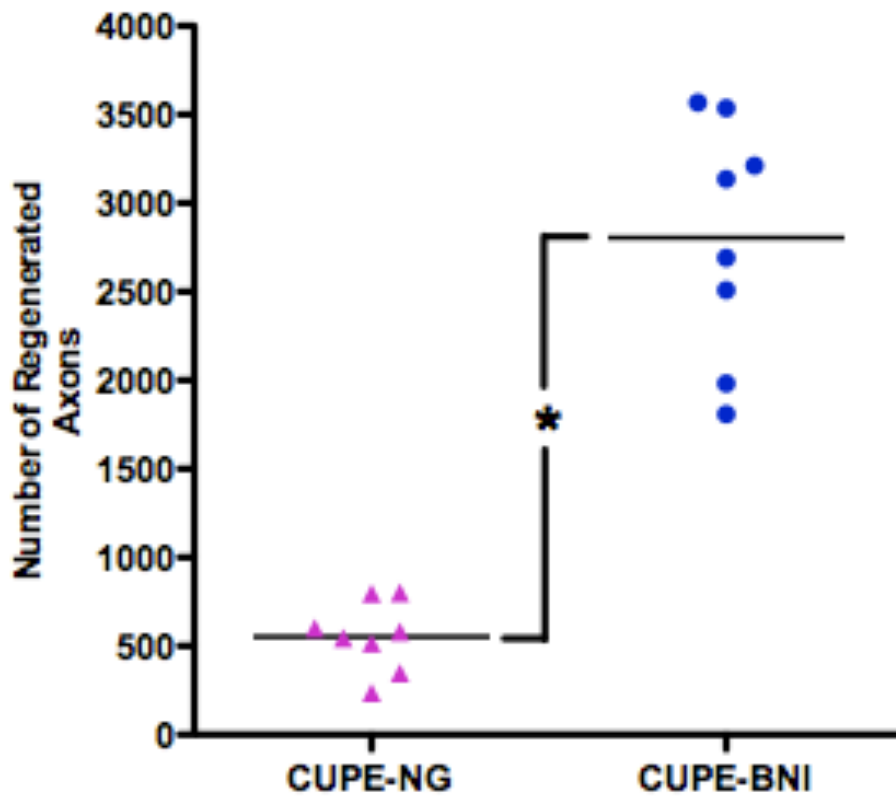


Figure 3.6: Comparison of regenerated axonal number quantification across a CUPE-NG and a CUPE-BNI indicates significant increase in the number of axons in the multi luminal BNI group (* $p < 0.001$).

Also, the regeneration of fascicle-like structures in the CUPE-BNI microchannels was confirmed by immunodetection of vimentin+ cells, a specific marker of perineural cells, in the periphery of the regenerated axon bundle within the microchannels (Fig 3.6 C, D).

To confirm that the observed increase in regenerated axons in the CUPE-BNI mediated improvement in function, we measured the restoration of nerve conduction.

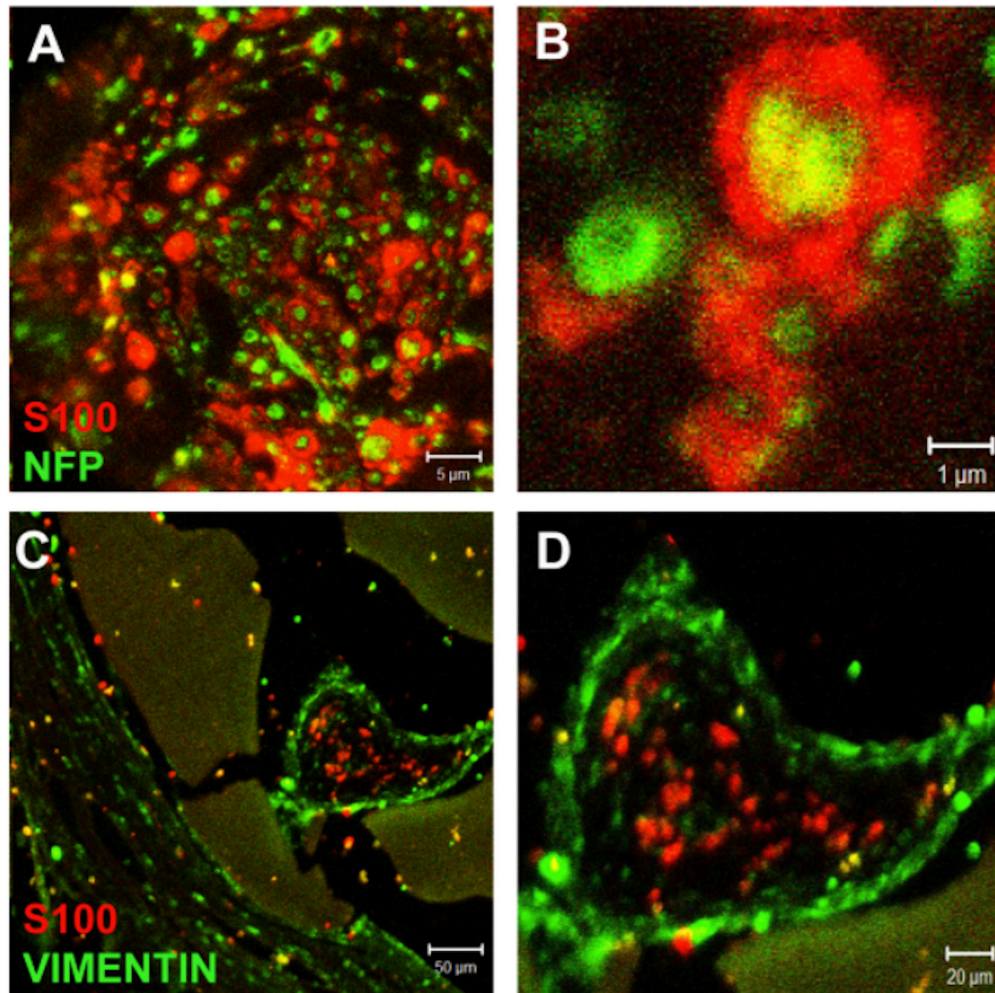


Figure 3.7: (A, B) Normal fascicular nerve regeneration is demonstrated by the co-localization of Schwann cells (red labeled S-100+) wrapping regenerated axons (green label NFP+); and by (C, D)Vimentin+ fibroblast (green) regeneration in the periphery of the regenerated nerve. Vimentin+ labeling marks the formation of perineurium around each micro channel packed with a regenerated nerve fascicle (Scale bars A=5 μm , B=1 μm , C=50 μm , D=20 μm)

Compound muscle action potentials (CMAP) recorded from the CUPE-BNI repaired group ($323.2 \pm 9.8 \mu\text{V}$) was significantly ($*p<0.01$) increased compared to those implanted with CUPE-

NG ($257.4 \pm 14.45 \mu\text{V}$; Fig. 3.7 A, B). Contraction of the gastrocnemius muscle was also visually confirmed in all animals. Together, this data indicates that the CUPE conduit is permissive for nerve repair and that normal axon regeneration, myelination, fasciculation and function can be facilitated through a long-gap injury using a multiluminal BNI design.

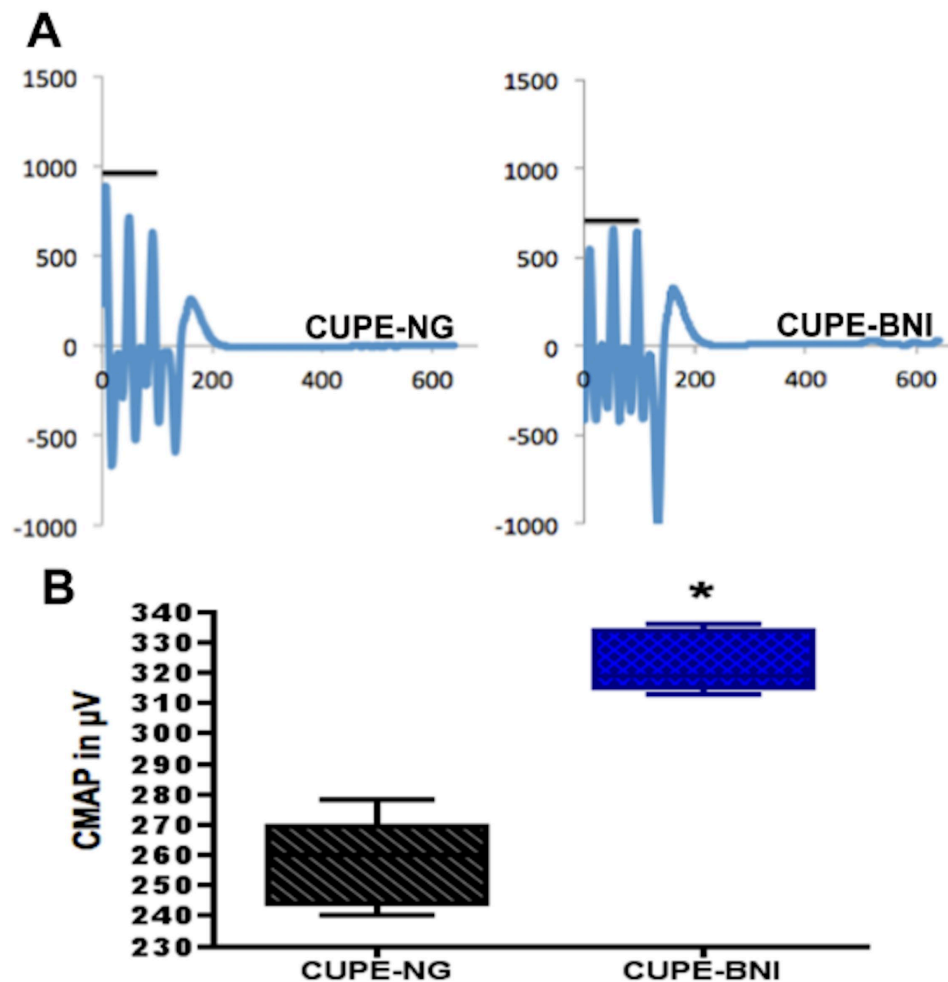


Figure 3.8: Compound muscle action potential recordings (CMAP) from the gastrocnemius muscles. All gastrocnemius muscles produced measurable signals. (A) Representation of CMAP in CUPE-NG and CUPE-BNI group (The bar indicates three stimulation peaks); (B) Comparison of CMAP between CUPE-NG (n=8) and CUPE-BNI (n=8) group showed significant increase in nerve conduction in the multiluminal BNI group (* $p < 0.01$).

3.3.3 Restricted inflammatory response elicited by CUPE revealed specific recruitment of macrophages and controlled polymer reabsorption.

Upon harvesting at 8 and 12 weeks post-implantation, the CUPE nerve guides showed signs of apparent degradation including increased translucency and flexibility. To directly ascertain whether the immune response to CUPE was restricted to the polymer, we evaluated the inflammatory response by direct visualization of the lysosomal macrophage activation antigen ED-1. This method revealed numerous macrophages infiltrating the CUPE tubing (Figs. 3.8 A, D), while few ED-1 cells were observed either in the fibrotic tissue covering the exterior walls of the conduits (Fig. 3.8 B, E), or in the regenerated nerve tissue located in the lumen of the nerve guide or the lumen of the BNI microchannels (Figs. 3.8 C, F).

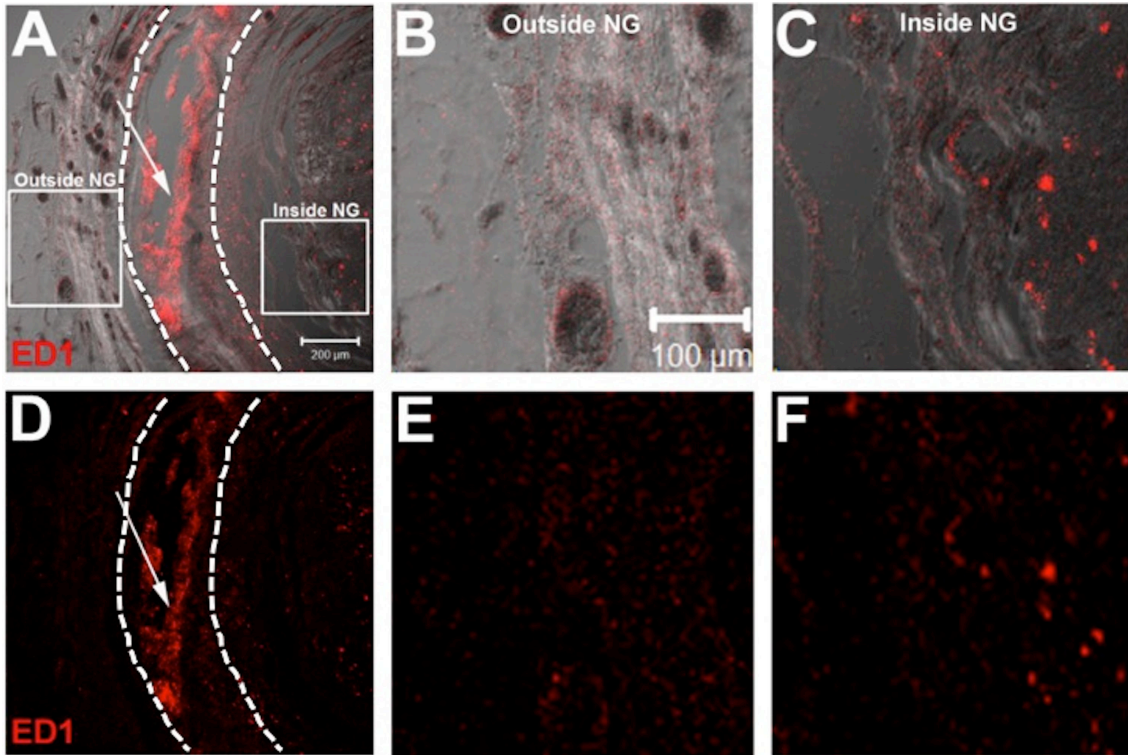


Figure 3.9: ED1+ Macrophages were localized on the CUPE-NG with minimal presence in regenerated epineurium or nerve fascicles. (A, D) ED1+ cells (arrows) present in surplus on the NG (marked by the dotted lines) and sparingly inside and outside the NG; (B, E) Magnification of the region within the box outside the NG (C, F) Magnification of the region within the box inside the NG (Scale bar A, D=200 μm; B, C, E, F=100 μm,).

Higher magnification confocal microscopy showed detail of the macrophage infiltration of the CUPE polymer, confirming the cellular-mediated degradation of CUPE over time. The macrophages were also visualized by DIC microscopy, which combined with ED-1 labeling, showed areas of high ED-1 immunoreactivity along the edges of the CUPE polymer, locating macrophages in the areas of polymer degradation (Fig. 3.9).

Using scanning electron microscopy we compared CUPE tubes before implantation and 8-weeks post-implantation. This method revealed clear polymer degradation overtime in the form of perforations and delamination observed in the tubing (Figs. 3.10 A, B). The amount of degradation was then estimated from mechanical testing and showed that peak stress of 23 ± 1.88 MPa prior to implantation, reduced to 11.36 ± 0.71 and 9.57 ± 1.05 MPa at 8 weeks and 12 weeks, respectively (* $p < 0.01$; Fig 9C). Similarly, the elongation to break reduced from 135.60 ± 13.31 to 51.53 ± 10.55 and 23.67 ± 6.37 % at 8 and 12 weeks, respectively (* $p < 0.001$, ** $p < 0.01$; Fig. 9D). This data confirmed the specific and control reabsorption of the CUPE tubing overtime, while supporting nerve regeneration and functional recovery.

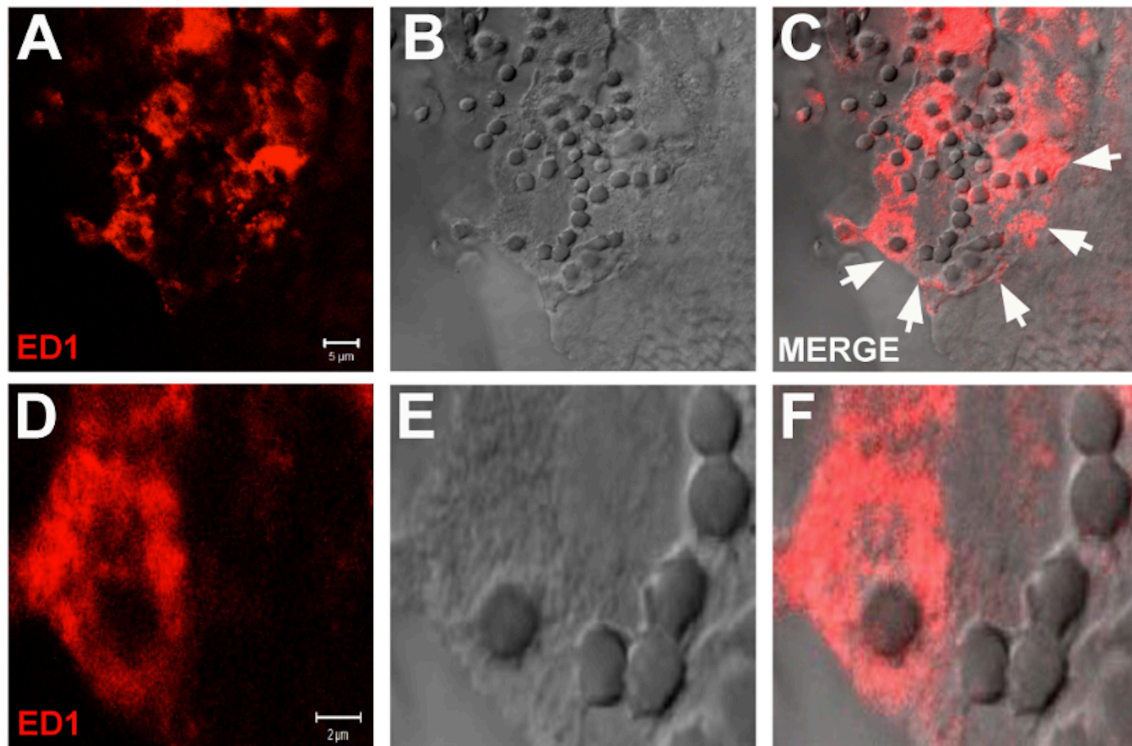


Figure 3.10: ED-1+ cells were observed on the NG eroding the CUPE at higher magnification. (A, B) ED+1 cells on the walls of the CUPE-NG; (C) Merged image of A and B (Scale bar=5 μm). The arrows indicate edge of the polymer being degraded; (D, E, F) Magnified images of A, B and C (Scale bar=2 μm).

3.4 Discussion

A variety of luminal fillers such collagen, microfilaments, aligned fibers, hydrogel microchannels, and Schwann cells, have been reported to enhance peripheral nerve regeneration across gap injuries (89, 90, 92, 102, 185, 186). Despite the observed growth-promoting effect of the luminal fillers, the opaque nature of the currently available nerve conduits prevents the identification of fabrication errors prior to implantation such as air bubbles, cell death, contamination, or misalignment of luminal structures. Here we demonstrated the use of CUPE as a biodegradable material with 70% light transmittance that allow the visualization of luminal filler integrity in nerve guides prior to implantation. The translucent nature of the CUPE conduits also provided confidence during the surgical implantation of the biosynthetic nerve, as compression or disruption of the luminal fillers are visualized and prevented during nerve stump insertion into the nerve guide, and nerve suturing can be more accurately approximated. Furthermore, the

CUPE conduits remained translucent after recovery from implantation even after 12 weeks, facilitating the inspection of luminal content and gross evaluation of nerve regeneration *in vivo* if needed. Peripheral nerves are normally under some tensile load, as evidenced by the fact that a nerve *in situ* retracts when severed. During limb movement, physical stresses are placed on peripheral nerve with tensile stress applied longitudinally resulting in steady elongation of the nerve which can reach 12 MPa. In the rabbit tibial nerve when the knee and ankle are each maintained at 90 degrees of flexion, the *in situ* strain is 11% (183).

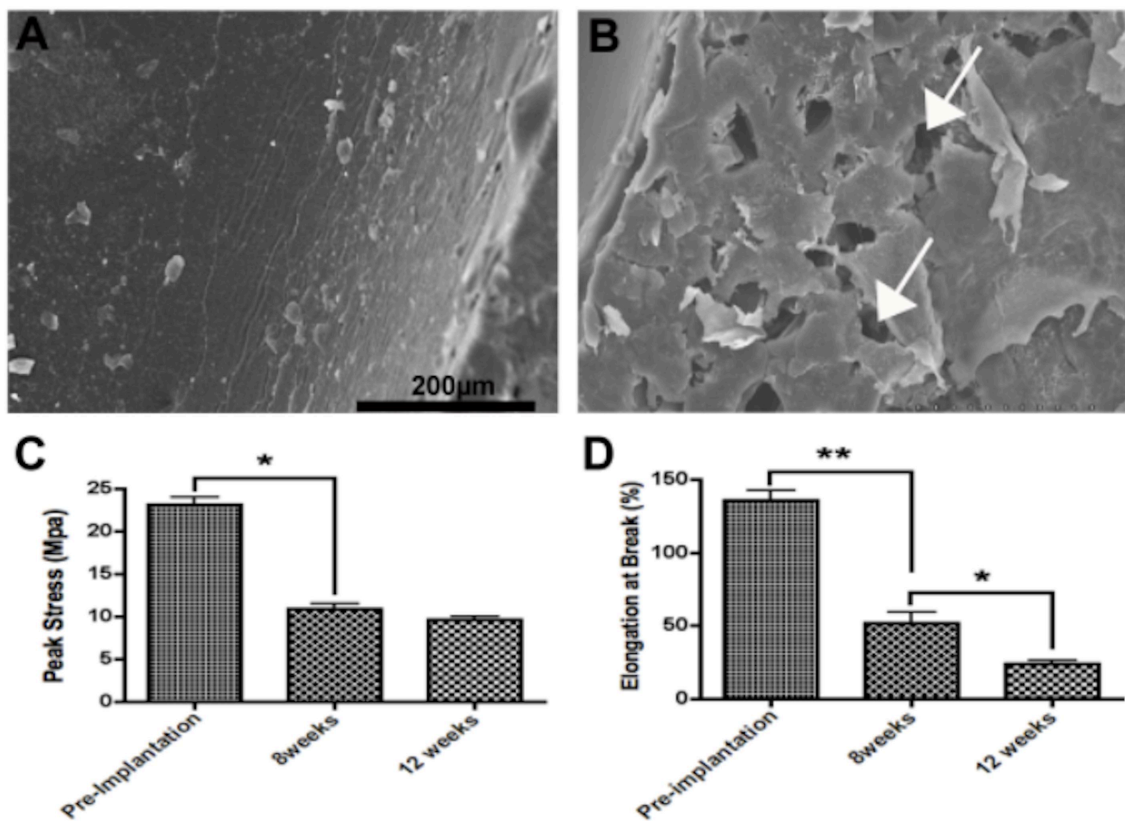


Figure 3.11: Scanning electron microscope (SEM) images of the CUPE-NG surface (A) before implantation and (B) 8 weeks after implantation, indicating the degradation of the NG over time (arrows point to the pores formed on the NG; Scale bar= 200 μm). Reduction in mechanical strength of CUPE-NGs after 8 and 12 weeks of implantation according to (C) Peak stress testing (* $p < 0.01$) and (D) Elongation at break (* $p < 0.01$, ** $p < 0.001$).

It is well established that Schwann cells promote axon regeneration, remyelination and improve functional recovery if placed in the lumen of biodegradable conduits, both in the peripheral

nerve (187) and the transected spinal cord (188, 189). However, some have reported disappointing nerve regeneration in Schwann cells containing conduits compared to autologous grafts (190).

While more research is needed to resolve this apparent controversy, the opaque nature of most nerve guides has limited the information that one can obtain from the luminal fillers. For instance, the number of surviving Schwann cells overtime inside the peripheral nerve conduits is unknown, thus the actual contribution of transplanted cells to integrate into host tissue and mediate functional improvement, remains to be determined. Furthermore, due to the large inflammatory response to the injury and implantation, it is highly likely that Schwann cells in the lumen of an implanted degradable conduits die shortly after transplantation. This clearly seems to be the case in the injured spinal cord, where most transplanted Schwann cells are known to die within two weeks post implantation due to necrosis and apoptosis (191). Clearly, survival of the transplanted cells is vital, and inadequate amount of these cells will hamper the repair process (186). Transparent conduits such as the CUPE nerve guides will facilitate proper evaluation of the transplanted cells within the tube prior to implantation, and assist in ascertaining cell survival after grafting. This approach can provide important insights as to specific contributions of luminal cells in nerve repair.

We observed that CUPE conduits are biocompatible and gradually reabsorbed. This was determined by the significant reduction in peak stress and elongation at break of the conduit after eight and twelve weeks of implantation, and confirmed by scanning electron microscopy showing several areas of polymer degradation in the same samples. Analysis of the immune response to the CUPE polymer revealed a very specific targeting of activated macrophages expressing lysosomal proteins recognized by the ED1 antibody, located inside the CUPE-NG, with almost no inflammation observed in the surrounding tissue. Since ED-1 staining was observed at the margins of the eroding zones within the conduit, it follows that the activated macrophages

are engaged in the enzymatic degradation of the polymer in a specific and restrictive manner. These observations support the use of CUPE conduits in peripheral nerve gap repair.

Furthermore, gross anatomical evaluation of nerve regeneration and histological visualization of regenerating axons in the distal end of the tube demonstrated successful nerve regeneration across a 15 mm gap using CUPE elastomeric conduits. However, the amount of nerve regeneration was significantly different between the collagen-filled NGs and those with collagen-filled multiple microchannels (i.e., BNI). Specifically, the number of NFP+ fibers was increased three-fold in the BNI as compared to the CUPE simple tubularization method. This result demonstrates that the multichannel luminal fillers are indeed beneficial for enticing and directing nerve regeneration across long gap injuries. This was further supported by the observed by the larger CMAPs recorded in the gastrocnemius muscle of animals with CUPE-BNI implant.

The robust increase in the number of axons regenerating across the multiluminal BNI could be the result of the restricted directional growth within the hydrogel macrochannels, as linear topographic cues are known to promote unidirectional nerve regeneration (90, 96). In addition, the multiluminal design provides a 60% increase in surface area compared to the empty tube, and this likely increases Schwann cell migration from both sides of the transected nerve facilitating axonal regeneration (18, 159, 192).

It also possible that higher concentration of various growth promoting factors released in the microchannels would be achieved in the microchannels compared to the simple conduits (18). Despite the observed increase in axonal regeneration and CMAP in the BNI-repaired animals, we were unable to observe a significant behavioral recovery in toe spreading after the 12 weeks compared to the NG group. This might be a result of muscle atrophy after nerve injury as we have observed muscle weight reduction of 60% within the first 6 weeks of injury. To alleviate this limitation in future studies, nerve electrical stimulation and treadmill training, which have been reported to stimulate axonal regeneration and functional recovery (18, 193), will need to be incorporated.

3.5 Conclusion

In Summary, the CUPE elastomer is has demonstrated transparency and biocompatibility to support its use in long gap peripheral nerve repair. Furthermore, multi luminal fillers enhanced axonal growth across long critical gaps and increase nerve conduction to the innervating muscles.

CHAPTER 4

FUTURE DIRECTIONS

4.1 Additional CUPE-NG assessments for clinical applications

CUPE proved to be an effective selection for nerve guide material. The CUPE-NGs were translucent before implantation and it helped in proper evaluation of the microchannel structures and loading of the collagen. After 8 weeks of implantation, the CUPE-NGs were similarly translucent which helped in visualization of nerve tissue regeneration across the length of the NG. There were no overt immune response to the CUPE-NG and a nice layer of tissue was surrounding the implant. ED-1 positive staining also revealed that the walls of the NGs are specifically targeted by the macrophages and the nerve tissue growing within the NGs are spared from these cells. Currently, this study was conducted in a rat sciatic nerve injury model to bridge a gap of 15mm. In future, extensive study needs to be carried out in larger animals such as rabbits and pigs to evaluate the immune response to this polymer. Furthermore, studies need to be done in a preclinical setting with primate models and if successful can be used for a clinical trial model. Also, in a 15mm CUPE-NG the agarose microchannels were completely intact and the regeneration was robust but in future the CUPE-NG needs to be tested for repair of gaps larger than 5cms. There are several FDA approved nerve guides currently available in the clinics for bridging of short gaps. Some of these NGs are made of collagen [Integra Sciences] (35, 179, 180), polyglycolic acid (PGA) [Synovis] (181, 182), and poly(di-lactide- ϵ -caprolactone) [Ascension] (35). These tubes do not have any luminal fillers and they are used in a single empty lumen approach. The CUPE-NGs with the agarose microchannels should be compared side to side in a future experimental design with all the FDA approved nerve guides to evaluate the best material for this approach.

The CUPE-NG was also tested as a spinal implant after complete spinal cord transection. There were no visible immune response to the biomaterial and there was nerve tissue regeneration inside these NGs as well as there were signs of vertebral column repair on top of the implant surface. Over all, CUPE-NGs could prove to be an efficient and effective solution for repairing traumatic peripheral nerve injuries and spinal cord injuries. Hence, further extensive characterization needs to be done on the CUPE-NGs to make way to the clinics for repair of long nerve injuries.

4.2 Combination of NGF/NT-3 and PTN for long gap repair

Despite recent studies demonstrating the added regenerative benefit of combinatorial treatments in the injured spinal cord (194, 195) and peripheral nerve (196), a systematic evaluation of combinatorial treatments that would promote peripheral nerve regeneration across critically long gaps remains unexplored. I hypothesize that combinatorial treatments aimed specifically at providing a suitable growth substrate to bridge the injury gap and a growth factor milieu that stimulates regeneration of most neuronal subpopulations in the peripheral nerve, will constitute a more robust and efficient method for the repair of critical long gap nerve injuries, which are currently poorly treated. To test this hypothesis we will have to systematically evaluate the relative regenerative potency of traditional growth factors from the neurotrophin family (nerve growth factor (NGF) and Neurotrophin-3 (NT-3)) alone or in combination to PTN. We recently obtained evidence that support the feasibility of this approach. In DRG explant cultures PTN was found to potentiate the axonal growth mediated by NGF and NT-3 added to the media. This preliminary study confirmed that the significant regenerative effect of NT-3/NGF can be further increased 2-3 folds by PTN. This result provides confidence that the NT-3/NGF and PTN combinatorial approach might indeed be able to stimulate an enhanced regenerative response across critically long peripheral nerve gaps.

Neurotrophic growth factors such as NGF and NT-3 are known to entice the regeneration of nociceptive and proprioceptive sensory neurons, respectively (197). In addition, PTN is known

to stimulate the regeneration of spinal cord motor neurons (124) and the proliferation and migration of Schwann cells, fibroblasts and endothelial cells (78, 160, 198). We postulate that multiluminal BNIs loaded with a combination of NGF, NT-3 and PTN in the microchannels will provide a more efficient regenerative strategy for the repair of critical long gap injuries. As shown in our Preliminary Studies, we have used polymeric growth factor encapsulation double emulsion evaporation method to produced bioactive VEGF and PTNPLGA microparticles with sustained release for at least 30 days. Here we will extend the fabrication of the polymeric microspheres to encapsulate and test the bioactivity of NGF and NT-3 alone, or in combination with PTN. In the first phase of this proposal, the drug load and release profiles, as well as their biological activity in eliciting axonal growth from neonatal DRGs will be carefully characterized.

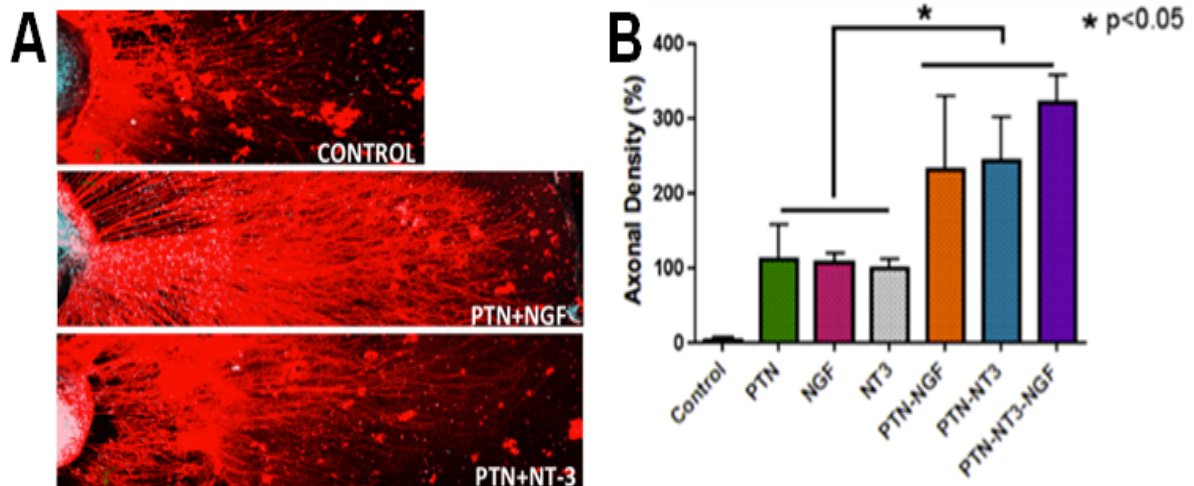


Figure 4.1: (A) DRG explants cultures from postnatal mice day 3 treated with combination of PTN and NT-3/NGF and the control group not treated with any growth factors. (B) Quantification of the axonal density from these explants cultures under the treatment of individual growth factors and combination of growth factors.

APPENDIX A

GROWTH FACTOR RELEASE MODELING WITHIN NERVE GUIDES OF COMPLEX
MATERIAL COMPOSITION

We recently reported the use of collagen-filled agarose multi luminal nerve guides as a method to linearly guide axonal regeneration after peripheral nerve gap injury repair (92). We have also demonstrated that poly lactic-co-glycolic acid (PLGA)-microparticles placed within the lumen of such microchannels provide sustained growth factor (GF) release, which in turns promotes cellular growth and tissue regeneration *in vitro*(130). However, the temporal dynamics of GF release within such multi-luminal nerve guides with complex material composition is unknown. Moreover, whether a particular luminal filler composition would offer optimal GF availability for nerve regeneration has not been determined. Here we design a mathematical model that predicts the spatial-temporal diffusion of GF within four types of materials including poly-lactic glycolic acid (PLGA), collagen, agarose, and extracellular fluid. This model was validated and used to compare the spatial-temporal GF diffusion rates across multiple physicochemical barriers (199-201). Three different types of luminal filler designs in nerve guides were compared: 1) Simple tube with GF, 2) BNI with GF within agarose microchannels and 3) BNI with GF-PLGA microparticles in collagen within agarose microchannels. The predicted GF release pattern was then used to select the most appropriate configuration for enticing nerve regeneration.

Growth factor diffusion is more symmetrical in the multiluminal nerve guides

The mathematical model was used to estimate the GF diffusion in four types of nerve conduits with increased complexity in luminal biomaterials composition: 1) simple conduit filled with GF/collagen, 2) conduit filled with agarose microchannels each filled with GF/collagen. 3) Simple conduit filled with GF-PLGA microparticles suspended in collagen, and 4) conduit filled with agarose microchannels each filled with GF-PLGA microparticles suspended in collagen. Our model showed that GF diffusion in the simple conduit filled with GF/collagen is asymmetrical due to increased diffusion at both ends of the conduit, which in turns forms bidirectional gradients from each end of the nerve guide, peaking at the center of the tube. In sharp contrast, GF diffusion in nerve guides containing agarose microchannels is more

symmetrical, as each microchannel filled with GF suspended in collagen, in addition of diffusing from both ends of the nerve guide, also diffuses into the agarose, which alters the diffusion dynamics in the nerve conduit with more linear concentration observed in the lumen of each microchannel. In the multiluminal agarose model, the GF is suspended in collagen and the total concentration is limited to the available volume within the microchannels. The total amount of initial GF is approximately 50% of that that can be loaded in the simple tube. The model also predicts a faster diffusion of the total GF load in the microchannels, which is estimated to elute 75% by 21 days and almost 90% at the end of the fourth week.

PLGA microparticles extend the GF release and reverse the diffusion dynamics.

The incorporation of GF-encapsulated PLGA microparticles to prolonged drug delivery in the lumen of the nerve guides was modeled for both the empty channel and the multiluminal conduit designs. The microparticles suspended in collagen generate small concentration peaks of GF according to the position of the microparticles in the lumen of each design, which is included an initial release burst over the first 24-48 hrs. In contrast to the diffusion models of GF suspended in the collagen, which is at maximum concentration from day 1, the use of GF-microparticles generates a much different effect as GF builds overtime both in the simple tube and in the multiluminal conduits, from very low levels at 48hrs to approximately 30ng/ml at the center of the simple tube by 21 days. Those levels remain constant at the center of the conduit from the 3rd week to the 30 days, indicating a more balanced dynamics between GF release and diffusion. In the multiluminal conduits, GF appears evenly diffused throughout the microchannels, as the microparticles suspended in collagen gradually release the growth factor, which in turn is diffusing both into the agarose and from both ends of the tube. This preparation maintains similar concentration of GF not only throughout the tube, but from 24hrs to 30 days, suggesting that this nerve guide design would better provide constant and uniform levels of growth factor along the nerve conduit a characteristic that is anticipated to be highly beneficial for nerve repair.

Visualization of the direct comparison of the average concentration for 30 days in the single channel and multiluminal arrangements with and without PLGA microparticles incorporated in the lumens clearly shows that GF release in simple conduits forms bidirectional gradients with epicenter at the middle of the tube, which is expected to limit nerve regeneration. In contrast, modeled GF diffusion in the lumen of agarose microchannels is more uniform, and controlled release from polymeric microparticles, can offer a more physiologically relevant GF distribution throughout the multiluminal nerve conduit.

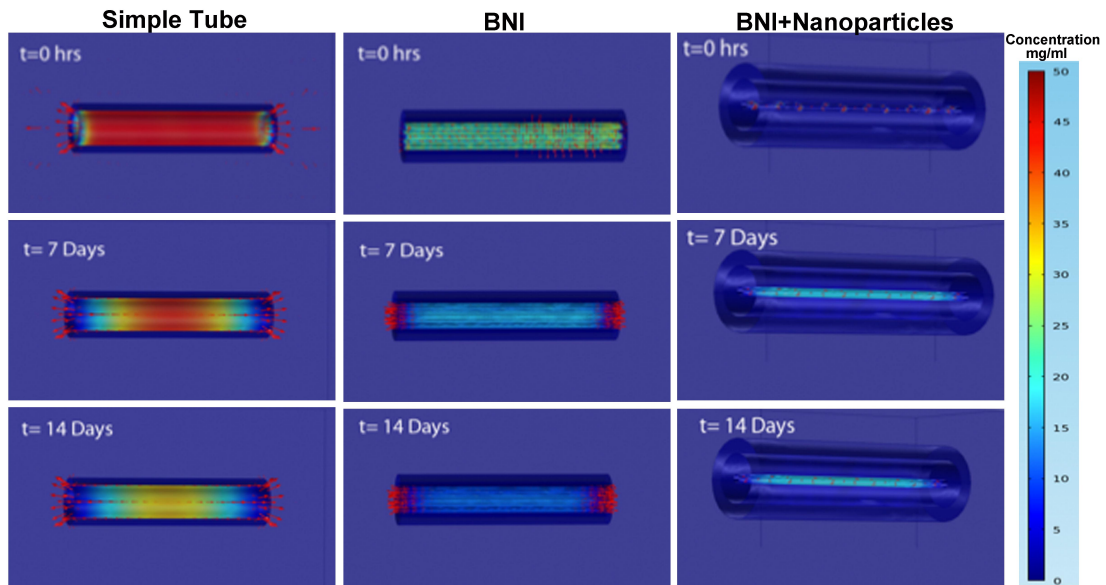


Figure: Comparison of Modeling of growth factor release among simple tube, BNI and BNI loaded with nanoparticles.

DISCUSSION

Several reports have demonstrated that nerve guides can be used successfully to enhance nerve regeneration across short gap defects (35). The regenerative effect is thought to rely in linearly restricting axonal growth. In addition, nerve conduits are thought to restrict GF diffusion from the lumen, thus forming a GF-enriched intraluminal milieu (202). To enhance even further nerve repair, GF have been delivered in the lumen of nerve conduits and reportedly have improved nerve repair and functional recovery(118). Despite such advances in the nerve

tissue engineering, GF release profiles in the nerve conduits have not been determined. In order to directly address this shortcoming, we developed a computer model that simulates GF diffusion in four specific types of nerve guides, from GF-collagen filled conduits, and to collagen-filled agarose microchannels with suspended GF-releasing PLGA microparticles. The mathematical modeling provides fundamental information to understand and predict the distribution of the GF concentration with different channel dimensions and filling material, when growth factor is the only exogenous material added. Moreover, it can provide an explanation to more complex designs (combination of several strategies; loading cells and growth factors) and possibly explain their less favorable result over the less complicated approach (203).

Existing drug delivery mathematical model have been limited to biodegradable polymer release and release from polymer matrixes(204, 205), and only few reports have described the kinetics of drug release and the diffusion into an external medium. A study reported the use of a multi particulate system with microcapsules where the release rate into a finite volume was estimated accurately (206). However, this model, cannot explain drug diffusion through a more complex environment. Here we described a multimediuum drug delivery mathematical model that incorporates several physical parameters such as diffusion, dissolution, and polymer degradation; and applies them into different spatiotemporal environments.

Our model showed that GF mixed in collagen accumulates in the center and diffuses at both ends of the conduit. This bilateral gradient might be suboptimal for axonal regeneration, as axons are known to follow increasing unilateral GF gradients(207). While direct axonal regeneration might not be enticed past the center of the tube if GF is at highest concentration there, if an appropriate GF to stimulate the migration of supportive glial Schwann cells from the distal and proximal nerve stumps is used, then these cells will aim at migrating to the center of the tube and in so doing, they would benefit nerve regeneration (208, 209). Specific experimental data would be necessary to determine whether enticing directly the axons or indirectly through Schwann cells migration would be better in terms of nerve repair and

functional recovery. Conversely, the use of polymeric GF release in the microchannels compared to GF loaded in the lumen of a single tube produces a more uniform distribution and constant concentration of GF throughout the tube overtime. Such GF diffusion dynamics are expected to favor nerve regeneration.

While the reported GF diffusion model has specific benefits in the design of nerve guides, the versatile capability of the mathematical model to incorporate defined volumes, solute release profiles and diffusion coefficient through multiple biomaterials such as collagen and agarose, strongly suggest that this modeling can also be useful for other tissue engineered scaffolds. For instance, bilateral GF concentration profiles such as that formed in the single lumen tubes can be also used to model cellular migration for bone regeneration or vascularization.

The limitation of the mathematical model of multi-medium drug delivery here reported is limited by some important assumptions such as the static nature and perfect spherical shape of the GF-loaded PLGA microparticles. It also fails to incorporate critical parameters involved in drug delivery such as temperature and pH that affect diffusion and drug release.

REFERENCES

1. Mohanna PN, Young RC, Wiberg M, Terenghi G. A composite poly-hydroxybutyrate-glial growth factor conduit for long nerve gap repairs. *J Anat.* 2003;203(6):553-65. Epub 2003/12/23. PubMed PMID: 14686691; PubMed Central PMCID: PMC1571193.
2. Chalfoun CT, Wirth GA, Evans GR. Tissue engineered nerve constructs: where do we stand? *J Cell Mol Med.* 2006;10(2):309-17. Epub 2006/06/27. doi: 010.002.05 [pii]. PubMed PMID: 16796801.
3. Noble J, Munro CA, Prasad VS, Midha R. Analysis of upper and lower extremity peripheral nerve injuries in a population of patients with multiple injuries. *J Trauma.* 1998;45(1):116-22. Epub 1998/07/29. PubMed PMID: 9680023.
4. Pondaag W, Malessy MJ, van Dijk JG, Thomeer RT. Natural history of obstetric brachial plexus palsy: a systematic review. *Dev Med Child Neurol.* 2004;46(2):138-44. Epub 2004/02/21. PubMed PMID: 14974639.
5. Hill BE, Williams G, Bialocerkowski AE. Clinimetric evaluation of questionnaires used to assess activity after traumatic brachial plexus injury in adults: a systematic review. *Arch Phys Med Rehabil.* 2011;92(12):2082-9. Epub 2011/12/03. doi: S0003-9993(11)00631-9 [pii] 10.1016/j.apmr.2011.07.188. PubMed PMID: 22133257.
6. Gaudet AD, Popovich PG, Ramer MS. Wallerian degeneration: gaining perspective on inflammatory events after peripheral nerve injury. *J Neuroinflammation.* 2011;8:110. Epub 2011/09/01. doi: 1742-2094-8-110 [pii] 10.1186/1742-2094-8-110. PubMed PMID: 21878126; PubMed Central PMCID: PMC3180276.
7. Lee SK, Wolfe SW. Peripheral nerve injury and repair. *The Journal of the American Academy of Orthopaedic Surgeons.* 2000;8(4):243-52. Epub 2000/08/22. PubMed PMID: 10951113.
8. Perry VH, Brown MC, Gordon S. The macrophage response to central and peripheral nerve injury. A possible role for macrophages in regeneration. *J Exp Med.* 1987;165(4):1218-23. Epub 1987/04/01. PubMed PMID: 3559478; PubMed Central PMCID: PMC2188570.
9. Stoll G, Muller HW. Nerve injury, axonal degeneration and neural regeneration: basic insights. *Brain Pathol.* 1999;9(2):313-25. Epub 1999/04/29. PubMed PMID: 10219748.
10. Arvidsson J, Ygge J, Grant G. Cell loss in lumbar dorsal root ganglia and transganglionic degeneration after sciatic nerve resection in the rat. *Brain Res.* 1986;373(1-2):15-21. Epub 1986/05/14. doi: 0006-8993(86)90310-0 [pii]. PubMed PMID: 3719303.
11. Tandrup T, Woolf CJ, Coggeshall RE. Delayed loss of small dorsal root ganglion cells after transection of the rat sciatic nerve. *J Comp Neurol.* 2000;422(2):172-80. Epub 2000/06/08. doi: 10.1002/(SICI)1096-9861(20000626)422:2<172::AID-CNE2>3.0.CO;2-H [pii]. PubMed PMID: 10842225.
12. Ygge J. Neuronal loss in lumbar dorsal root ganglia after proximal compared to distal sciatic nerve resection: a quantitative study in the rat. *Brain Res.* 1989;478(1):193-5. Epub 1989/01/23. doi: 0006-8993(89)91497-2 [pii]. PubMed PMID: 2924117.
13. Lowrie MB, Lavalette D, Davies CE. Time course of motoneurone death after neonatal sciatic nerve crush in the rat. *Dev Neurosci.* 1994;16(5-6):279-84. Epub 1994/01/01. PubMed PMID: 7768206.
14. Snider WD, Elliott JL, Yan Q. Axotomy-induced neuronal death during development. *J Neurobiol.* 1992;23(9):1231-46. Epub 1992/11/01. doi: 10.1002/neu.480230913. PubMed PMID: 1469386.
15. Tornqvist E, Aldskogius H. Motoneuron survival is not affected by the proximo-distal level of axotomy but by the possibility of regenerating axons to gain access to the distal nerve

- stump. *J Neurosci Res.* 1994;39(2):159-65. Epub 1994/10/01. doi: 10.1002/jnr.490390206. PubMed PMID: 7837285.
16. Kawamura Y, Dyck PJ. Permanent axotomy by amputation results in loss of motor neurons in man. *J Neuropathol Exp Neurol.* 1981;40(6):658-66. Epub 1981/11/01. PubMed PMID: 7299422.
 17. Fried K, Govrin-Lippmann R, Rosenthal F, Ellisman MH, Devor M. Ultrastructure of afferent axon endings in a neuroma. *J Neurocytol.* 1991;20(8):682-701. Epub 1991/08/01. PubMed PMID: 1719140.
 18. Deumens R, Bozkurt A, Meek MF, Marcus MA, Joosten EA, Weis J, et al. Repairing injured peripheral nerves: Bridging the gap. *Prog Neurobiol.* 2010;92(3):245-76. Epub 2010/10/19. doi: S0301-0082(10)00172-3 [pii] 10.1016/j.pneurobio.2010.10.002. PubMed PMID: 20950667.
 19. Allodi I, Udina E, Navarro X. Specificity of peripheral nerve regeneration: Interactions at the axon level. *Prog Neurobiol.* 2012;98(1):16-37. Epub 2012/05/23. doi: 10.1016/j.pneurobio.2012.05.005. PubMed PMID: 22609046.
 20. Domeniconi M, Filbin MT. Overcoming inhibitors in myelin to promote axonal regeneration. *Journal of the neurological sciences.* 2005;233(1-2):43-7. Epub 2005/06/14. doi: 10.1016/j.jns.2005.03.023. PubMed PMID: 15949495.
 21. Lindwall C, Kanje M. Retrograde axonal transport of JNK signaling molecules influence injury induced nuclear changes in p-c-Jun and ATF3 in adult rat sensory neurons. *Molecular and cellular neurosciences.* 2005;29(2):269-82. Epub 2005/05/25. doi: 10.1016/j.mcn.2005.03.002. PubMed PMID: 15911351.
 22. Navarro X, Vivo M, Valero-Cabre A. Neural plasticity after peripheral nerve injury and regeneration. *Prog Neurobiol.* 2007;82(4):163-201. Epub 2007/07/24. doi: S0301-0082(07)00109-8 [pii] 10.1016/j.pneurobio.2007.06.005. PubMed PMID: 17643733.
 23. Stoll G, Jander S, Myers RR. Degeneration and regeneration of the peripheral nervous system: from Augustus Waller's observations to neuroinflammation. *J Peripher Nerv Syst.* 2002;7(1):13-27. Epub 2002/04/10. PubMed PMID: 11939348.
 24. Deckwerth TL, Johnson EM, Jr. Neurites can remain viable after destruction of the neuronal soma by programmed cell death (apoptosis). *Dev Biol.* 1994;165(1):63-72. Epub 1994/09/01. doi: S0012-1606(84)71234-6 [pii] 10.1006/dbio.1994.1234. PubMed PMID: 8088451.
 25. Glass JD, Brushart TM, George EB, Griffin JW. Prolonged survival of transected nerve fibres in C57BL/Ola mice is an intrinsic characteristic of the axon. *J Neurocytol.* 1993;22(5):311-21. Epub 1993/05/01. PubMed PMID: 8315413.
 26. Ann ES, Mizoguchi A, Okajima S, Ide C. Motor axon terminal regeneration as studied by protein gene product 9.5 immunohistochemistry in the rat. *Arch Histol Cytol.* 1994;57(4):317-30. Epub 1994/10/01. PubMed PMID: 7880586.
 27. Son YJ, Thompson WJ. Schwann cell processes guide regeneration of peripheral axons. *Neuron.* 1995;14(1):125-32. Epub 1995/01/01. doi: 0896-6273(95)90246-5 [pii]. PubMed PMID: 7826630.
 28. Beirowski B, Adalbert R, Wagner D, Grumme DS, Addicks K, Ribchester RR, et al. The progressive nature of Wallerian degeneration in wild-type and slow Wallerian degeneration (WldS) nerves. *BMC Neurosci.* 2005;6:6. Epub 2005/02/03. doi: 1471-2202-6-6 [pii] 10.1186/1471-2202-6-6. PubMed PMID: 15686598; PubMed Central PMCID: PMC549193.
 29. Chaudhry V, Cornblath DR. Wallerian degeneration in human nerves: serial electrophysiological studies. *Muscle Nerve.* 1992;15(6):687-93. Epub 1992/06/01. doi: 10.1002/mus.880150610. PubMed PMID: 1324426.
 30. Lubinska L. Early course of Wallerian degeneration in myelinated fibres of the rat phrenic nerve. *Brain Res.* 1977;130(1):47-63. Epub 1977/07/08. doi: 0006-8993(77)90841-1 [pii]. PubMed PMID: 884520.

31. Markus A, Patel TD, Snider WD. Neurotrophic factors and axonal growth. *Curr Opin Neurobiol.* 2002;12(5):523-31. Epub 2002/10/09. doi: S0959438802003720 [pii]. PubMed PMID: 12367631.
32. Boyd JG, Gordon T. Neurotrophic factors and their receptors in axonal regeneration and functional recovery after peripheral nerve injury. *Mol Neurobiol.* 2003;27(3):277-324. Epub 2003/07/08. doi: MN:27:3:277 [pii] 10.1385/MN:27:3:277. PubMed PMID: 12845152.
33. Persson H, Ibanez CF. Role and expression of neurotrophins and the trk family of tyrosine kinase receptors in neural growth and rescue after injury. *Curr Opin Neurol Neurosurg.* 1993;6(1):11-8. Epub 1993/02/01. PubMed PMID: 8428057.
34. Pabari A, Yang SY, Seifalian AM, Mosahebi A. Modern surgical management of peripheral nerve gap. *J Plast Reconstr Aesthet Surg.* 2010;63(12):1941-8. Epub 2010/01/12. doi: S1748-6815(09)00862-6 [pii] 10.1016/j.bjps.2009.12.010. PubMed PMID: 20061198.
35. de Ruyter GC, Malessy MJ, Yaszemski MJ, Windebank AJ, Spinner RJ. Designing ideal conduits for peripheral nerve repair. *Neurosurgical focus.* 2009;26(2):E5. Epub 2009/05/14. doi: 10.3171/FOC.2009.26.2.E5. PubMed PMID: 19435445; PubMed Central PMCID: PMC2978041.
36. Daly W, Yao L, Zeugolis D, Windebank A, Pandit A. A biomaterials approach to peripheral nerve regeneration: bridging the peripheral nerve gap and enhancing functional recovery. *J R Soc Interface.* 2012;9(67):202-21. Epub 2011/11/18. doi: rsif.2011.0438 [pii] 10.1098/rsif.2011.0438. PubMed PMID: 22090283; PubMed Central PMCID: PMC3243399.
37. Moradzadeh A, Borschel GH, Luciano JP, Whitlock EL, Hayashi A, Hunter DA, et al. The impact of motor and sensory nerve architecture on nerve regeneration. *Experimental neurology.* 2008;212(2):370-6. Epub 2008/06/14. doi: S0014-4886(08)00165-9 [pii] 10.1016/j.expneurol.2008.04.012. PubMed PMID: 18550053; PubMed Central PMCID: PMC2761727.
38. Alluin O, Wittmann C, Marqueste T, Chabas JF, Garcia S, Lavaut MN, et al. Functional recovery after peripheral nerve injury and implantation of a collagen guide. *Biomaterials.* 2009;30(3):363-73. Epub 2008/10/22. doi: S0142-9612(08)00692-3 [pii] 10.1016/j.biomaterials.2008.09.043. PubMed PMID: 18929405.
39. Mackinnon SE, Doolabh VB, Novak CB, Trulock EP. Clinical outcome following nerve allograft transplantation. *Plast Reconstr Surg.* 2001;107(6):1419-29. Epub 2001/05/04. PubMed PMID: 11335811.
40. Siemionow M, Sonmez E. Nerve allograft transplantation: a review. *J Reconstr Microsurg.* 2007;23(8):511-20. Epub 2008/01/15. doi: 10.1055/s-2007-1022694. PubMed PMID: 18189213.
41. Ray WZ, Mackinnon SE. Management of nerve gaps: autografts, allografts, nerve transfers, and end-to-side neurorrhaphy. *Experimental neurology.* 2009;223(1):77-85. Epub 2009/04/08. doi: S0014-4886(09)00122-8 [pii] 10.1016/j.expneurol.2009.03.031. PubMed PMID: 19348799; PubMed Central PMCID: PMC2849924.
42. Chiono V, Tonda-Turo C, Ciardelli G. Chapter 9: Artificial scaffolds for peripheral nerve reconstruction. *Int Rev Neurobiol.* 2009;87:173-98. Epub 2009/08/18. doi: S0074-7742(09)87009-8 [pii] 10.1016/S0074-7742(09)87009-8. PubMed PMID: 19682638.
43. FF IJ, Van De Graaf RC, Meek MF. The early history of tubulation in nerve repair. *J Hand Surg Eur Vol.* 2008;33(5):581-6. Epub 2008/08/13. doi: 1753193408091349 [pii] 10.1177/1753193408091349. PubMed PMID: 18694914.
44. Braga-Silva J. The use of silicone tubing in the late repair of the median and ulnar nerves in the forearm. *J Hand Surg Br.* 1999;24(6):703-6. Epub 2000/02/15. doi: 10.1054/jhsb.1999.0276

- S0266-7681(99)90276-0 [pii]. PubMed PMID: 10672808.
45. Kehoe S, Zhang XF, Boyd D. FDA approved guidance conduits and wraps for peripheral nerve injury: a review of materials and efficacy. *Injury*. 2012;43(5):553-72. Epub 2011/01/29. doi: 10.1016/j.injury.2010.12.030. PubMed PMID: 21269624.
46. Kemp SW, Syed S, Walsh W, Zochodne DW, Midha R. Collagen nerve conduits promote enhanced axonal regeneration, schwann cell association, and neovascularization compared to silicone conduits. *Tissue Eng Part A*. 2009;15(8):1975-88. Epub 2009/02/07. doi: 10.1089/ten.tea.2008.0338
10.1089/ten.tea.2008.0338 [pii]. PubMed PMID: 19196132.
47. Brown JM, Shah MN, Mackinnon SE. Distal nerve transfers: a biology-based rationale. *Neurosurgical focus*. 2009;26(2):E12. Epub 2009/05/07. doi: 10.3171/FOC.2009.26.2.E12. PubMed PMID: 19416056.
48. Timmer M, Robben S, Muller-Ostermeyer F, Nikkhah G, Grothe C. Axonal regeneration across long gaps in silicone chambers filled with Schwann cells overexpressing high molecular weight FGF-2. *Cell Transplant*. 2003;12(3):265-77. Epub 2003/06/12. PubMed PMID: 12797381.
49. Nilsson A, Dahlin L, Lundborg G, Kanje M. Graft repair of a peripheral nerve without the sacrifice of a healthy donor nerve by the use of acutely dissociated autologous Schwann cells. *Scandinavian journal of plastic and reconstructive surgery and hand surgery / Nordisk plastikkirurgisk forening [and] Nordisk klubb for handkirurgi*. 2005;39(1):1-6. Epub 2005/04/26. doi: GABVJM7U3V7EVCMW [pii]
10.1080/02844310410017979. PubMed PMID: 15848958.
50. Haastert K, Lipokatic E, Fischer M, Timmer M, Grothe C. Differentially promoted peripheral nerve regeneration by grafted Schwann cells over-expressing different FGF-2 isoforms. *Neurobiology of disease*. 2006;21(1):138-53. Epub 2005/08/27. doi: 10.1016/j.nbd.2005.06.020. PubMed PMID: 16122933.
51. Hood B, Levene HB, Levi AD. Transplantation of autologous Schwann cells for the repair of segmental peripheral nerve defects. *Neurosurgical focus*. 2009;26(2):E4. Epub 2009/05/14. doi: 10.3171/FOC.2009.26.2.E4. PubMed PMID: 19435444.
52. Ngo TT, Waggoner PJ, Romero AA, Nelson KD, Eberhart RC, Smith GM. Poly(L-Lactide) microfilaments enhance peripheral nerve regeneration across extended nerve lesions. *J Neurosci Res*. 2003;72(2):227-38. Epub 2003/04/03. doi: 10.1002/jnr.10570. PubMed PMID: 12671998.
53. Okamoto H, Hata K, Kagami H, Okada K, Ito Y, Narita Y, et al. Recovery process of sciatic nerve defect with novel bioabsorbable collagen tubes packed with collagen filaments in dogs. *Journal of biomedical materials research Part A*. 2010;92(3):859-68. Epub 2009/03/13. doi: 10.1002/jbm.a.32421. PubMed PMID: 19280630.
54. Gordon T. The role of neurotrophic factors in nerve regeneration. *Neurosurgical focus*. 2009;26(2):E3. Epub 2009/02/21. doi: 10.3171/FOC.2009.26.2.E3
10.3171/FOC.2009.26.2.E3 [pii]. PubMed PMID: 19228105.
55. Koopmans G, Hasse B, Sinis N. Chapter 19: The role of collagen in peripheral nerve repair. *Int Rev Neurobiol*. 2009;87:363-79. Epub 2009/08/18. doi: 10.1016/S0074-7742(09)87019-0. PubMed PMID: 19682648.
56. Szpak P. Fish bone chemistry and ultrastructure: implications for taphonomy and stable isotope analysis. *Journal of Archaeological Science*. 2011.
57. Kadler KE, Hill A, Canty-Laird EG. Collagen fibrillogenesis: fibronectin, integrins, and minor collagens as organizers and nucleators. *Current opinion in cell biology*. 2008;20(5):495-501. Epub 2008/07/22. doi: 10.1016/j.ceb.2008.06.008. PubMed PMID: 18640274; PubMed Central PMCID: PMC2577133.
58. Armstrong SJ, Wiberg M, Terenghi G, Kingham PJ. ECM molecules mediate both Schwann cell proliferation and activation to enhance neurite outgrowth. *Tissue Eng*.

- 2007;13(12):2863-70. Epub 2007/08/31. doi: 10.1089/ten.2007.0055. PubMed PMID: 17727337.
59. Pankov R, Yamada KM. Fibronectin at a glance. *Journal of cell science*. 2002;115(Pt 20):3861-3. Epub 2002/09/24. PubMed PMID: 12244123.
60. de Ruitter GC, Malessy MJ, Alaid AO, Spinner RJ, Engelstad JK, Sorenson EJ, et al. Misdirection of regenerating motor axons after nerve injury and repair in the rat sciatic nerve model. *Experimental neurology*. 2008;211(2):339-50. Epub 2008/05/02. doi: S0014-4886(07)00497-9 [pii] 10.1016/j.expneurol.2007.12.023. PubMed PMID: 18448099.
61. Guenard V, Kleitman N, Morrissey TK, Bunge RP, Aebischer P. Syngeneic Schwann cells derived from adult nerves seeded in semipermeable guidance channels enhance peripheral nerve regeneration. *The Journal of neuroscience : the official journal of the Society for Neuroscience*. 1992;12(9):3310-20. Epub 1992/09/01. PubMed PMID: 1527582.
62. Anselin AD, Fink T, Davey DF. Peripheral nerve regeneration through nerve guides seeded with adult Schwann cells. *Neuropathology and applied neurobiology*. 1997;23(5):387-98. Epub 1997/11/19. PubMed PMID: 9364464.
63. Fang Y, Mo X, Guo W, Zhang M, Zhang P, Wang Y, et al. A new type of Schwann cell graft transplantation to promote optic nerve regeneration in adult rats. *Journal of tissue engineering and regenerative medicine*. 2010;4(8):581-9. Epub 2010/10/12. doi: 10.1002/term.264. PubMed PMID: 20936715.
64. Oudega M, Xu XM. Schwann cell transplantation for repair of the adult spinal cord. *J Neurotrauma*. 2006;23(3-4):453-67. Epub 2006/04/25. doi: 10.1089/neu.2006.23.453. PubMed PMID: 16629629.
65. Ishikawa N, Suzuki Y, Dezawa M, Kataoka K, Ohta M, Cho H, et al. Peripheral nerve regeneration by transplantation of BMSC-derived Schwann cells as chitosan gel sponge scaffolds. *Journal of biomedical materials research Part A*. 2009;89(4):1118-24. Epub 2009/04/04. doi: 10.1002/jbm.a.32389. PubMed PMID: 19343770.
66. Matsuse D, Kitada M, Kohama M, Nishikawa K, Makinoshima H, Wakao S, et al. Human umbilical cord-derived mesenchymal stromal cells differentiate into functional Schwann cells that sustain peripheral nerve regeneration. *J Neuropathol Exp Neurol*. 2010;69(9):973-85. Epub 2010/08/20. doi: 10.1097/NEN.0b013e3181eff6dc. PubMed PMID: 20720501.
67. Pereira Lopes FR, Frattini F, Marques SA, Almeida FM, de Moura Campos LC, Langone F, et al. Transplantation of bone-marrow-derived cells into a nerve guide resulted in transdifferentiation into Schwann cells and effective regeneration of transected mouse sciatic nerve. *Micron*. 2010;41(7):783-90. Epub 2010/08/24. doi: 10.1016/j.micron.2010.05.010. PubMed PMID: 20728816.
68. Raivich G, Hellweg R, Kreutzberg GW. NGF receptor-mediated reduction in axonal NGF uptake and retrograde transport following sciatic nerve injury and during regeneration. *Neuron*. 1991;7(1):151-64. Epub 1991/07/01. doi: 0896-6273(91)90083-C [pii]. PubMed PMID: 1648938.
69. Meyer M, Matsuoka I, Wetmore C, Olson L, Thoenen H. Enhanced synthesis of brain-derived neurotrophic factor in the lesioned peripheral nerve: different mechanisms are responsible for the regulation of BDNF and NGF mRNA. *J Cell Biol*. 1992;119(1):45-54. Epub 1992/10/01. PubMed PMID: 1527172; PubMed Central PMCID: PMC2289627.
70. Funakoshi H, Frisen J, Barbany G, Timmusk T, Zachrisson O, Verge VM, et al. Differential expression of mRNAs for neurotrophins and their receptors after axotomy of the sciatic nerve. *J Cell Biol*. 1993;123(2):455-65. Epub 1993/10/01. PubMed PMID: 8408225; PubMed Central PMCID: PMC2119843.
71. Harpf C, Dabernig J, Humpel C. Receptors for NGF and GDNF are highly expressed in human peripheral nerve neuroma. *Muscle Nerve*. 2002;25(4):612-5. Epub 2002/04/05. doi: 10.1002/mus.10103 [pii]. PubMed PMID: 11932982.

72. Donato R, Cheema S, Finkelstein D, Bartlett P, Morrison W. Role of leukaemia inhibitory factor (LIF) in rat peripheral nerve regeneration. *Ann Acad Med Singapore*. 1995;24(4 Suppl):94-100. Epub 1995/07/01. PubMed PMID: 8572536.
73. Sun W, Sun C, Lin H, Zhao H, Wang J, Ma H, et al. The effect of collagen-binding NGF-beta on the promotion of sciatic nerve regeneration in a rat sciatic nerve crush injury model. *Biomaterials*. 2009;30(27):4649-56. Epub 2009/07/04. doi: S0142-9612(09)00542-0 [pii] 10.1016/j.biomaterials.2009.05.037. PubMed PMID: 19573907.
74. Fine EG, Decosterd I, Papaloizos M, Zurn AD, Aebischer P. GDNF and NGF released by synthetic guidance channels support sciatic nerve regeneration across a long gap. *Eur J Neurosci*. 2002;15(4):589-601. Epub 2002/03/12. PubMed PMID: 11886440.
75. Lindsay RM. Nerve growth factors (NGF, BDNF) enhance axonal regeneration but are not required for survival of adult sensory neurons. *The Journal of neuroscience : the official journal of the Society for Neuroscience*. 1988;8(7):2394-405. Epub 1988/07/01. PubMed PMID: 3249232.
76. Sterne GD, Brown RA, Green CJ, Terenghi G. Neurotrophin-3 delivered locally via fibronectin mats enhances peripheral nerve regeneration. *Eur J Neurosci*. 1997;9(7):1388-96. Epub 1997/07/01. PubMed PMID: 9240396.
77. Romero MI, Rangappa N, Li L, Lightfoot E, Garry MG, Smith GM. Extensive sprouting of sensory afferents and hyperalgesia induced by conditional expression of nerve growth factor in the adult spinal cord. *The Journal of neuroscience : the official journal of the Society for Neuroscience*. 2000;20(12):4435-45. Epub 2000/06/14. doi: 20/12/4435 [pii]. PubMed PMID: 10844012.
78. Romero MI, Rangappa N, Garry MG, Smith GM. Functional regeneration of chronically injured sensory afferents into adult spinal cord after neurotrophin gene therapy. *The Journal of neuroscience : the official journal of the Society for Neuroscience*. 2001;21(21):8408-16. Epub 2001/10/19. doi: 21/21/8408 [pii]. PubMed PMID: 11606629.
79. Boyd JG, Gordon T. A dose-dependent facilitation and inhibition of peripheral nerve regeneration by brain-derived neurotrophic factor. *Eur J Neurosci*. 2002;15(4):613-26. Epub 2002/03/12. PubMed PMID: 11886442.
80. Midha R, Munro CA, Dalton PD, Tator CH, Shoichet MS. Growth factor enhancement of peripheral nerve regeneration through a novel synthetic hydrogel tube. *Journal of neurosurgery*. 2003;99(3):555-65. Epub 2003/09/10. doi: 10.3171/jns.2003.99.3.0555. PubMed PMID: 12959445.
81. Sun W, Sun C, Zhao H, Lin H, Han Q, Wang J, et al. Improvement of sciatic nerve regeneration using laminin-binding human NGF-beta. *PLoS One*. 2009;4(7):e6180. Epub 2009/07/10. doi: 10.1371/journal.pone.0006180. PubMed PMID: 19587785; PubMed Central PMCID: PMC2703785.
82. Wood MD, Hunter D, Mackinnon SE, Sakiyama-Elbert SE. Heparin-binding-affinity-based delivery systems releasing nerve growth factor enhance sciatic nerve regeneration. *J Biomater Sci Polym Ed*. 2010;21(6):771-87. Epub 2010/05/21. doi: 10.1163/156856209X445285. PubMed PMID: 20482984.
83. Romero MI, Lin L, Lush ME, Lei L, Parada LF, Zhu Y. Deletion of Nf1 in neurons induces increased axon collateral branching after dorsal root injury. *The Journal of neuroscience : the official journal of the Society for Neuroscience*. 2007;27(8):2124-34. Epub 2007/02/23. doi: 27/8/2124 [pii] 10.1523/JNEUROSCI.4363-06.2007. PubMed PMID: 17314307.
84. Patel M, Mao L, Wu B, Vandevord PJ. GDNF-chitosan blended nerve guides: a functional study. *Journal of tissue engineering and regenerative medicine*. 2007;1(5):360-7. Epub 2007/11/27. doi: 10.1002/term.44. PubMed PMID: 18038430.
85. Guzen FP, de Almeida Leme RJ, de Andrade MS, de Luca BA, Chadi G. Glial cell line-derived neurotrophic factor added to a sciatic nerve fragment grafted in a spinal cord gap ameliorates motor impairments in rats and increases local axonal growth. *Restor Neurol*

- Neurosci. 2009;27(1):1-16. Epub 2009/01/24. doi: 10.3233/RNN-2009-0454. PubMed PMID: 19164849.
86. Kokai LE, Ghaznavi AM, Marra KG. Incorporation of double-walled microspheres into polymer nerve guides for the sustained delivery of glial cell line-derived neurotrophic factor. *Biomaterials*. 2010;31(8):2313-22. Epub 2009/12/09. doi: S0142-9612(09)01319-2 [pii] 10.1016/j.biomaterials.2009.11.075. PubMed PMID: 19969346.
87. Boyd JG, Gordon T. Glial cell line-derived neurotrophic factor and brain-derived neurotrophic factor sustain the axonal regeneration of chronically axotomized motoneurons in vivo. *Experimental neurology*. 2003;183(2):610-9. Epub 2003/10/14. doi: S0014488603001833 [pii]. PubMed PMID: 14552902.
88. Magill CK, Moore AM, Yan Y, Tong AY, Macewan MR, Yee A, et al. The differential effects of pathway- versus target-derived glial cell line-derived neurotrophic factor on peripheral nerve regeneration. *Journal of neurosurgery*. 2009. Epub 2009/12/01. doi: 10.3171/2009.10.JNS091092. PubMed PMID: 19943736.
89. Cai J, Peng X, Nelson KD, Eberhart R, Smith GM. Permeable guidance channels containing microfilament scaffolds enhance axon growth and maturation. *Journal of biomedical materials research Part A*. 2005;75(2):374-86. Epub 2005/08/10. doi: 10.1002/jbm.a.30432. PubMed PMID: 16088902.
90. Kim YT, Haftel VK, Kumar S, Bellamkonda RV. The role of aligned polymer fiber-based constructs in the bridging of long peripheral nerve gaps. *Biomaterials*. 2008;29(21):3117-27. Epub 2008/05/02. doi: S0142-9612(08)00226-3 [pii] 10.1016/j.biomaterials.2008.03.042. PubMed PMID: 18448163; PubMed Central PMCID: PMC2483242.
91. Yao L, de Ruitter GC, Wang H, Knight AM, Spinner RJ, Yaszemski MJ, et al. Controlling dispersion of axonal regeneration using a multichannel collagen nerve conduit. *Biomaterials*. 2010;31(22):5789-97. Epub 2010/05/01. doi: 10.1016/j.biomaterials.2010.03.081. PubMed PMID: 20430432.
92. Tansey KE SJ, Botterman B, Delgado MR, Romero MI. Peripheral Nerve Repair Through Multi-Luminal Biosynthetic Implants. *Ann Biomed Eng* 2011. 2011(Epub ahead of print). Epub Feb 24., 2011.
93. Lundborg G, Dahlin L, Dohi D, Kanje M, Terada N. A new type of "bioartificial" nerve graft for bridging extended defects in nerves. *J Hand Surg Br*. 1997;22(3):299-303. Epub 1997/06/01. PubMed PMID: 9222905.
94. Itoh M, Fukumoto S, Iwamoto T, Mizuno A, Rokutanda A, Ishida HK, et al. Specificity of carbohydrate structures of gangliosides in the activity to regenerate the rat axotomized hypoglossal nerve. *Glycobiology*. 2001;11(2):125-30. Epub 2001/04/05. PubMed PMID: 11287399.
95. Hu W, Gu J, Deng A, Gu X. Polyglycolic acid filaments guide Schwann cell migration in vitro and in vivo. *Biotechnol Lett*. 2008;30(11):1937-42. Epub 2008/07/10. doi: 10.1007/s10529-008-9795-1. PubMed PMID: 18612593.
96. Clements IP, Kim YT, English AW, Lu X, Chung A, Bellamkonda RV. Thin-film enhanced nerve guidance channels for peripheral nerve repair. *Biomaterials*. 2009;30(23-24):3834-46. Epub 2009/05/19. doi: S0142-9612(09)00417-7 [pii] 10.1016/j.biomaterials.2009.04.022. PubMed PMID: 19446873; PubMed Central PMCID: PMC2753861.
97. de Ruitter GC, Spinner RJ, Malessy MJ, Moore MJ, Sorenson EJ, Currier BL, et al. Accuracy of motor axon regeneration across autograft, single-lumen, and multichannel poly(lactic-co-glycolic acid) nerve tubes. *Neurosurgery*. 2008;63(1):144-53; discussion 53-5. Epub 2008/08/30. doi: 10.1227/01.NEU.0000335081.47352.78 00006123-200807000-00017 [pii]. PubMed PMID: 18728579.
98. de Ruitter GC, Onyeneho IA, Liang ET, Moore MJ, Knight AM, Malessy MJ, et al. Methods for in vitro characterization of multichannel nerve tubes. *Journal of biomedical*

- materials research Part A. 2008;84(3):643-51. Epub 2007/07/20. doi: 10.1002/jbm.a.31298. PubMed PMID: 17635012.
99. Matsumoto K, Ohnishi K, Sekine T, Ueda H, Yamamoto Y, Kiyotani T, et al. Use of a newly developed artificial nerve conduit to assist peripheral nerve regeneration across a long gap in dogs. *ASAIO J.* 2000;46(4):415-20. Epub 2000/08/05. PubMed PMID: 10926137.
100. Whitlock EL, Tuffaha SH, Luciano JP, Yan Y, Hunter DA, Magill CK, et al. Processed allografts and type I collagen conduits for repair of peripheral nerve gaps. *Muscle Nerve.* 2009;39(6):787-99. Epub 2009/03/18. doi: 10.1002/mus.21220. PubMed PMID: 19291791.
101. Hess JR, Brenner MJ, Fox IK, Nichols CM, Myckatyn TM, Hunter DA, et al. Use of cold-preserved allografts seeded with autologous Schwann cells in the treatment of a long-gap peripheral nerve injury. *Plast Reconstr Surg.* 2007;119(1):246-59. Epub 2007/01/27. doi: 10.1097/01.prs.0000245341.71666.97
00006534-200701000-00035 [pii]. PubMed PMID: 17255680.
102. Sinis N, Schaller HE, Becker ST, Schlosshauer B, Doser M, Roesner H, et al. Long nerve gaps limit the regenerative potential of bioartificial nerve conduits filled with Schwann cells. *Restor Neurol Neurosci.* 2007;25(2):131-41. Epub 2007/08/30. PubMed PMID: 17726272.
103. Kim BS, Yoo JJ, Atala A. Peripheral nerve regeneration using acellular nerve grafts. *Journal of biomedical materials research Part A.* 2004;68(2):201-9. Epub 2004/01/06. doi: 10.1002/jbm.a.10045. PubMed PMID: 14704961.
104. Suzuki K, Kawauchi A, Nakamura T, Itoi S, Ito T, So J, et al. Histologic and electrophysiological study of nerve regeneration using a polyglycolic acid-collagen nerve conduit filled with collagen sponge in canine model. *Urology.* 2009;74(4):958-63. Epub 2009/08/18. doi: S0090-4295(09)00328-8 [pii]
10.1016/j.urology.2009.02.057. PubMed PMID: 19683805.
105. Yan H, Zhang F, Chen MB, Lineaweaver WC. Chapter 10: Conduit luminal additives for peripheral nerve repair. *Int Rev Neurobiol.* 2009;87:199-225. Epub 2009/08/18. doi: S0074-7742(09)87010-4 [pii]
10.1016/S0074-7742(09)87010-4. PubMed PMID: 19682639.
106. Hadlock T, Sundback C, Hunter D, Cheney M, Vacanti JP. A polymer foam conduit seeded with Schwann cells promotes guided peripheral nerve regeneration. *Tissue Eng.* 2000;6(2):119-27.
107. Dey J, Xu H, Nguyen KT, Yang J. Crosslinked urethane doped polyester biphasic scaffolds: Potential for in vivo vascular tissue engineering. *Journal of biomedical materials research Part A.* 2010;95(2):361-70. Epub 2010/07/16. doi: 10.1002/jbm.a.32846. PubMed PMID: 20629026; PubMed Central PMCID: PMC2944010.
108. Dey J, Xu H, Shen J, Thevenot P, Gondi SR, Nguyen KT, et al. Development of biodegradable crosslinked urethane-doped polyester elastomers. *Biomaterials.* 2008;29(35):4637-49. Epub 2008/09/20. doi: S0142-9612(08)00605-4 [pii]
10.1016/j.biomaterials.2008.08.020. PubMed PMID: 18801566; PubMed Central PMCID: PMC2747515.
109. Chen MB, Zhang F, Lineaweaver WC. Luminal fillers in nerve conduits for peripheral nerve repair. *Ann Plast Surg.* 2006;57(4):462-71. Epub 2006/09/26. doi: 10.1097/01.sap.0000237577.07219.b6
00000637-200610000-00021 [pii]. PubMed PMID: 16998343.
110. Yoshii S, Ito S, Shima M, Taniguchi A, Akagi M. Functional restoration of rabbit spinal cord using collagen-filament scaffold. *Journal of tissue engineering and regenerative medicine.* 2008. Epub 2008/11/18. doi: 10.1002/term.130. PubMed PMID: 19012267.
111. Al-Majed AA, Neumann CM, Brushart TM, Gordon T. Brief electrical stimulation promotes the speed and accuracy of motor axonal regeneration. *The Journal of neuroscience : the official journal of the Society for Neuroscience.* 2000;20(7):2602-8.

112. Schmidt CE, Leach JB. Neural tissue engineering: strategies for repair and regeneration. *Annu Rev Biomed Eng.* 2003;5:293-347. Epub 2003/10/07. doi: 10.1146/annurev.bioeng.5.011303.120731. PubMed PMID: 14527315.
113. Gordon T, Sulaiman O, Boyd JG. Experimental strategies to promote functional recovery after peripheral nerve injuries. *J Peripher Nerv Syst.* 2003;8(4):236-50. Epub 2003/12/04. PubMed PMID: 14641648.
114. Pellegrino RG, Politis MJ, Ritchie JM, Spencer PS. Events in degenerating cat peripheral nerve: induction of Schwann cell S phase and its relation to nerve fibre degeneration. *J Neurocytol.* 1986;15(1):17-28. Epub 1986/02/01. PubMed PMID: 3086507.
115. Wood MD, Moore AM, Hunter DA, Tuffaha S, Borschel GH, Mackinnon SE, et al. Affinity-based release of glial-derived neurotrophic factor from fibrin matrices enhances sciatic nerve regeneration. *Acta Biomater.* 2009;5(4):959-68. Epub 2008/12/24. doi: S1742-7061(08)00358-9 [pii] 10.1016/j.actbio.2008.11.008. PubMed PMID: 19103514; PubMed Central PMCID: PMC2678870.
116. Wood MD, Borschel GH, Sakiyama-Elbert SE. Controlled release of glial-derived neurotrophic factor from fibrin matrices containing an affinity-based delivery system. *Journal of biomedical materials research Part A.* 2009;89(4):909-18. Epub 2008/05/10. doi: 10.1002/jbm.a.32043. PubMed PMID: 18465825.
117. Wang CY, Liu JJ, Fan CY, Mo XM, Ruan HJ, Li FF. The effect of aligned core-shell nanofibres delivering NGF on the promotion of sciatic nerve regeneration. *J Biomater Sci Polym Ed.* 2012;23(1-4):167-84. Epub 2011/01/05. doi: jbs3255 [pii] 10.1163/092050610X545805. PubMed PMID: 21192836.
118. Pfister LA, Papaloizos M, Merkle HP, Gander B. Nerve conduits and growth factor delivery in peripheral nerve repair. *J Peripher Nerv Syst.* 2007;12(2):65-82. Epub 2007/06/15. doi: 10.1111/j.1529-8027.2007.00125.x. PubMed PMID: 17565531.
119. Rabinovsky ED. The multifunctional role of IGF-1 in peripheral nerve regeneration. *Neurological research.* 2004;26(2):204-10. Epub 2004/04/10. doi: 10.1179/016164104225013851. PubMed PMID: 15072640.
120. Rabinovsky ED, Draghia-Akli R. Insulin-like growth factor I plasmid therapy promotes in vivo angiogenesis. *Molecular therapy : the journal of the American Society of Gene Therapy.* 2004;9(1):46-55. Epub 2004/01/27. PubMed PMID: 14741777.
121. Aebischer P, Salessiotis AN, Winn SR. Basic fibroblast growth factor released from synthetic guidance channels facilitates peripheral nerve regeneration across long nerve gaps. *J Neurosci Res.* 1989;23(3):282-9. Epub 1989/07/01. doi: 10.1002/jnr.490230306. PubMed PMID: 2769793.
122. Hobson MI. Increased vascularisation enhances axonal regeneration within an acellular nerve conduit. *Ann R Coll Surg Engl.* 2002;84(1):47-53. Epub 2002/03/14. PubMed PMID: 11890626; PubMed Central PMCID: PMC2503765.
123. Zachary I. Neuroprotective role of vascular endothelial growth factor: signalling mechanisms, biological function, and therapeutic potential. *Neurosignals.* 2005;14(5):207-21. Epub 2005/11/23. doi: 88637 [pii] 10.1159/000088637. PubMed PMID: 16301836.
124. Mi R, Chen W, Hoke A. Pleiotrophin is a neurotrophic factor for spinal motor neurons. *Proc Natl Acad Sci U S A.* 2007;104(11):4664-9. Epub 2007/03/16. doi: 10.1073/pnas.0603243104. PubMed PMID: 17360581; PubMed Central PMCID: PMC1838658.
125. Islamov RR, Chintalgattu V, Pak ES, Katwa LC, Murashov AK. Induction of VEGF and its Flt-1 receptor after sciatic nerve crush injury. *Neuroreport.* 2004;15(13):2117-21. Epub 2004/10/16. doi: 00001756-200409150-00024 [pii]. PubMed PMID: 15486493.
126. Sondell M, Lundborg G, Kanje M. Vascular endothelial growth factor stimulates Schwann cell invasion and neovascularization of acellular nerve grafts. *Brain Res.*

- 1999;846(2):219-28. Epub 1999/11/11. doi: S0006-8993(99)02056-9 [pii]. PubMed PMID: 10556639.
127. Deuel TF, Zhang N, Yeh HJ, Silos-Santiago I, Wang ZY. Pleiotrophin: a cytokine with diverse functions and a novel signaling pathway. *Arch Biochem Biophys*. 2002;397(2):162-71. Epub 2002/02/14. doi: 10.1006/abbi.2001.2705 S0003986101927055 [pii]. PubMed PMID: 11795867.
128. Li YS, Milner PG, Chauhan AK, Watson MA, Hoffman RM, Kodner CM, et al. Cloning and expression of a developmentally regulated protein that induces mitogenic and neurite outgrowth activity. *Science*. 1990;250(4988):1690-4. Epub 1990/12/21. PubMed PMID: 2270483.
129. Blondet B, Carpentier G, Lafdil F, Courty J. Pleiotrophin cellular localization in nerve regeneration after peripheral nerve injury. *J Histochem Cytochem*. 2005;53(8):971-7. Epub 2005/08/02. doi: 53/8/971 [pii] 10.1369/jhc.4A6574.2005. PubMed PMID: 16055750.
130. A. F. Dawood PL, S. N. Dash, S. K. Kona, K. T. Nguyen and Mario I. Romero-Ortega. VEGF Release in Multiluminal Hydrogels Directs Angiogenesis from Adult Vasculature In Vitro. *CARDIOVASCULAR ENGINEERING AND TECHNOLOGY*. 2011.
131. Kona S, Specht D, Rahimi M, Shah BP, Gilbertson TA, Nguyen KT. Targeted biodegradable nanoparticles for drug delivery to smooth muscle cells. *J Nanosci Nanotechnol*. 2012;12(1):236-44. Epub 2012/04/25. PubMed PMID: 22523971.
132. Seifert JL, Bell JE, Elmer BB, Sucato DJ, Romero MI. Characterization of a novel bidirectional distraction spinal cord injury animal model. *Journal of neuroscience methods*. 2011;197(1):97-103. Epub 2011/02/22. doi: 10.1016/j.jneumeth.2011.02.003. PubMed PMID: 21334381.
133. Mizobuchi S, Matsuoka Y, Obata N, Kaku R, Itano Y, Tomotsuka N, et al. Antinociceptive effects of intrathecal landiolol injection in a rat formalin pain model. *Acta medica Okayama*. 2012;66(3):285-9. Epub 2012/06/26. PubMed PMID: 22729110.
134. Mark A. Suckow KASaRPW. *The Laboratory Rabbit, Guinea Pig, Hamster, and Other Rodents*
135. Recknor JBaSKM. *Nerve Regeneration: Tissue Engineering Strategies. The Biomedical Engineering Handbook: Tissue Engineering and Artificial Organs*. 2006.
136. Fu SY, Gordon T. The cellular and molecular basis of peripheral nerve regeneration. *Mol Neurobiol*. 1997;14(1-2):67-116. Epub 1997/02/01. doi: 10.1007/BF02740621. PubMed PMID: 9170101.
137. Tria MA, Fusco M, Vantini G, Mariot R. Pharmacokinetics of nerve growth factor (NGF) following different routes of administration to adult rats. *Experimental neurology*. 1994;127(2):178-83. Epub 1994/06/01. doi: 10.1006/exnr.1994.1093. PubMed PMID: 8033961.
138. Lee AC, Yu VM, Lowe JB, 3rd, Brenner MJ, Hunter DA, Mackinnon SE, et al. Controlled release of nerve growth factor enhances sciatic nerve regeneration. *Experimental neurology*. 2003;184(1):295-303. Epub 2003/11/26. doi: S0014488603002589 [pii]. PubMed PMID: 14637100.
139. Terris DJ, Toft KM, Moir M, Lum J, Wang M. Brain-derived neurotrophic factor-enriched collagen tubule as a substitute for autologous nerve grafts. *Archives of otolaryngology--head & neck surgery*. 2001;127(3):294-8. Epub 2001/03/20. PubMed PMID: 11255474.
140. Ohta M, Suzuki Y, Chou H, Ishikawa N, Suzuki S, Tanihara M, et al. Novel heparin/alginate gel combined with basic fibroblast growth factor promotes nerve regeneration in rat sciatic nerve. *Journal of biomedical materials research Part A*. 2004;71(4):661-8. Epub 2004/10/27. doi: 10.1002/jbm.a.30194. PubMed PMID: 15505831.
141. Hobson MI, Green CJ, Terenghi G. VEGF enhances intraneural angiogenesis and improves nerve regeneration after axotomy. *J Anat*. 2000;197 Pt 4:591-605. Epub 2001/02/24. PubMed PMID: 11197533; PubMed Central PMCID: PMC1468175.

142. Wells MR, Kraus K, Batter DK, Blunt DG, Weremowitz J, Lynch SE, et al. Gel matrix vehicles for growth factor application in nerve gap injuries repaired with tubes: a comparison of biomatrix, collagen, and methylcellulose. *Experimental neurology*. 1997;146(2):395-402. Epub 1997/08/01. doi: S0014-4886(97)96543-2 [pii] 10.1006/exnr.1997.6543. PubMed PMID: 9270050.
143. Mohanna PN, Terenghi G, Wiberg M. Composite PHB-GGF conduit for long nerve gap repair: a long-term evaluation. *Scandinavian journal of plastic and reconstructive surgery and hand surgery / Nordisk plastikkirurgisk forening [and] Nordisk klubb for handkirurgi*. 2005;39(3):129-37. Epub 2005/07/16. doi: P575387510XH361W [pii] 10.1080/02844310510006295. PubMed PMID: 16019744.
144. McKay Hart A, Wiberg M, Terenghi G. Exogenous leukaemia inhibitory factor enhances nerve regeneration after late secondary repair using a bioartificial nerve conduit. *Br J Plast Surg*. 2003;56(5):444-50. Epub 2003/08/02. doi: S0007122603001346 [pii]. PubMed PMID: 12890457.
145. Menei P, Pean JM, Nerriere-Daguin V, Jollivet C, Brachet P, Benoit JP. Intracerebral implantation of NGF-releasing biodegradable microspheres protects striatum against excitotoxic damage. *Experimental neurology*. 2000;161(1):259-72. Epub 2000/02/23. doi: 10.1006/exnr.1999.7253. PubMed PMID: 10683292.
146. Pean JM, Menei P, Morel O, Montero-Menei CN, Benoit JP. Intraseptal implantation of NGF-releasing microspheres promote the survival of axotomized cholinergic neurons. *Biomaterials*. 2000;21(20):2097-101. Epub 2000/08/31. PubMed PMID: 10966020.
147. Xu X, Yee WC, Hwang PY, Yu H, Wan AC, Gao S, et al. Peripheral nerve regeneration with sustained release of poly(phosphoester) microencapsulated nerve growth factor within nerve guide conduits. *Biomaterials*. 2003;24(13):2405-12. Epub 2003/04/18. doi: S0142961203001091 [pii]. PubMed PMID: 12699678.
148. Apel PJ, Garrett JP, Sierpinski P, Ma J, Atala A, Smith TL, et al. Peripheral nerve regeneration using a keratin-based scaffold: long-term functional and histological outcomes in a mouse model. *J Hand Surg Am*. 2008;33(9):1541-7. Epub 2008/11/06. doi: S0363-5023(08)00460-7 [pii] 10.1016/j.jhsa.2008.05.034. PubMed PMID: 18984336.
149. Solomon LB, Ferris L, Tedman R, Henneberg M. Surgical anatomy of the sural and superficial fibular nerves with an emphasis on the approach to the lateral malleolus. *J Anat*. 2001;199(Pt 6):717-23. Epub 2002/01/15. PubMed PMID: 11787825; PubMed Central PMCID: PMC1468389.
150. Schmitz HC, Beer GM. The toe-spreading reflex of the rabbit revisited--functional evaluation of complete peroneal nerve lesions. *Laboratory animals*. 2001;35(4):340-5. Epub 2001/10/24. PubMed PMID: 11669318.
151. Hu J, Zhu QT, Liu XL, Xu YB, Zhu JK. Repair of extended peripheral nerve lesions in rhesus monkeys using acellular allogenic nerve grafts implanted with autologous mesenchymal stem cells. *Experimental neurology*. 2007;204(2):658-66. Epub 2007/02/24. doi: S0014-4886(06)00651-0 [pii] 10.1016/j.expneurol.2006.11.018. PubMed PMID: 17316613.
152. Matsumoto K, Ohnishi K, Kiyotani T, Sekine T, Ueda H, Nakamura T, et al. Peripheral nerve regeneration across an 80-mm gap bridged by a polyglycolic acid (PGA)-collagen tube filled with laminin-coated collagen fibers: a histological and electrophysiological evaluation of regenerated nerves. *Brain Res*. 2000;868(2):315-28. Epub 2000/06/16. PubMed PMID: 10854584.
153. Yoshii S, Oka M. Collagen filaments as a scaffold for nerve regeneration. *Journal of biomedical materials research*. 2001;56(3):400-5. Epub 2001/05/24. doi: 10.1002/1097-4636(20010905)56:3<400::AID-JBM1109>3.0.CO;2-7 [pii]. PubMed PMID: 11372058.

154. Yoshii S, Oka M, Shima M, Taniguchi A, Akagi M. Bridging a 30-mm nerve defect using collagen filaments. *Journal of biomedical materials research Part A*. 2003;67(2):467-74. Epub 2003/10/21. doi: 10.1002/jbm.a.10103. PubMed PMID: 14566787.
155. Labrador RO, Buti M, Navarro X. Influence of collagen and laminin gels concentration on nerve regeneration after resection and tube repair. *Experimental neurology*. 1998;149(1):243-52. Epub 1998/02/10. doi: S0014-4886(97)96650-4 [pii] 10.1006/exnr.1997.6650. PubMed PMID: 9454634.
156. Huang EJ, Reichardt LF. Trk receptors: roles in neuronal signal transduction. *Annu Rev Biochem*. 2003;72:609-42. Epub 2003/04/05. doi: 10.1146/annurev.biochem.72.121801.161629 121801.161629 [pii]. PubMed PMID: 12676795.
157. Lin LF, Doherty DH, Lile JD, Bektesh S, Collins F. GDNF: a glial cell line-derived neurotrophic factor for midbrain dopaminergic neurons. *Science*. 1993;260(5111):1130-2. Epub 1993/05/21. PubMed PMID: 8493557.
158. Ho PR, Coan GM, Cheng ET, Niell C, Tarn DM, Zhou H, et al. Repair with collagen tubules linked with brain-derived neurotrophic factor and ciliary neurotrophic factor in a rat sciatic nerve injury model. *Archives of otolaryngology--head & neck surgery*. 1998;124(7):761-6. Epub 1998/07/24. PubMed PMID: 9677110.
159. Weis J, May R, Schroder JM. Fine structural and immunohistochemical identification of perineurial cells connecting proximal and distal stumps of transected peripheral nerves at early stages of regeneration in silicone tubes. *Acta Neuropathol*. 1994;88(2):159-65. Epub 1994/01/01. PubMed PMID: 7985496.
160. Hoke A, Redett R, Hameed H, Jari R, Zhou C, Li ZB, et al. Schwann cells express motor and sensory phenotypes that regulate axon regeneration. *The Journal of neuroscience : the official journal of the Society for Neuroscience*. 2006;26(38):9646-55. Epub 2006/09/22. doi: 26/38/9646 [pii] 10.1523/JNEUROSCI.1620-06.2006. PubMed PMID: 16988035.
161. Blondet B, Carpentier G, Ferry A, Courty J. Exogenous pleiotrophin applied to lesioned nerve impairs muscle reinnervation. *Neurochem Res*. 2006;31(7):907-13. Epub 2006/06/29. doi: 10.1007/s11064-006-9095-x. PubMed PMID: 16804756.
162. Jin L, Jianghai C, Juan L, Hao K, Ruiz de Almodovar C, Lambrechts D, et al. Pleiotrophin and peripheral nerve injury Role and therapeutic potential of VEGF in the nervous system. *Neurosurg Rev*. 2009;32(4):387-93. Epub 2009/05/09 2009/04/04. doi: 10.1007/s10143-009-0202-8 89/2/607 [pii] 10.1152/physrev.00031.2008. PubMed PMID: 19424734.
163. Mi R, Chen W, Höke A. Pleiotrophin is a neurotrophic factor for spinal motor neurons. *Proceedings of the National Academy of Sciences*. 2007;104(11):4664.
164. Zhang N, Deuel T. Pleiotrophin and midkine, a family of mitogenic and angiogenic heparin-binding growth and differentiation factors. *Current Opinion in Hematology*. 1999;6(1):44.
165. Yeh H, He Y, Xu J, Hsu C, Deuel T. Upregulation of pleiotrophin gene expression in developing microvasculature, macrophages, and astrocytes after acute ischemic brain injury. *Journal of Neuroscience*. 1998;18(10):3699.
166. Jin L, Jianghai C, Juan L, Hao K. Pleiotrophin and peripheral nerve injury. *Neurosurg Rev*. 2009;32(4):387-93. Epub 2009/05/09. doi: 10.1007/s10143-009-0202-8. PubMed PMID: 19424734.
167. Yu CQ, Zhang M, Matis KI, Kim C, Rosenblatt MI. Vascular endothelial growth factor mediates corneal nerve repair. *Investigative ophthalmology & visual science*. 2008;49(9):3870-8. Epub 2008/05/20. doi: iovs.07-1418 [pii] 10.1167/iov.07-1418. PubMed PMID: 18487369.

168. Rovak JM, Mungara AK, Aydin MA, Cederna PS. Effects of vascular endothelial growth factor on nerve regeneration in acellular nerve grafts. *J Reconstr Microsurg.* 2004;20(1):53-8. Epub 2004/02/20. doi: 10.1055/s-2004-818050. PubMed PMID: 14973776.
169. Ruiz de Almodovar C, Lambrechts D, Mazzone M, Carmeliet P. Role and therapeutic potential of VEGF in the nervous system. *Physiol Rev.* 2009;89(2):607-48. Epub 2009/04/04. doi: 89/2/607 [pii] 10.1152/physrev.00031.2008 [doi]. PubMed PMID: 19342615.
170. Haninec P, Kaiser R, Bobek V, Dubovy P. Enhancement of musculocutaneous nerve reinnervation after vascular endothelial growth factor (VEGF) gene therapy. *BMC Neurosci.* 2012;13(1):57. Epub 2012/06/08. doi: 1471-2202-13-57 [pii] 10.1186/1471-2202-13-57. PubMed PMID: 22672575.
171. Gupta R, Gray M, Chao T, Bear D, Modafferi E, Mozaffar T. Schwann cells upregulate vascular endothelial growth factor secondary to chronic nerve compression injury. *Muscle Nerve.* 2005;31(4):452-60. Epub 2005/02/03. doi: 10.1002/mus.20272. PubMed PMID: 15685607.
172. Schratzberger P, Schratzberger G, Silver M, Curry C, Kearney M, Magner M, et al. Favorable effect of VEGF gene transfer on ischemic peripheral neuropathy. *Nat Med.* 2000;6(4):405-13. Epub 2000/03/31. doi: 10.1038/74664. PubMed PMID: 10742147.
173. Yang F, Murugan R, Ramakrishna S, Wang X, Ma YX, Wang S. Fabrication of nanostructured porous PLLA scaffold intended for nerve tissue engineering. *Biomaterials.* 2004;25(10):1891-900. Epub 2004/01/24. PubMed PMID: 14738853.
174. Bini TB, S. Gao, S. Wang and S. Mamakrishna. Poly(l-lactide-co-glycolide) biodegradable microfibers and electrospun nanofibers for nerve tissue engineering: An in vitro study. *J Mater Sci.* 2006.
175. Nicoli Aldini N, Perego G, Cella GD, Maltarello MC, Fini M, Rocca M, et al. Effectiveness of a bioabsorbable conduit in the repair of peripheral nerves. *Biomaterials.* 1996;17(10):959-62. Epub 1996/05/01. PubMed PMID: 8736729.
176. Wen X, Tresco PA. Fabrication and characterization of permeable degradable poly(DL-lactide-co-glycolide) (PLGA) hollow fiber phase inversion membranes for use as nerve tract guidance channels. *Biomaterials.* 2006;27(20):3800-9. Epub 2006/03/28. doi: 10.1016/j.biomaterials.2006.02.036. PubMed PMID: 16564567.
177. Lietz M, Ullrich A, Schulte-Eversum C, Oberhoffner S, Fricke C, Muller HW, et al. Physical and biological performance of a novel block copolymer nerve guide. *Biotechnology and bioengineering.* 2006;93(1):99-109. Epub 2005/09/28. doi: 10.1002/bit.20688. PubMed PMID: 16187339.
178. N. Kotsaeng YBaYS. Preparation and in vitro Degradation of Methoxy Poly (Ethylene Glycol)-b-Poly (D, L-Lactide) Tubes for Nerve Tissue Engineering. *International Journal of Chemical Technology.* 2009.
179. Archibald SJ, Krarup C, Shefner J, Li ST, Madison RD. A collagen-based nerve guide conduit for peripheral nerve repair: an electrophysiological study of nerve regeneration in rodents and nonhuman primates. *J Comp Neurol.* 1991;306(4):685-96. Epub 1991/04/22. doi: 10.1002/cne.903060410. PubMed PMID: 2071700.
180. Fields RD EM. Axons Regenerated through Silicone Tube Splices. II. Functional morphology. *Experimental neurology.* 1986(92):61-74.
181. Dellon AL, Mackinnon SE. An alternative to the classical nerve graft for the management of the short nerve gap. *Plast Reconstr Surg.* 1988;82(5):849-56. Epub 1988/11/01. PubMed PMID: 2845455.
182. Dunnen WFAD, Lei Bvd, Schakenraad JM, Stokroos I, Blaauw E, Bartels H, et al. Poly(DL-lactide- ϵ -caprolactone) nerve guides perform better than autologous nerve grafts. *Microsurgery.* 1996;17(7):348-57.

183. Kwan MK, Wall EJ, Massie J, Garfin SR. Strain, stress and stretch of peripheral nerve. Rabbit experiments in vitro and in vivo. *Acta orthopaedica Scandinavica*. 1992;63(3):267-72. Epub 1992/06/01. PubMed PMID: 1609588.
184. Yang J, Motlagh D, Webb AR, Ameer GA. Novel biphasic elastomeric scaffold for small-diameter blood vessel tissue engineering. *Tissue Eng*. 2005;11(11-12):1876-86. Epub 2006/01/18. doi: 10.1089/ten.2005.11.1876. PubMed PMID: 16411834.
185. Sinis N, Schaller HE, Schulte-Eversum C, Schlosshauer B, Doser M, Dietz K, et al. Nerve regeneration across a 2-cm gap in the rat median nerve using a resorbable nerve conduit filled with Schwann cells. *Journal of neurosurgery*. 2005;103(6):1067-76. Epub 2005/12/31. doi: 10.3171/jns.2005.103.6.1067. PubMed PMID: 16381194.
186. di Summa PG, Kalbermatten DF, Pralong E, Raffoul W, Kingham PJ, Terenghi G. Long-term in vivo regeneration of peripheral nerves through bioengineered nerve grafts. *Neuroscience*. 2011;181:278-91. Epub 2011/03/05. doi: S0306-4522(11)00222-3 [pii] 10.1016/j.neuroscience.2011.02.052. PubMed PMID: 21371534.
187. Kalbermatten DF, Erba P, Mahay D, Wiberg M, Pierer G, Terenghi G. Schwann cell strip for peripheral nerve repair. *J Hand Surg Eur Vol*. 2008;33(5):587-94. Epub 2008/11/04. doi: 10.1177/1753193408090755. PubMed PMID: 18977829.
188. Bunge MB. Bridging the transected or contused adult rat spinal cord with Schwann cell and olfactory ensheathing glia transplants. *Prog Brain Res*. 2002;137:275-82. Epub 2002/11/21. PubMed PMID: 12440373.
189. Cao Q, Xu XM, Devries WH, Enzmann GU, Ping P, Tsoulfas P, et al. Functional recovery in traumatic spinal cord injury after transplantation of multilineurotrophin-expressing glial-restricted precursor cells. *The Journal of neuroscience : the official journal of the Society for Neuroscience*. 2005;25(30):6947-57. Epub 2005/07/29. doi: 10.1523/JNEUROSCI.1065-05.2005. PubMed PMID: 16049170; PubMed Central PMCID: PMC2813488.
190. Stang F, Fansa H, Wolf G, Keilhoff G. Collagen nerve conduits--assessment of biocompatibility and axonal regeneration. *Biomed Mater Eng*. 2005;15(1-2):3-12. Epub 2004/12/30. PubMed PMID: 15623925.
191. Hill CE, Moon LD, Wood PM, Bunge MB. Labeled Schwann cell transplantation: cell loss, host Schwann cell replacement, and strategies to enhance survival. *Glia*. 2006;53(3):338-43. Epub 2005/11/04. doi: 10.1002/glia.20287. PubMed PMID: 16267833.
192. Longo FM, Hayman EG, Davis GE, Ruoslahti E, Engvall E, Manthorpe M, et al. Neurite-promoting factors and extracellular matrix components accumulating in vivo within nerve regeneration chambers. *Brain Res*. 1984;309(1):105-17. Epub 1984/08/20. doi: 0006-8993(84)91014-X [pii]. PubMed PMID: 6488001.
193. Sabatier MJ, Redmon N, Schwartz G, English AW. Treadmill training promotes axon regeneration in injured peripheral nerves. *Experimental neurology*. 2008;211(2):489-93. Epub 2008/04/19. doi: S0014-4886(08)00078-2 [pii] 10.1016/j.expneurol.2008.02.013. PubMed PMID: 18420199; PubMed Central PMCID: PMC2584779.
194. Fouad K, Schnell L, Bunge MB, Schwab ME, Liebscher T, Pearse DD. Combining Schwann cell bridges and olfactory-ensheathing glia grafts with chondroitinase promotes locomotor recovery after complete transection of the spinal cord. *The Journal of neuroscience : the official journal of the Society for Neuroscience*. 2005;25(5):1169-78. Epub 2005/02/04. doi: 10.1523/JNEUROSCI.3562-04.2005. PubMed PMID: 15689553.
195. Kadoya K, Tsukada S, Lu P, Coppola G, Geschwind D, Filbin MT, et al. Combined intrinsic and extrinsic neuronal mechanisms facilitate bridging axonal regeneration one year after spinal cord injury. *Neuron*. 2009;64(2):165-72. Epub 2009/10/31. doi: S0896-6273(09)00698-9 [pii]

- 10.1016/j.neuron.2009.09.016. PubMed PMID: 19874785; PubMed Central PMCID: PMC2773653.
196. Udina E, Ladak A, Furey M, Brushart T, Tyreman N, Gordon T. Rolipram-induced elevation of cAMP or chondroitinase ABC breakdown of inhibitory proteoglycans in the extracellular matrix promotes peripheral nerve regeneration. *Experimental neurology*. 2009. Epub 2009/09/08. doi: S0014-4886(09)00365-3 [pii] 10.1016/j.expneurol.2009.08.026. PubMed PMID: 19733561.
197. McMahon SB, Armanini MP, Ling LH, Phillips HS. Expression and coexpression of Trk receptors in subpopulations of adult primary sensory neurons projecting to identified peripheral targets. *Neuron*. 1994;12(5):1161-71. Epub 1994/05/01. doi: 0896-6273(94)90323-9 [pii]. PubMed PMID: 7514427.
198. Dijkhuizen PA, Hermens WT, Teunis MA, Verhaagen J. Adenoviral vector-directed expression of neurotrophin-3 in rat dorsal root ganglion explants results in a robust neurite outgrowth response. *J Neurobiol*. 1997;33(2):172-84. Epub 1997/08/01. doi: 10.1002/(SICI)1097-4695(199708)33:2<172::AID-NEU6>3.0.CO;2-# [pii]. PubMed PMID: 9240373.
199. Wu XY, Zhou Y. Finite element analysis of diffusional drug release from complex matrix systems. I complex geometries and composite structures. *J Control Release*. 1997;51(1):57-71.
200. The finite element method and applications in engineering using ANSYS, (2006).
201. Finite element analysis (FEA): applying an engineering method to functional morphology in anthropology and human biology, (2009).
202. Danielsen N, Vahlsing HL, Manthorpe M, Varon S. A two-compartment modification of the silicone chamber model for nerve regeneration. *Experimental neurology*. 1988;99(3):622-35. Epub 1988/03/01. PubMed PMID: 3342845.
203. Bryan DJ, Holway AH, Wang KK, Silva AE, Trantolo DJ, Wise D, et al. Influence of glial growth factor and Schwann cells in a bioresorbable guidance channel on peripheral nerve regeneration. *Tissue Eng*. 2000;6(2):129-38. Epub 2000/08/15. doi: 10.1089/107632700320757. PubMed PMID: 10941208.
204. Grassi M, Grassi G. Mathematical modelling and controlled drug delivery: matrix systems. *Current drug delivery*. 2005;2(1):97-116. PubMed PMID: 16992988178690593545related:CdNDP7c40-sJ.
205. Mathematical modeling of drug release from bioerodible microparticles: effect of gamma-irradiation, (2003).
206. Modeling and analysis of dispersed-drug release into a finite medium from sphere ensembles with a boundary layer, (2003).
207. Chung BG, Flanagan LA, Rhee SW, Schwartz PH, Lee AP, Monuki ES, et al. Human neural stem cell growth and differentiation in a gradient-generating microfluidic device. *Lab Chip*. 2005;5(4):401-6. Epub 2005/03/26. doi: 10.1039/b417651k. PubMed PMID: 15791337.
208. Bryan DJ, Wang KK, Summerhayes C. Migration of schwann cells in peripheral-nerve regeneration. *J Reconstr Microsurg*. 1999;15(8):591-6. Epub 1999/12/23. doi: 10.1055/s-2007-1000143. PubMed PMID: 10608740.
209. Tseng CY, Hu G, Ambron RT, Chiu DT. Histologic analysis of Schwann cell migration and peripheral nerve regeneration in the autogenous venous nerve conduit (AVNC). *J Reconstr Microsurg*. 2003;19(5):331-40. Epub 2003/09/25. doi: 10.1055/s-2003-42502. PubMed PMID: 14506582.

BIOGRAPHICAL INFORMATION

Swarup Dash is a member of the Regenerative Neurobiology Lab at UT Arlington & UT Southwestern Medical Center – where he is currently pursuing his doctoral degree in Biomedical Engineering. He holds a Bachelor's degree in Biotechnology from Amity University, India. His PhD thesis involves regeneration of long gap defects in the peripheral nervous system using advanced nerve implant which constitutes of a novel biodegradable nerve guide and a growth factor delivery system to regain lost function. He has extensive training in aseptic cell/tissue culture techniques, molecular gateway cloning, drug delivery, viral vector formulations, and gene therapy and testing in various animal models as well as DNA and protein assay. He has worked for Life Technologies (Invitrogen), Carlsbad, California, where he accomplished a research project involving multisite gateway cloning of an 18kb plasmid for Jump In cells and developed a potential molecular biology product for stem cell research. He met his wife in the bioengineering program at UT Arlington and they live in Arlington, TX.